Title

Expeditious Data Center Sustainability, Flow, and Temperature Modeling: Life-Cycle Exergy Consumption Combined with a Potential Flow Based, Rankine Vortex Superposed, Predictive Method

Author

Lettieri, David

Publication Date

2012

Peer reviewed|Thesis/dissertation

Expeditious Data Center Sustainability, Flow, and Temperature Modeling: Life-Cycle Exergy Consumption Combined with a Potential Flow Based, Rankine Vortex Superposed, Predictive Method

by

David Joseph Lettieri

A dissertation submitted in partial satisfaction of the
requirements for the degree of
Doctor of Philosophy

in

Mechanical Engineering

and the Designated Emphasis

in

Energy Science and Technology

in the

Graduate Division

of the

University of California, Berkeley

Committee in charge:

Professor Van P. Carey, Chair
Adjunct Professor Samuel Mao
Professor Edward Arens

Spring 2012

The dissertation of David Joseph Lettieri, titled Expeditious Data Center Sustainability, Flow, and Temperature Modeling: Life-Cycle Exergy Consumption Combined with a Potential Flow Based, Rankine Vortex Superposed, Predictive Method, is approved:

Chair _____ Date _____

_____ Date _____

_____ Date _____

University of California, Berkeley

Expeditious Data Center Sustainability, Flow, and Temperature Modeling: Life-Cycle Exergy Consumption Combined with a Potential Flow Based, Rankine Vortex Superposed, Predictive Method

Abstract

Expeditious Data Center Sustainability, Flow, and Temperature Modeling: Life-Cycle Exergy Consumption Combined with a Potential Flow Based, Rankine Vortex Superposed, Predictive Method

by

David Joseph Lettieri

Doctor of Philosophy in Mechanical Engineering

University of California, Berkeley

Professor Van P. Carey, Chair

Traditionally data centers were designed with reliability, functionality, and up front cost as the primary design drivers, with secondary consideration given to cost of operation and sustainability. In the past decade, data center design has shifted giving more weight to operational energy use and sustainability. This thesis outlines two work streams aimed at allowing data center designers and operators to design more efficient, cost effective, sustainable data centers. The first track deals with evaluating data center sustainability quickly and easily. The metric chosen to quantify data center sustainability is life-cycle exergy consumption. Other sustainability indicators are investigated, and reasons for choosing this metric for data centers are provided. Two case studies are provided to illustrate the sustainability ramifications of different design and operation decisions. A Life-Cycle Assessment (LCA), perhaps the most widely accepted industry practice of assessing the environmental ramifications of a product or process, is also completed for comparison purposes. A MATLAB based graphical user interface (GUI) developed to perform a life-cycle exergy consumption analysis (LCEA) on data centers was designed and its usefulness is demonstrated.

The second track of this thesis deals with expeditious velocity and temperature field prediction in data centers, developed to be an ultrafast alternative to conventional computational fluid dynamics (CFD) code. This expeditious predictive scheme is based on a potential flow velocity prediction method with a Rankine vortex superposition correction scheme to correct for physical processes neglected by the relatively simpler but much more computationally efficient potential flow equations. Energy considerations are accomplished through convective energy transport equations. It is shown that without the Rankine vortex superposition correction, potential flow is inadequate for accurately predicting velocity and temperature fields in data centers. It is also shown that with the Rankine vortex superposition, in areas of interest within data centers, temperature predictions are as accurate or are more accurate than a commercially available, conventional CFD software package that uses the full Navier-Stokes and energy equations to solve for velocity and temperature fields.

Three case studies are carried out based on experiments that were conducted in a data center at HP Labs in Palo Alto, California. Measurements taken in that data center are used for comparison with CFD predictions from ANSYS FLUENT and a MATLAB based, potential flow with Rankine Vortex code named COMPACT (Compact Model of Potential Flow and Convective Transport) . FLUENT's temperature field predictions are also compared with COMPACT's predictions for both computational speed and accuracy.

The ultimate goal of these two streams, when combined, is to give a data center designer or operator an ultrafast, comprehensive tool to make data center sustainability decisions while constrained by operational temperature limit considerations. It is shown in this work that such a goal is attainable.

To my family.

By giving me a strong foundation you enabled me to chase my dreams. Your constant support is all I need to achieve them.

Contents

List of Figures

List of Tables

Nomenclature

β	Volumentric thermal expansion coefficient . . . 59
$\Delta\rho$	Density difference between heated air and air at reference temperature 59
δm	Mass of heated parcel of air . . . 59
ΔP_b	Pressure loss as air travels through CRAC unit . . . 43
ΔT_R	Measured temperature rise across server . . . 65
ΔT_{water}	Temperature difference of chilled water across condensor in CRAC unit 43
$\dot{m}$	Mass flow rate . . . 39
$\dot{W}_b$	Rate of work done by blower in CRAC unit . . . 45
$\dot{W}_c$	Rate of work done by compressor in CRAC unit . . . 45
$\dot{W}_{cv}$	Rate of work done by control volume . . . 39
$\dot{X}_d$	Rate of exergy consumption (alternatively called rate of exergy destruction) . . . 39
η_b	Efficiency of blowers in CRAC unit . . . 43
γ	Ratio of specific heat at constant pressure and volume . . . 44
ϕ	Mass specific exergy value in flow field . . . 39
ϕ	Velocity potential . . . 57
ρ_o	Density at reference temperature . . . 59
υ	Specific volume . . . 44
A	Area of server rack face . . . 65
AL	Average Load . . . 47
C	Specific heat capaity multiplied by mass flow rate . . . 57
c_p	Specific heat at constant pressure . . . 44
COP	Coefficient of performance . . . 45
D	Duration . . . 47
$F_{\delta m}$	Buoyancy force . . . 59
g	Gravitational constant . . . 40
H	Height . . . 59
h	Enthalpy . . . 40
I	Current . . . 52
k_v	Vortex strength . . . 60
P	Pressure . . . 44
Q_j	Rate of heat transfer at location j . . . 39

Acknowledgments

I would like to thank the many people that have helped me with my studies throughout my life. Beginning with my parents homework help as a kid, and continuing with all my teachers and classmates, those around me have always made learning exciting. You instilled in me a curiosity and determination to learn that I hope never fades. One very important aspect of life is finding the right balance, and my lab-mates and friends often convinced me to put aside my work and just enjoy the moment. I am a better person for having gotten to know you all, and I have made countless wonderful memories over the last five years. I can't imagine interacting with a better group of people in the future.

Working on this project has been a great learning experience. First, I would like to thank Professor Carey for his guidance and support. You taught me how to frame and carry out a research project, and for that I am grateful. I am also grateful for the help and guidance of Amip Shah and Cullen Bash at HP labs. I appreciate all of your instruction and guidance as I conducted experiments in your data center. I would especially like to acknowledge Mike for all of his efforts. We spent a lot of time working together on this project. I, as well as all those who have to read my code in the future, am thankful for everything I learned from you as we worked together.

Finally, support for this research from both a grant from the Hewlett Packard Laboratories Innovation Research program and the UC Discovery Grant program is gratefully acknowledged.

Chapter 1

Introduction

1.1 Motivation for Sustainable Data Centers

Information technology (IT) equipment in data centers use considerable amounts of energy and in the process generate large amounts of heat. In 2006, data centers used approximately 61 billion kWh of electricity, accounting for about 1.5% of total U.S. energy consumption. More troubling than the large amount of electricity use is the fact that the usage has approximately doubled since 2000 [4]. Figure 1.1, taken from [4], shows electricity use in data centers from 2000 to 2006 and estimates what the electricity use in data centers could be in future years if different courses of action are taken. The figure shows the doubling of electricity use by data centers from 2000 to 2006 and extrapolates to what future electric usage may be achieved. The potentially favorable trends rely on implementing current efficiency practices, such as better load sharing of servers to reduce idle and number of servers needed, as well as improved operating conditions, such as direct liquid cooling or the use of air and water side economizers.

Before proceeding further, it is advantageous to define what is meant by the term data center. The definition in this study will be that used by Tschudi, et al. [112]. A data center will be defined as "a facility that contains concentrated equipment to perform one or more of the following functions: store, manage, process, and exchange digital data and information." Since the temperature of the IT equipment must be controlled both to ensure reliable operation and to prevent premature failure of said equipment, energy usage involves, amongst other things, both actual server electricity use and the power needed to run cooling infrastructure. Removing the heat generated by the IT equipment is most commonly achieved by circulating cooled air through the data center; air warmed by this process is then removed from the room and often re-cooled for use in the server room [97]. The energy expended in this fashion is comparable to and sometimes even larger than the energy needed to power the IT equipment [28]. When viewing an entire data center system, the electricity used by cooling equipment can be more than half of the total data center energy use. In light of growing economic and environmental concerns over energy use, it is advantageous

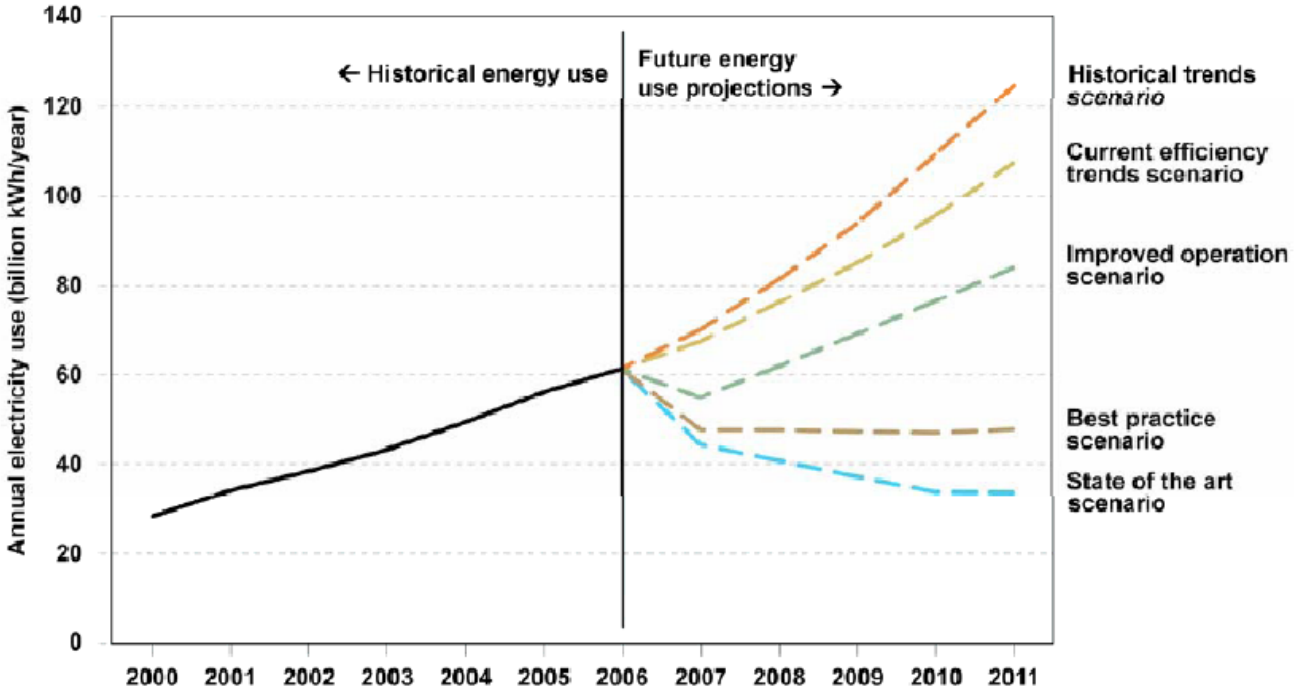

Figure 1.1: Past U.S. data center electricity use and future electricity use projections, taken from the EPA Report on Server and Data Center Energy Efficiency [4].

to expend effort and capital on data center energy efficiency. As is pointed out in [112], the concentrated equipment to perform data center functions usually includes energy intensive computer equipment, cooling equipment, and electrical infrastructure to handle high levels of power consumption with a high level of reliability. This definition of a data center is not applicable to spaces that house office computers as well as small rooms of servers.

Billions of dollars and kWh, and all of the environmental implications of generating 61 billion kWh, is motivation enough for the continued study of data centers and their environmental footprint. Due to the large scale of operational energy use, even small improvements in overall data center efficiency can lead to large financial and environmental savings. However, this motivation deals only with the operational portion of the life-cycle of a data center. Data center life-cycles have other portions other than the operational leg. Traditional cradle-to-grave life-cycle analyses include raw material extraction and processing, manufacturing, operation, recycling or some other end-of-life treatment, and transportation throughout. All of these stages of a life-cycle contribute to the overall environmental footprint of a product, process, or service. In the case of the data center, almost all of the research efforts have been focused only on the operational portion. The reason for this is likely twofold. First, data center equipment uses a high level of power continuously for years. Second, by far the easiest

attainable measure of data center environmental performance is electricity consumption.

The assumption often made is that the environmental effects of a high level of fairly constant operational energy use over years are much larger than the other life-cycle stages. Therefore, if an exotic material were to be used in data centers to increase data center operational efficiency, but at the cost of requiring more energy to manufacture, the assumption is that the operational energy savings and associated environmental savings achieved through the use of the exotic material will by far outweigh the increased environmental consequences of manufacturing the new exotic material. In addition, tallying the electric bills for a data center is an easy and straightforward process requiring little skill and time.

While this approach is the easiest and may be satisfactory if the operational leg truly is exceedingly dominant when compared to the rest of the life-cycle, to the authors knowledge, there is presently no holistic analysis to confirm this assumption. Several frameworks exist to quantify the environmental effects of a product, process, or service. These frameworks are discussed in chapter 2. It is a goal of this study to perform a life-cycle analysis of a data center to show the sustainability implications of the entire life-cycle.

1.2 Data Center Basics

1.2.1 Equipment in a Data Center

Data centers come in many different sizes and configurations, but almost always consist of five groups of similar equipment. The most obvious group of equipment is the IT equipment. This includes the servers, routers, switches, and other related equipment. IT equipment is usually stored in cabinets called racks. These racks are approximately 7 feet tall and 2 feet wide. The racks are usually organized in rows (more information on why that is in subsection 1.2.2). The IT equipment uses a large amount of electricity, and dissipates this electricity as heat. This concentrated heat load must be removed to maintain cool operating conditions required by the IT equipment. The second group of equipment included in data centers is the cooling equipment. This group of equipment includes computer room air handler units (CRAH units), computer room air conditioning units (CRAC units), water chillers, cooling towers and all of the ductwork, piping, and other related equipment needed to move heat from within the data center to outside the data center. The third group of equipment traditionally in data centers is the power distribution equipment. Power distribution units (PDU), both on a large room level scale and a smaller rack level scale, are used to step voltages down thousands of volts to hundreds of volts for IT equipment to use. The fourth group of equipment is the group of equipment used to maintain reliable power to the data center. Depending on the size of the data center, power reliability consists of both uninterruptible power supplies (UPS) as well as backup generators. The uninterruptible power supplies are devices which, in the event of power loss, provide power to the data center for a short period of time until the power is restored or the backup generators are turned on and brought online. The next group of equipment is some kind of building structure or housing for a data center.

Often this is a traditional bricks and mortar building or lately metal shipping containers. A final group of equipment includes economizers, either air or water side economizers. A description of how these equipment work is given in subsection 1.2.2, but for now it is sufficient to know that economizers are used to take advantage of cool outside air to reduce air conditioning costs of the CRAC and chiller units.

In order to evaluate the sustainability ramifications of the equipment in a data center, this thesis includes two different life-cycle analyses of a combination of the equipment listed above from all five of these groups. Not all of the equipment in each category will be analyzed, primarily due to a lack of information on certain equipment. However, the most important equipment from all five groups is included. The study focuses on equipment housed in the data center, and will not include equipment outside of the physical data center (electricity grid, step down transforms, cooling towers, air and water side economizers, etc.).

1.2.2 Cooling Strategy in a Data Center

To cool a data center, different methodologies can be employed. IT equipment uses a lot of electricity, almost all of which is transformed into heat. This heat must be removed for two reasons. First, if IT equipment becomes too hot, it cannot perform its tasks. The equipment must be below design thresholds to function. Second, even if below design thresholds, if equipment is kept too close to the design temperature limit, the lifetime of the IT equipment shortens. For this reason, an effective cooling strategy is needed. In the past, when electricity use and environmental effects took a backseat to system reliability and facility upfront cost, the cooling strategy often involved providing more cooling than needed to ensure reliable operation and equipment longevity. Recently, concern over operational costs (as energy becomes more expensive) and environmental effects (as data centers become more prevalent), motivate more efficient cooling strategies.

The most common cooling strategy is a raised floor configuration with an underfloor plenum, where air is cyclically cooled and warmed. Figure 1.2 shows an example of a data center cooling strategy. Racks are organized into rows which separate cold aisles from warm aisles. Cold air is pumped from the underfloor plenum into the cold aisle. Fans in the racks pull cold air in through the front of the racks over the hot IT equipment, cooling the IT equipment. The warm air is blown out of the back of the racks into the hot aisle, where it leaves the room through either ceiling or wall return tiles.

Cold air is generated either directly by chillers and then moved around by CRAH units, or is made cool by direct expansion (DX) CRAC units. Chillers are large refrigeration units which make cool water. The air that is to be cooled in the data center is passed through a heat exchanger, where the hot air gives up its heat to the cool water. In this case, a CRAH unit is used to move warm air from the data center to the chiller evaporator coils. In the latter case, a DX CRAC unit uses a refrigerant rather than water to exchange heat with warm air. CRAC units can be located directly in the data center and often give operators and designers more flexibility in the cooling strategy. The warm working fluid of the CRAC unit is often cooled by chilled water supplied by a chiller, so a chiller is still required. As

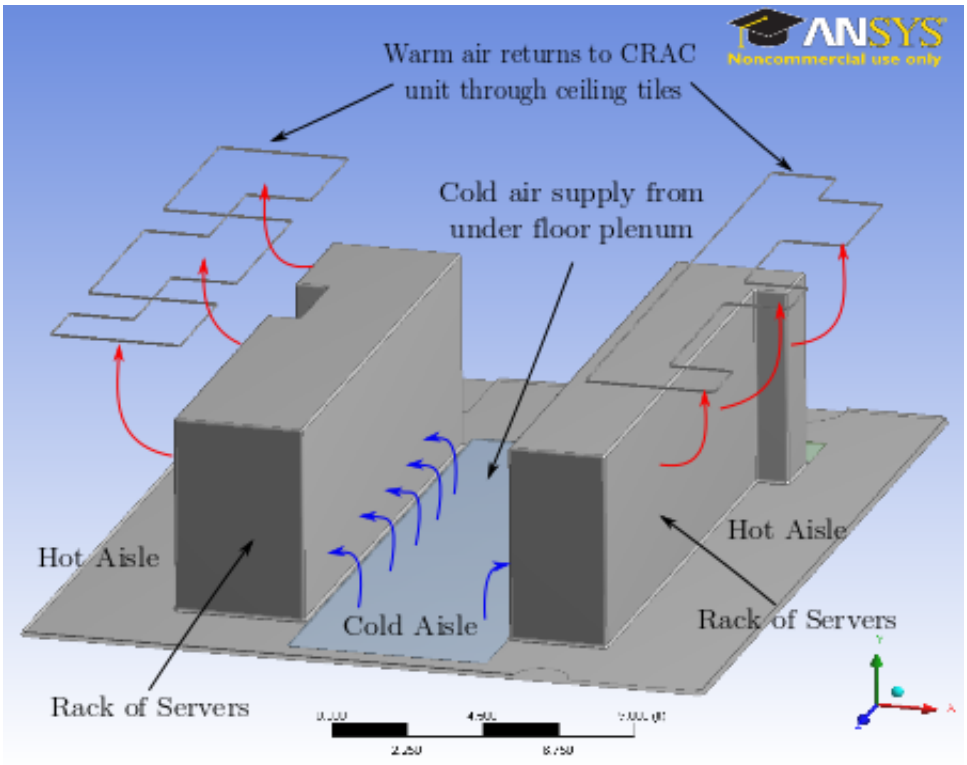

Figure 1.2: Most common data center layout, showing hot and cold aisles.

pointed out in [46], this is the dominant cooling strategy in mid to large data centers [112]. The warm working fluid of a chiller is cooled using air or water and a cooling tower.

A more recent cooling strategy uses cold air from the environment when available to save on cooling costs [46]. This can be done using economizers which use free, cool outside air to minimize cooling energy needed. There are two types of economizers, air and water side, both of which make use of cold outside temperatures when available. Air side economizers make use of the fact that it can be more energy efficient to condition cool outside air than to condition recirculating interior air [59]. The outside air is conditioned to ensure proper humidity and particulate matter levels to meet standards necessary for IT equipment, and is pumped inside a data center using CRAH units. Warm exhaust air from the data center is exhausted out of the data center to the environment. This strategy bypasses the vapor-compression cycle of the CRAC units and chillers, and can save energy. However, more ducting is needed to pump in outside air, resulting in more air resistance. Achieving 100% use of outside air could result in more overall cooling energy used due to the increased pumping energy needed, so care must be used when using air side economizers to ensure energy savings when compared to a baseline case of no air side economizer.

A water side economizer is used to directly cool the working fluid of CRAC units without having to use a chiller [100]. Additional heat exchangers are installed between the CRAC

unit and the cooling tower. Using cold outside air and cooling towers, cold water is generated to cool the working fluid of a CRAC unit. If weather conditions are sufficient, a chiller can be bypassed altogether. In this case, outside air does not have to be introduced into the data center, dismissing concerns over ducting losses and humidity and particulate control that afflict air side economizers.

In order to evaluate the cooling strategies in data centers, this thesis employees two different types of computational fluid dynamics (CFD) studies: tradition CFD and reduced-order CFD. The CFD studies focus on predicting velocity and temperature fields in the data center room, and do not model flow upstream of the room. The boundary conditions for the CFD studies are the room inlet and outlet tiles.

1.3 Motivation for Faster Data Center Velocity and Temperature Field Prediction

The arguments for sustainable data centers illustrate two competing goals for data center thermal management. The first goal is to maintain temperatures in the data center so that IT equipment stays below rated operational temperature thresholds. The second goal is to provide the needed cooling as efficiently as possible to minimize energy use and subsequently the associated operational costs and potential environmental consequences associated with energy consumption. Related to the improvement in energy efficiency is the improvement in cooling capacity that results from accurate prediction of thermo-fluidic behavior in the data center. Improved capacity utilization can result in reduced capital costs, since less infrastructure is needed to remove a given load. Furthermore, improved capacity utilization can result in increased potential to utilize alternative cooling resources like air or water side economization which result in improved operational efficiency of cooling microgrids that blend economization schemes with traditional mechanical refrigeration [60].

Accordingly, flow and temperature prediction allows data center designers to build data centers that provide cooling to IT equipment when and where it is needed. Prediction is also useful for active operation, allowing managers to control cooling equipment to efficiently adapt to dynamic IT loads and/or cooling equipment failure. Current state-of-the-art CFD models use the full Navier-Stokes equations, coupled with the energy equation and even turbulence models, to model airflow and predict the velocity and temperature fields in a data center. There are many commercially available CFD packages that exist and allow for this rigorous analysis. While these packages do provide accurate modeling of airflow in data centers, there are several drawbacks to their use.

1. The CFD packages themselves are often expensive and differ in their use. This requires not only the purchase of the CFD package, but also the employment of someone with knowledge of how to use the CFD package. Even for someone well versed in the use of a particular CFD package, it may be time consuming to set up the CFD study, especially if the design envelope being studied is expansive.

2. CFD studies are often computationally expensive and require expensive, high powered workstations to manage the large number of calculations required by the sophisticated model.

3. CFD models can take long periods of time, often on the scale of hours, to achieve convergence. This is prohibitively long for a real time controller or for design optimization with a large number of design parameters.

These drawbacks are not insurmountable and are often not of large consequence. One may argue that when designing a data center, the capital expense and time commitment needed to carry out a CFD study are of little significance compared to the overall design and construction of a data center. It is much cheaper and faster to complete a CFD study than the alternative of building a data center and using trial and error to choose the location and cooling levels of cooling equipment. However, it would still be advantageous to have faster, less computationally expensive methods of predicting temperatures in a data center. This is generally achieved at the expense of accuracy, but this trade-off is nonetheless deemed beneficial for the following reasons:

1. Investigation of the data center design envelope would be expedited with faster predictive capabilities. When a final design or small group of potential final designs are identified as promising after the use of the faster prediction, a more rigorous CFD analysis could be used to confirm the findings of the simpler prediction. This will speed up optimization of data centers with many parameters.

2. Often in CFD analyses, convergence can be accelerated if the initial conditions are closer to the final solution. The faster, simpler analysis could be used to generate an initial guess for more complicated CFD analyses, facilitating faster overall convergence times.

3. Simplified models could be used in automated, real time controllers that optimize the cooling in a data center. In this case, the controller would likely not be a powerful workstation and analyses would have to be completed on the scale of minutes or even seconds rather than hours. This will not be possible in the foreseeable future with full CFD simulations.

4. A MATLAB based program has been developed concurrently with COMPACT to assess on a system level the life-cycle efficiency ramifications of different data center decisions [64, 63]. Whether used by a data center designer when initially designing a data center or by a controller when operating the data center, a simpler MATLAB based flow and temperature prediction model could be easily incorporated with this software to rank decisions based on the efficiency implications on an overall data center system level. This will allow for the most efficient decision overall. The MATLAB based efficiency program could be integrated with a commercially available CFD program, but it would

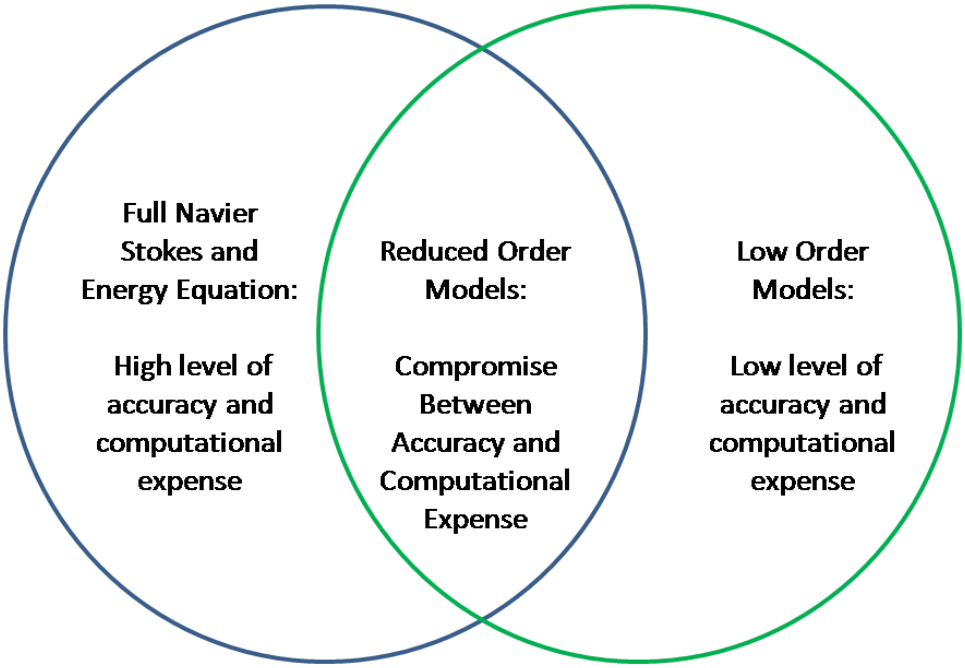

Figure 1.3: Comparison of full numerical model to reduced order models.

be more difficult, time consuming, and potentially expensive. It is important to note that while the efficiency and simpler flow and temperature modeling programs are written with MATLAB, they are not restricted to MATLAB, and could be written in other languages, such as C or JAVA. MATLAB was chosen because it is ubiquitous in industry and academia.

It is the goal of this study to find an acceptable balance between full Navier-Stokes and energy equation consideration and low order consideration. An example of a low order model is BLAST or DOE-2 [6]. Low order models are much less computationally expensive, but would not be accurate in assessing temperature or velocity fields in data centers. Low order models are useful for looking at an overall energy balance, including building heat loads due to building equipment or weather, on a simplified basis to estimate building energy usage. For example, someone using these programs might be trying to solve for building energy usage necessary to maintain a certain average temperature, but not to solve for temperature fields within the building to find hot-spots. The middle ground reduced order model, with the appropriate balance of accuracy and speed, needs to be computational cheap but predict temperature fields accurately. Figure 1.3 illustrates the balance that needs to be achieved.

Although accuracy is generally lost when a simplified model is used, this assumes that the boundary conditions supplied to said model are well-specified. Not every data center may be well-instrumented enough to provide accurate boundary conditions (e.g. room inlet flow rate, server rack power consumption, server rack volumetric flow rate). If they are not, then

the effectiveness of a full commercial CFD package is lessened. If the accuracy of a full CFD analysis is comparable to a simpler analysis, or if the simpler analysis is deemed accurate enough, then the simplified model may be more desirable due to much quicker computation time. It is the goal of this paper to make that comparison. A small data center was studied, and the results of a full CFD analysis and simpler potential flow analysis were compared to experimental results and to each other.

1.4 Thesis Layout

This thesis is composed of nine chapters. Chapters 2 and 3 provide a background of work that has already been done with regard to sustainability modeling and indicators as well as temperature and velocity field prediction, respectively. The literature review is broken into two chapters: one for the sustainability track of this thesis, the other for the temperature and velocity field prediction. Similarly, the methodology for the two tracks are laid out separately in chapters 4 and 5. The results of sustainability modeling as well as temperature and velocity field predictions are also laid out separately in chapters 6 and 7. The two tracks are brought together in chapters 8 and 9, where the results from each track are discussed and a case study is performed to show how they can be combined for their ultimate goal: data center sustainable design and operation.

Chapter 2

Literature Review of Sustainability Modeling

Sections 2.1.1 through 2.3.3 are sections that were included almost verbatim in [64, 62]. They are also included here in this thesis because they are necessary to motivate why life-cycle exergy consumption is a good sustainability metric for data centers.

2.1 Review of Sustainability Modeling

2.1.1 Need for Sustainability Indicators

Energy, pollution, and resource use are currently issues of growing relevance and importance. On many levels, from the individual to the international, efforts have been and are continuing to be made to increase sustainability. The most logical place to begin is with a definition of sustainability. One of the first and the most widely cited definitions for sustainable development comes from the Brundtland Commission's resolution 42/187 [24]. This resolution stated that "Sustainable development is development that meets the needs of the present without compromising the ability of future generations to meet their own needs." As is often pointed out, there are several practical shortfalls of this definition. First, the term "needs" is rather vague. For example, few would argue that access to clean drinking water is a need, but is access to the Internet or air conditioning a need? The second shortcoming deals with the needs of the "future generations". There is no mention of how far in the future we should be concerned. Taking it to the extreme limit, sustainable development could be development that could be continued indefinitely. Someone attempting to use this strict interpretation would have to decide what level of technological sophistication to factor into their calculations. For example, when considering whether or not a car is sustainable, should one use today's standard fuel economy or fuel economy of future, more technologically advanced and efficient cars. Is it sustainable to drain our oil reserves now if cars in the future will be powered by batteries? This definition of sustainability, as with many others,

shows the inherent difficulty in assessing whether a certain decision, product, or process is sustainable.

Setting aside the difficulty in defining sustainability, efforts to be more sustainable are increasing. However, mere effort does not guarantee that more sustainable practices will be achieved. An example is corn based ethanol biofuel. In principle, creating fuel from plant material, a renewable resource, might increase a nation's level of sustainability. But it has been argued that more energy may be required to produce and distribute the ethanol than the ethanol itself contains, resulting in a net loss [76]. For this reason, it is imperative to have indicators that can be used to evaluate the level of sustainability for different activities. By using such indicators, decision makers can perform more thorough assessments of the sustainability of future actions. Indicators are typically used to show which is the more sustainable option between several different options. In this way, the relatively difficult task of defining absolute sustainability is sidestepped in favor of a practically feasible method of a relative assessment of sustainability.

2.1.2 Overview of Sustainability Indicators

Over the last several decades, a myriad of sustainability indicators have been proposed. An individual attempting to assess the sustainability of an action is faced with the daunting task of choosing a suitable and accurate indicator to measure the action's sustainability. In an effort to remedy this problem, the Scientific Committee on Problems of the Environment (SCOPE) published an extensive review [37] of sustainability indicators. Some of their conclusions are summarized below:

1. Hundreds of sustainability indicators have been defined and used, and are grouped into what the report labels three "pillars". These three pillars, often also referred to as the triple bottom line [23], categorize sustainability into environmental, economic, and social considerations. However, there is no scientific consensus on a common set of indicators appropriate for use within or between the pillars of sustainability.

2. Most indicators quantify behavior within one of the three pillars, although some indicators attempt to link the three pillars. This linkage of the pillars, while difficult, provides for a more complete indicator.

3. Good indicators are modular in nature. This allows for varying levels of accuracy in the analysis depending on the desired investment into generating the indicator. Thus, issues that are not considered important can be added later if then deemed relevant. This also allows for easy updating of the indicator when new information becomes available or when processes are changed.

Good indicators strike a balance between the accuracy of the model used to generate the indicator and ease at which the indicator is generated. Indicators that model a system with an excessively high level of accuracy at the cost of being overly expensive and time

consuming to generate are not necessarily effective. On the other hand, indicators that are easy to generate but that do not model a process well are also not effective.

In an age of relative information abundance, a good indicator is not only one that effectively models a system, but does so in a way that results in a simple index or expression that can be used by decision makers to achieve a "scientifically verifiable trajectory" towards a goal [37].

2.2 General Classification of Sustainability Indicators

There are hundreds of sustainability indicators. An attempt to analyze and compare all recently proposed indicators would be overly complex. One aim of this study is to compare life-cycle exergy consumption with other proposed sustainability metrics for use with data center design and operation. To refine the comparison of indicators, they will first be classified and only those that are applicable to information technology will be compared, citing specific indicators for illustration when necessary.

On the broadest level, sustainability indicators can be classified by which pillar of the triple bottom line they attempt to measure. While some indicators attempt to quantify more than one pillar, most do not. For example, the human development index [113, 86], which ranks countries by their level of human development, exemplifies a social indicator. The index computes human development by factoring in life expectancy, education, and standard of living. An example of an economic indicator is gross domestic product (GDP), which can be used to quantify the income and output of a nation's economy. Data centers can affect all three pillars of sustainability. For example, information stored in data centers may enable an increased level of education, thus increasing a nation's human development index. Data centers may also lead to more efficient businesses, thus increasing economic sustainability.

Of interest in this thesis is how data centers affect the environmental pillar. It should be noted that while some indicators may measure sustainability in more than one pillar, not all of these pillars are relevant for this study. Only indicators or portions of indicators related to the environmental pillar will be analyzed.

2.3 Thermodynamic Metrics used as Environmental Indicators

2.3.1 Environmental Indicators

Human activities rely on the environment to provide resources and absorb wastes [33]. Environmental indicators assess how such activities affect the environment and, based on the effect, quantify the sustainability of the process. Environmental indices often do not have a value which can be used to determine whether or not sustainability has been reached.

Rather, most environmental indicators are used in a comparative manner. Using the index in this way, two different activities can be analyzed, and the indicator can quantify which activity is less sustainable. An example of an environmental indicator is the Environmental Sustainability Indicator (ESI) [25]. The ESI takes 76 variables, chosen through an environmental literature review, and obtains a single index for the sustainability of a country through weighting of the different variables. A problem with the ESI is one that faces many indices: the index is arrived at through subjective decisions as to the importance of different variables. For example, two variables are child death rate from respiratory disease and environmental efficiency. When determining the ESI, these two factors were weighted the same. Weighting these two or any other factors differently may lead to an alternate conclusion as to the sustainability of the country. A better index might be one that is not so subjective and is instead based on scientifically rigorous calculations.

Thermodynamic assessments provide such scientific rigor. The fundamental laws of thermodynamics provide means to quantify mass and energy transfer in processes. While mass conservation and the first law of thermodynamics track mass and energy exchanges, the second law of thermodynamics can be used to assess how well energy is being used. Thus thermodynamics can directly be used to quantify materials required and produced by a process, energy required by the process, and how well the energy is used by the process. This information can then be used as an indicator to compare different technologies. While a thermodynamic analysis does not necessarily produce an index, one could use a thermodynamic analysis to compare necessary inputs to a process, including materials and energy, as well as the products of the process. Some thermodynamic quantities, such as exergy consumption, can even be used as a single index. Thermodynamic indicators generally have two main parameters that differentiate them. The first parameter is what thermodynamic quantity the indicator is tracking. Some indicators track mass flow, while others track energy flow, and still others track exergy or emergy flow. The second parameter is the scale the analysis will include. The scale of the indicators is linked to the design goals. In past times of relatively inexpensive energy, initial cost of manufacturing and installation was generally more significant than operating costs [5]. As a result, design decisions were based on manufacturing and installation. However, higher energy prices and the prevalence of more active work-consuming devices shifted the design emphasis towards operating costs.

Indicators generated to assess products will vary in the scope of their assessment as design goals vary. Some indicators focus on certain portions of the life-cycle of a product, such as the operations phase. Others look at the broader picture and evaluate more of the life-cycle of a product. What is considered the life-cycle of a product is somewhat arbitrary. The cradle-to-grave cycle, which includes raw material extraction, manufacturing, operation, disposal, and all necessary transportation, is usually considered a complete life-cycle [10]. These phases are usually considered the most influential and will be the parts of a life-cycle for the purposes of this paper.

Hau [41] provides an extensive review of recently proposed and utilized thermodynamically based metrics. Some of the more influential metrics are the following:

1. Mass Based Metrics
2. Energy Analyses
3. Life-Cycle Exergy Analysis (LCEA)
4. Life-Cycle Assessment (LCA)
5. Exergetic Life-Cycle Assessment (ELCA)
6. Emergy Analysis

The goal of this section, set forth in section 2.3.1, was to begin with all indicators and refine their classification until only those pertinent to data centers remained (see figure 2.1). The six thermodynamic indicator types are those that will be analyzed in their relevance to data centers.

2.3.2 Specific Thermodynamic Indicators

Material Input per Service Unit (MIPS) exemplifies mass based metrics [45, 44]. It quantifies the material necessary to produce a unit of service. In the context of information technology, MIPS can be used to analyze a server. In the point of view of the MIPS indicator, the data transferred (and not the server itself) is the service being provided. The total material required over the life-cycle of the server normalized by the data transferred would be the MIPS for the server. The advantage of the MIPS metric as well as other mass based metrics is that because only material or mass is tracked over the life of a product, it may be easier to calculate than other proposed metrics. However, this is also the disadvantage of the MIPS method. Since only mass is tracked, mass based metrics do not give a complete assessment of the process. They sacrifice a more thorough model for ease of generating the indicator and are not as complete as those discussed below.

Energy analyses provide a more thorough picture of a system by tracking not only material flows in a process, but also energy flows [32]. These types of analyses can vary in the scope of the life-cycle they evaluate. Even a life-cycle energy analysis has its drawbacks. Energy analyses use mass and energy conservation but do not make use of the second law of thermodynamics. Therefore, there is no distinction made between energy of different forms. A life-cycle exergy analysis (LCEA), which tracks lifetime exergy consumption, does use the second law of thermodynamics and rates energy based on its "quality" [41].

Exergy is defined as the maximum work retrievable when a system is brought into thermodynamic equilibrium with its surroundings [68]. Exergy measures a system's ability to do useful work. The advantage of exergy analyses is that since the quantity being compared is the ability to do useful work, different material and energy flows of varying quality can all be compared in a scientifically rigorous manner. An example might be two processes, A and B, each that use 100 kJ of energy. However, process A involves a heat engine that uses 100 kJ of heat or thermal energy, and process B involves an electric motor which uses 100

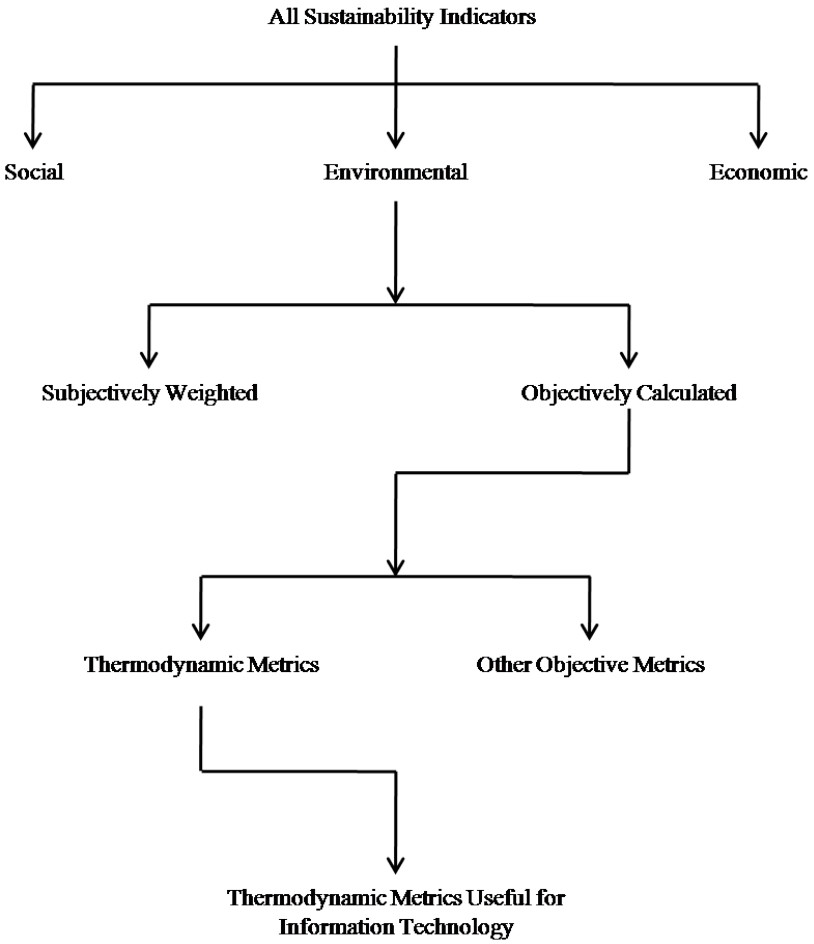

Figure 2.1: Classification of sustainability indicators.

kJ of electricity. Since heat and electricity are of different qualities, they cannot be directly compared. This is because electricity is of a high quality, and essentially all of the electricity can be converted into useful work. However, a heat engine is limited in its ability to convert thermal energy to work with the upper limit being the reversible Carnot engine. A Carnot engine analysis dictates that the amount of thermal energy converted to useful work is limited by the temperature at which heat transfer takes place. The main advantage of an LCEA metric is that exergy provides an equal comparison for different forms of material and energy, thus allowing for comparison between the heat use of process A and the electricity use of process B. By examining the life-cycle of a process, a complete appraisal is provided. The disadvantage of an LCEA metric is that it does not provide a complete picture of the environmental impacts of a process. For example, an LCEA might find that some hypothetical process C consumes 10 MJ of exergy. This evaluation is incomplete. There is no accounting for how this affects the environment. Was rainwater acidified or a species made

extinct in the consumption of this 10 MJ of exergy?

Life-Cycle Assessment (LCA) was defined by the International Organization for Standardization's (ISO) 14040 series [50]. LCA is not a metric by itself, but instead provides a framework for metrics to estimate environmental effects due to existence of a product or process over its life-cycle [10]. This is done by systematically tracking all inputs and outputs of a product or service over its lifetime. Since LCA is only a framework for how the inputs and outputs should be tracked, there are many different variations, but the variations often focus on emissions [41]. The advantage of an LCA analysis is that depending on how it is done, it can give a very complete analysis of how a process affects the environment. It can account for mass and energy inputs into a process, as well as mass products of a process. While an LCA analysis is very complete in its description of environmental effects, there are several disadvantages. First, in general, an LCA analysis does not lead to a single quantity that can be used to compare different processes. For instance, if two hypothetical processes A and B were analyzed, an LCA would find that process A produces sulfuric acid while process B produces mercury as pollutants. Directly comparing these emissions is difficult, and an LCA uses databases of standardized impact factors to compare aggregate effects from different processes. But comparing across different impact categories - for example, ecotoxicity versus global warming potential - is still difficult, and users must often rely upon subjective interpretations of different impacts to evaluate competing trade-offs in different processes. Second, the accurate assessment of how a process affects the environment achieved by an LCA is accomplished at the cost of being time consuming and expensive to produce. An LCA requires the scope of the problem to be defined and extensive libraries to be assembled. SimaPro [3] and GaBi Software [79] are two commercial LCA software packages available, but even using such software packages, an LCA analysis is more difficult to obtain than other metrics.

Attempts have been made to combine LCA with exergy in the ELCA [9, 14]. When this is done, the rigor of an LCA is achieved, but resource depletion and pollution are accounted for through exergy values. The result is a single metric available for comparison (exergy). This method has the advantages of both the LCA and LCEA, but still requires more effort to generate than an LCEA. Also, like an LCEA, a disadvantage is that the evaluation is incomplete. The examples of rainwater acidification and species extinction presented for an LCEA would work equally as well for an ELCA.

The last thermodynamic metric of interest is emergy. Emergy, a quantity defined by Odum [72], "is the available energy of one kind previously used up directly and indirectly to make a service or product," where available energy is defined by Odum as "potential energy capable of doing work and being degraded in the process (exergy)." Odum indicates that emergy quantifies the work of nature as well as humans in production of a product or service. As discussed earlier, different forms of energy are not equivalent in their ability to do work, which motivated the use of exergy. In an attempt to make energy comparisons more convenient, Odum expresses given energy inputs in equivalent amounts of solar energy that would be required to generate the input. The idea is that nearly all of the energy available on Earth comes from the sun (with small contributions from tidal and deep Earth energy).

Emergy is similar to an LCEA, as described earlier, with the difference that the life-cycle has been extended. In a cradle-to-grave LCEA, the normal starting point is the raw material extraction. However, with this starting point, the exergy necessary for nature to produce the raw material is neglected. Emergy has the advantage that it provides a more complete picture over the entire life-cycle of a product or service, including the portion of the life-cycle where nature provides the necessary inputs. This is also a disadvantage of emergy analyses. Like an LCA analysis, the more complete analysis provided by emergy is more time consuming and difficult to attain than an LCEA. This is so because the amount of emergy involved with a raw material is path dependent while in an exergy analysis, path is independent. For example, in an exergy analysis, a block of wood has some exergetic value irrespective of how the block of wood came to be. In an emergy analysis, the block of wood could have different emergy values if it were grown naturally in a forest or if it was grown in a tree farm. In the latter case, the available energy involved with planting the tree, fertilizing and watering the tree, and other farming energy expenditures would have to be accounted for, complicating the analysis. There are also other criticisms of emergy analysis, many of which are detailed in [42]. Many of these criticisms deal with other emergy principles, such as how emergy measures economic value and how emergy dictates the organization of a system (the maximum empower principle). While these are often criticisms of emergy, they do not directly relate to environmental sustainability, and will not be further discussed here.

2.3.3 Application to Data Centers

Thermodynamic Indicators to Evaluate Data Centers

Table 2.1 provides a summary of the different types of environmental, thermodynamically based sustainability metrics commonly used and their respective advantages and disadvantages. The task still remains to investigate how these indicators would quantify the sustainability of data centers.

Mass based indices would not be the best type of metric for information technologies, as they track mass only. While it is useful to know the materials that go into and are produced by information technologies, a mass based index alone is not preferred, in that it neglects energy resource considerations, a very important aspect of information technology.

An energy analysis of information technologies is favored if the analysis is over the life-cycle of the information technology, as this captures many important energy inputs that would otherwise be neglected. In addition, energy analyses that compare exergy (LCEA), rather than simply energy, are better because different forms of energy have different abilities to do useful work. Comparing the exergy required to produce, operate, and dispose of information technologies generates a more useful metric because many different technologies can be compared. Exergy analyses have been found to be a useful indicator of operational optimality for various types of information technologies [98, 99].

An LCA analysis provides a more complete analysis of the environmental consequences of an information technology than an LCEA. It tracks all inputs and outputs required to

Table 2.1: Thermodynamic metric advantages and disadvantages.

Indicator Type	**Advantage**	**Disadvantage**
Mass Based	Relative ease of computation.	Lacks full description.
Energy Analysis	Includes mass and energy accounting through mass conservation and 1^{st} law of thermodynamics.	Cannot compare different forms of energy, does not directly track pollution, resource depletion.
LCEA	Those of energy analyses but also can compare different forms of energy, easier to derive than LCA, arrives at single index.	Involves more effort to compute than mass based metrics, does not directly track environmental impacts.
LCA	Very complete picture of environmental effect.	Difficult to compute, no single index for comparison of different products or processes.
ELCA	Complete picture, single metric.	Difficult to compute and does not directly track environmental impacts.
Emergy	Expansion of life-cycle incorporates ecological inputs to analysis.	Difficult and time consuming to compute (path dependent on history of exergy input).

make, operate, and dispose of the information technology. Emissions and pollutants, as well as natural resource depletion involved with a given information technology, can be evaluated. This cannot be done with an LCEA. However, a list of depleted resources and pollutants is not easily comparable for different information technologies. Moreover, because a large fraction of the environmental impacts of information technologies stem from the direct or indirect consumption of material or energy resources across the system life-cycle - which are adequately captured by an LCEA analysis - information technology choices based on LCEA often agree with the technology choices based on other impact assessment methods of an LCA. In addition, because of the cumbersome nature of an LCA analysis, it has been argued that an LCA analysis is useful for evaluating already proposed or existing systems, but an LCEA is much more useful in designing a sustainable product or process [32].

Finally, emergy analyses are comparable to LCEA but are perhaps more useful in that they capture the natural or ecological inputs to a product or service. However, like an LCA analysis, an emergy analysis is more burdensome to generate than a life-cycle energy analysis. Databases of emergy values are not easy to produce or readily assessable and depend on the

path taken to reach a state, so are not retrospectively deterministic.

For these reasons, it can be argued that an LCEA, which tracks lifetime exergy consumption, provides the best compromise among the different thermodynamic metrics for designing sustainable information technologies. It is important to note that an LCEA is a sustainability metric that meets the standards outlined by SCOPE for good indicators. An LCEA is modular in nature since the components of the life-cycle can be updated as new information becomes available or is deemed important. An LCEA also strikes a balance between ease of generation and scope of what it models. If more details are required, an LCA or an ELCA can be performed. Finally, an LCEA provides the total exergy consumed in generating a good or service, thus providing a single, scientifically rigorous, comparable metric.

Application: LCEA of Computer Servers in Data Center

An LCEA model generated by Hannemann et al. [40] will be used to exemplify a life-cycle exergy analysis for a data center server. Specifically, a 2U-rack-mounted server with two Intel Pentium III 1.0 GHz processors, one 36 GB SCSI hard disk drive, one CD-ROM drive, and one floppy disk drive, in addition to other necessary components, will be analyzed. The model examines the exergy for extracting and processing raw materials, manufacturing and assembling components, operating the server (including cooling), recycling and disposing of the server, and transporting the server and its components throughout.

Database Needs

In order to generate this model, databases are needed to provide the following information:

1. Mass of elements that make up different components
2. Exergy consumption to extract and process raw materials
3. Exergy consumption for different manufacturing processes
4. Operational parameters of technology of interest - max device power, average device load, cooling requirements, operational duration, uptime, etc.
5. Locations of raw material extraction, assembly, distribution, operation, and disposal as well as mode of transportation
6. Exergy consumption for different modes of transportation
7. Exergy consumption for recycling and disposal of different technologies

Hannemann et al. [40] devised methods to estimate these as well as server specific quantities for a 2U-rack-mounted server based data center. The base values for the analysis that follows are provided in table 2.2.

Table 2.2: Input variables representative of 2U-rack-mounted server.

Input Parameter	**Input Value**
Assembly Location	Taipei, Taiwan
Transportation Mode	Ship
Distribution Location	San Francisco, USA
Transportation Mode	Truck
Operation Location	New York, USA
Max Device Power (kW)	0.265
Average Device Load (%)	50
Operation Duration (years)	3
Estimated Uptime (%)	95
Cooling Scales with Load	Yes
Maximum Cooling Load	0.265

Results of Server Analysis

Figure 2.2 shows the exergy consumption in the five different stages of the life-cycle for typical data center parameters. In a data center, it is of interest to know the exergy consumption required to cool the servers, as it is a large portion of the operational exergy consumption. Consequently, this part of the operational exergy consumption is plotted separately.

Varying the design parameters changes the exergy consumed in the life-cycle of a server based data center. If an LCA analysis were done, it would be more difficult and take more time to vary the design parameters and complete a new analysis. However, an LCEA can be done quickly, letting a designer change many parameters to immediately find a design that minimizes exergy destruction. For example, the second set of data in figure 2.2 depicts the exergy destruction for the same server as described in table 2.2, except the operational duration has been changed to one year and the average device load has been changed to 25 %.

Theoretically, the decreased operational duration might be necessary if server technology accelerates at such a fast pace that servers need to be replaced every year. The average device load reduction might take place if it is found that many servers are needed during peak use certain times of the day, but at other times some servers may be powered down due to reduced use.

There are a multitude of variations that a designer may wish to analyze, and the LCEA provides a tool that is easy to use and is fairly complete in its analysis. A breakdown of where exergy is consumed in the life-cycle is provided, so a designer can focus attention to areas of largest exergy consumption. Once a design is decided upon based on minimization of life-cycle exergy consumption, an LCA can be done to analyze other environmental ramifications.

Once an LCEA model is built, all that is necessary to analyze different information technologies is a respective database of the components. For instance, all that would be

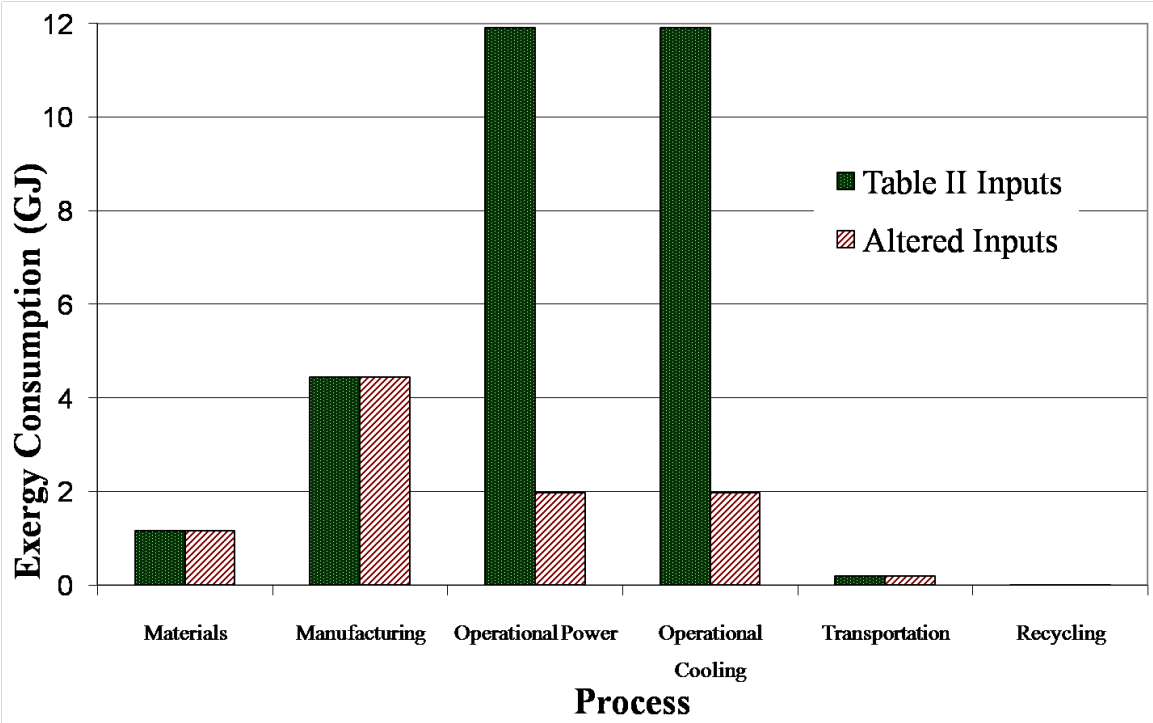

Figure 2.2: LCEA for server with properties described in table 2.2 as well as server with operational duration and average device load alterations.

required to extend the server model of Hannemann et al. [40] to do a LCEA of a laptop or smart phone would be the information described in the database needs of this report. Other minor adjustments to the model might be required, such as updating the cooling requirements, but these changes can be done with ease due to the modular nature of the LCEA analysis.

Chapter 3

Literature Review of Data Center Velocity and Temperature Prediction

Data center thermal management has been an area of intense research for over a decade. Over that time, there has been much work devoted to predicting velocity and, more importantly, temperature fields in data centers. Several comprehensive literature reviews have been performed. This author finds the review by Joshi and Kumar [115] to be thorough and complete. In the review by Joshi and Kumar, they note two other expansive reviews on data center thermal management: one is by Schmidt and Shaukatullah [94], and the other is by Rambo and Joshi [81]. The interested reader is directed to any of these three lengthly literature reviews for a more thorough literature review, the sum of which is on the same order in length as this entire thesis. The Joshi and Kumar review is summarized and augmented in this chapter.

3.1 Computational Fluid Dynamics: Solving full Navier Stokes and Energy Equations

As was discussed in chapter 1, the most historically prevalent method of cooling data centers has been through the use of an under-floor cold air supply with warm air ceiling return. One might assume this would be an efficient method of cooling, since warm air is less dense than relatively cooler air and naturally rises. It would seem logical to thus put the return vents on the ceiling and the cold air supply on the floor.

This under-floor plenum strategy has some inherent problems. One of the major problems that arises is ensuring that each floor tile achieves the target airflow through it that is desired. Much numerical work, especially the earlier numerical models in data centers, dealt with this problem [54, 55, 57, 95, 56, 73]. These studies examined variables such as under-floor plenum height, open area of perforated floor tiles, under-floor obstacles, and plenum partitions and their effects on airflow distribution through floor tiles.

Under-floor plenum numerical studies were just the beginning of data center numerical

analysis. Another area of numerical study was choosing operational parameters and data center layouts. These studies sought to find the optimal data center dimensions, rack layout, CRAC placement, cold air supply temperature and flow rate, etc. One of the first of such studies was performed by Schmidt [89]. Schmidt performed CFD studies examining hot aisle and cold aisle arrangement in data centers. One of his key findings was that in data centers recirculation can be caused by lower racks drawing in cold air from the supply floor tiles. Recirculation is when warm air that has already passed through servers recirculates around the rack and flows to the cold aisle in a data center. This can lead to hot air at the inlets to servers, the exact opposite of what is desired. Schmidt and Cruz performed other CFD studies analyzing different design scenarios, such as introducing cold air in hot aisles in an attempt to combat recirculation [90], mixing high and low power racks [91], and removing adjacent racks [92]. A logical thought, if concerned about recirculation, is to create physical barriers which prevent mixing of cold and hot aisle air. Gondipalli et al. [30, 31]. performed numerical case studies of containment using doors and roofs, with and without slits.

Patel et. al [75] investigated using CFD to examine changes caused by different data center layouts and CRAC cooling levels. They used their CFD work to find guidelines for data center design. They showed in some cases they could achieve 35% energy savings by choosing optimal CRAC settings.

Another logical questions in data center design is where is the optimal placement of supply and return vents. While it seems logical to have an under-floor cold air supply plenum and ceiling return vent, numerous CFD studies have sought to quantify the optimality of this setup [69, 71, 74, 101, 43, 93, 80, 83]. Different scenarios investigated include under-floor supply and overhead return, overhead supply and horizontal return, overhead supply and under-floor return, and finally overhead supply and horizontal return. The general consensus in these CFD studies is that the under-floor supply and overhead return minimizes mean and max rack inlet temperatures, and is the optimal supply and return setup. It was also shown that the worst setup, with the highest mean and max server inlet temperatures, is generally the overhead supply and under-floor return.

It is also important to note that the majority of numerical analysis of data centers is done at steady state. It is assumed that the server heat load is constant, that the cold supply air is kept at the same temperature and flow rate, and that there are no equipment failures. In reality, data centers are transient. Amongst other transient events, server loads vary over time, CRAC units fail, or inlet tiles have changes in flow rate or temperature to match server loads. There has been numerical work on the transient nature of data center operation [104]. Other transient CFD modeling looked at CRAC failure and the transient response [11] as well as varying server heat loads [48].

3.2 Reduced Order Models

Others have been working to make reduced order models as well. They have the same goal as the fast prediction methods of this work - to acquire relatively accurate temperature

field predictions at faster than conventional CFD speeds. Karki and Patankar created a one-dimensional computational model instead of using full CFD [58]. Their model generated decent predictions in certain flow regimes. Rambo and Joshi [82], and Rambo [85], solved RANS turbulence problems using proper orthogonal decomposition. The authors predicted reduced model size by a factor of 10^4 with errors as low as 5%. Shrivastava et al. created a software package to estimate cooling of groups of racks placed together in a cold aisle [102, 103]. Their tool produced temperature field solutions in 10-30 seconds.

There are also other researchers concurrently attempting to use potential flow theory to arrive at reduced order models. Lopez and Hamman use a physical model, based on potential flow theory, combined with real-time sensor data [66]. Due to the reduced complexity, they developed a model "suitable for operational and real-time usage". They conclude, as does this work, that "although the model is simpler than those based on the use of the Navier-Stokes equations for fluid flow, numerical experiments suggest that it can nevertheless provide useful information for use in data center energy management." Hamman went on to further explore using this model to ascertain optimal CRAC settings in a data center [38]. VanGilder and Shrivastava also developed a tool that is loosely based on potential flow theory [114]. They argue that in the bulk of most flow cases, the majority of the velocity field in a data center can be modeled by potential flow. In order to make this simplification, they must ignore buoyancy forces. With these forces ignored, the governing equations reduce to the potential flow equations and ultimately to the Laplacian of a potential function. These linear equations indicate that solutions can be superposed. VanGilder and Shrivastava use this thought process to compute thousands of flow scenarios. They then develop an algorithm to combine these flow scenarios to generate any flow scenario of interest through superposition.

All of the potential flow theories do not deal with buoyancy considerations. As was found in [110], buoyancy can play an important role in data center flow patterns, and this thesis details corrections to conventional potential flow theory to account for these forces.

3.3 Data Center Experimental Setups

Velocity and temperature fields in a data center are complex. Historically, researches have conducted many experiments both in an attempt to gain knowledge about data centers and to validate their numerical studies. Boucher [13] focused on controlling cooling equipment and analyzing different cooling equipment settings and their effects on server inlet temperature. In particular, CRAC temperature, fan speed, and vent tile openings were varied. It was concluded that since inlet temperatures varied linearly with CRAC supply temperature, that buoyancy was not important, at least for the operating conditions they studied. However, other experimental work has shown that buoyancy can be an important factor in data center operation [110, 47]. Another experimental study focused on comparing under floor plenum CFD simulations to experimental results [96]. The CFD analysis compared decently in trends with the experimental results, but there were sometimes large deviations in flow rates through tiles. Samadiani [87] used CFD to predict flow rates in an underfloor plenum to

investigate under-floor obstructions and tile openness and their effects on CRAC flow rates and distribution. The predictions were compared with experiments conducted by Rambo et al. [84] and were found to have average errors of approximately 10-13%.

Iyengar [51] performed an experiment in a small data center, consisting of one rack and one CRAC unit. In this study, the average absolute error between the CFD predictions and absolute error was found to be 3 K. Iyengar claimed that the dominant form of error was the $k-\epsilon$ method and a simplistic modeling of the rack since exhaust airflow was considered uniform. It was argued that both of these modeling limitations hinder mixing in the numerical model and lead to more extreme hot and cold spots than occur in reality. This brings up an important point: when performing a numerical model of airflow in a data center, one will have to choose a turbulence model. Cruz compared CFD results generated with seven different turbulence models and three different experimental data center layouts in two separate studies [17, 18] . Cruz found that the zero equation (or mixing length model) and the Spalart-Allmaras turbulence models had the smallest error when compared to experiments. The zero equation model required one-fifth the computational effort as the Spalart-Allmaras turbulence model. The laminar flow model was twice as fast the zero equation model and had similar errors to the six $k-\epsilon$ turbulence models investigated.

Perhaps the most methodical comparison of CFD to experiments can be found in [74]. In this work, unlike the others mentioned so far, a "controlled data center" was constructed to avoid experimental errors that plague many of the other studies. For example, the servers were simulated by heaters that had specific heat loads. Fan speeds on the simulated servers were set to a know constant and did not change. In other studies, including the one performed in this thesis, this luxury was not possible. Dynamic data centers are approximated as quasi-steady state and modeled as steady. This data center experiment actually was steady. A $k-\epsilon$ turbulence model was used, and the average error in temperature prediction was found to be between 7-17%, depending on the height of the experimental measurement. In the study, error was defined as follows:

$$Error = \frac{|(T_{sim} - T_{c,in}) - (T_{exp} - T_{c,in})|}{T_{exp} - T_{c,in}} \tag{3.1}$$

In this equation, T_{sim} is the temperature predicted by the numerical simulation at a point, T_{exp} is the experimentally determined temperature at the same point, and $T_{c,in}$ is the temperature of the cold inlet air.

Chapter 4

Sustainability Modeling Methodology

Two different sustainability analyses were performed in this thesis. The first analysis was a LCA. This was performed to be a point of comparison for the second analysis, a LCEA. The LCEA of a data center is one of the primary objectives of this thesis. The LCA, however, is more widely known and practiced and for this reason the LCEA results will be compared to the LCA results. Also, it was argued in subsection 2.3.2 that the results of an LCA and LCEA often agree. This claim will be quantified.

4.1 Life-Cycle Assessment (LCA)

A full blown LCA would take a very long time to generate and could be a thesis of its own. Instead of a full blown LCA, an LCA is carried out that deals only with the global warming potential of data centers. The questions which this study seeks to answer are what is the global warming potential of a traditional data center, how does this footprint differ for different data center configurations, and what are the best ways of reducing these impacts. In addition, the different legs of the life-cycle will be compared to see if the operational leg dominates over the other life-cycle stages as is often implicitly assumed. As has been discussed in the introduction, data centers can vary by size and configuration. It is therefore important to normalize both spatially and temporally. Spatial normalization refers to the fact that data centers can be of different sizes. Without normalization, it does not require much analysis to deduce the environmental impacts of a 100 MW data center are more than those of a 1 MW data center. The functional unit chosen for normalization spatially is the number of gigabytes (GB) available for data storage in the data center. A temporal normalization is also required because the different components identified as being present in all data centers have different lifetimes. Comparisons of the global warming potential of different equipment within the data center would not be fair without a temporal normalization. For example, the IT equipment in a data center may be used for 3 years without major maintenance or replacement, while the CRAC unit and chiller may be used for 10 years without major maintenance or replacement, and the building shell may last for 50 years without major

maintenance or replacement. The environmental footprint of a data center will thus be normalized by the lifetime of the respective equipment as well as the GB of storage of the data center.

Information for all components of a data center is not readily available. This study will focus on the following data center equipment for which information was available: building shell, servers, room level PDU, UPS, CRAC unit, and chiller. This equipment constitutes the bulk of what makes up data centers and represents all five groups identified as being present in all data center configurations.

A hybrid LCA is used to find the global warming potential for a typical data center. When performing an LCA, there are several different techniques, usually categorized into two main categories: process based and economic input-output LCA (EIO-LCA) [49]. A process based LCA is one that utilizes databases of information to ascertain process inputs and outputs through the supply chain. An EIO-LCA uses economic data from the product or process being investigated along with different sectors of the economy, in combination with the environmental consequences of different sectors of the economy, to generate an estimate of the environmental ramifications of a product or process. The EIO-LCA method takes economic value for a sector of the economy as an input and outputs different environmental information based on the economic activity in that sector. The EIO-LCA method is useful for well defined, homogeneous sectors of the economy, such as printed circuit assembly manufacturing, but less useful for non-homogeneous sectors of the economy, such as non-ferrous metal rolling, drawing, extruding, and alloying. In some cases in this study, the economic values could be found for the different data center components and the economic sector was acceptable, so the EIO-LCA tool [49] was used. This was the case for the resource extraction and manufacturing leg of the life-cycle for the server, CRAC unit, chiller, PDU, and UPS. For the other life-cycle stages, as well as the building shell, the process-based LCA method was used. Process-based data came from other LCA literature, such as Junnila and Horvath's paper on the environmental effects of an office building [52].

A hybrid method was used to minimize both the aggregate errors of the EIO-LCA method as well as truncation errors of the process based method. Aggregate error is error introduced because an entire sector of the economy is being reduced to one average. Within the sector, there are likely differences that get blurred. For example, if one is looking at the electricity generation sector of the economy, there is an average emissions factor per kWh (or $) for the entire country. However, the emissions per kWh in California are significantly different from the average of the United States. This error is an example of aggregate error. Truncation error is error due to the boundary of the problem being studied being truncated. Examining a supply chain can help to illustrate this point. When trying to ascertain the emissions of making a computer server, one would start by looking at the company that made the server. This company, however, buys parts from other vendors, has workers that drive to work and eat every day, and is housed in a building that has emissions of its own, etc. The list of emissions associated with the supply chain of this server is extensive. Often, the boundary of analysis is chosen to simplify the analysis and make the problem tractable. Error is introduced by narrowing the boundary of the problem, and this is called truncation

error. The EIO-LCA method cleverly avoids truncation error at the expense of introducing aggregate error. A hybrid method seeks to minimize both errors, hopefully resulting in an LCA with the least possible error [106].

Subsection 4.1.1 is an overview of how the life-cycle global warming potential of a typical data center was modeled, followed by a subsection with specific information on the calculations performed for each piece of equipment and how the equipment was put together to form a data center.

4.1.1 Overview

In this overview, the strategies behind the calculations in the four life-cycle stages studied are described. These four life-cycle stages were applied to the six pieces of equipment studied, and then a fictitious but realistic data center was created using combinations of the six pieces of equipment. When discussing the four life-cycle stages, what is being addressed in each life-cycle leg is only the activity of a particular piece of equipment in that leg. A simple example helps to illustrate this point. In the resource extraction and manufacturing life-cycle leg for a server, different materials and components had to be transported to make a server. In addition, the equipment used to make the server has a useful life and there are global warming ramifications associated with their disposal. However, in the context of this report, the global warming potential of transporting around the raw materials used to make the server and disposing of the equipment used to make the server will be counted in the resource extraction and processing life-cycle leg. The transportation life-cycle leg refers only to global warming potential of the emissions used to transport the finished server throughout its life. Similarly, the end-of-life leg refers specifically to the emissions resulting from the end-of-life treatment of the server. This thought process holds for all six data center equipment analyzed.

Resource Extraction and Manufacturing

The resource extraction and manufacturing portion of the life-cycle refers to all activities that were necessary to make the piece of equipment of interest. When possible, as was the case for the CRAC unit and chiller, mass breakdown data for equipment was obtained. Economic values were found for the different masses in the breakdown and using this information economic values were determined for different materials that made up the equipment. For example, knowing the mass of steel and aluminum in a CRAC unit, and also knowing the price of manufactured steel and aluminum per kg, the price of these materials in a CRAC unit were calculated. Using the price of the materials, the EIO-LCA tool was used to find the global warming potential of the supply chain in making the respective piece of equipment. The method of finding the mass breakdown, then the value of the masses in the breakdown, and then using the EIO-LCA tool, was done in an attempt to avoid error that would result from using non-homogeneous economic sectors in the EIO-LCA tool. It is important to note that it was assumed the assembly of different materials was negligible compared to

the resource extraction and manufacturing of the individual components. For example, in the case of the CRAC unit, the global warming potential was found for making steel and aluminum components, but not for putting that steel and aluminum together into a CRAC unit.

When it was not possible to obtain a mass breakdown of the individual pieces of equipment, as was the case for the server, PDU, and UPS, monetary values were assumed for the equipment and the EIO-LCA tool was used directly to estimate the global warming potential for that component. This likely led to some error, since the PDU and UPS were analyzed using economic sectors that are not unique to data center equipment. While not as accurate, this method of modeling was necessary since detailed mass breakdowns of these components could not be obtained. In the case of the building shell, the EIO-LCA tool was not directly used. Data from [52] was used to estimate the global warming potential of procuring the building materials as well as the actual construction of the building. Both of these activities were considered resource extraction and manufacturing to compare to other data center equipment.

Operation

The modeled global warming impacts of data center operation were limited to only the life-cycle emissions related to the electricity used by the data center. As a first order approximation, with the exception of the building shell, maintenance of the data center equipment was not modeled. The life-cycle data used for the building shell [52] did incorporate maintenance, and the global warming potential due to the maintenance was counted in the operational leg of the life-cycle for the building. The other traditional operational parameters associated with a building, such as HVAC, were not counted towards the building shell operational global warming potential since they had dedicated equipment and were analyzed separately. Other than electrical inputs and maintenance, the only other significant operational input to a data center is water into the cooling towers. Data could not be obtained for cooling towers and as a result they were omitted from this study. However, this is not a catastrophic omission, since not all data centers use cooling towers. It is possible to cool the working fluid of a refrigeration cycle with air and this is done in some circumstances. Future work could analyze the effect of the cooling tower as data becomes available. A more thorough description of the electricity calculations is given in the more detailed analysis descriptions below.

Transportation

Transportation modeling required estimating the distances data center components traveled, the mode of transportation over those distances, and the global warming potential of the different modes of transportation. Due to data availability as well as simplifying the study, the modes of transportation studied were limited to air, ship, rail, and truck. For all six of the data center components, except the building shell, it was assumed the components were

made in China and shipped via ship to southern California. From southern California the components were loaded on a train and sent to northern California. From the rail yard, the components were loaded on a truck and delivered to their final destination. As described above, the transportation section here refers only to the transportation of the finished data center component. As a result, the transportation for the building shell is zero since the building shell is not transported anywhere. There is, however, transportation required in the construction of the building shell. The global warming potential of this transportation is included in the raw material extraction and manufacturing life-cycle leg for the building shell. A more thorough description of the transportation calculations is given in the more detailed analysis descriptions below.

End-of-Life

To estimate the global warming potential of the end-of-life activities, data was used from the HP computer recycling facility in Roseville, California. This facility uses shredders, meshes, eddy current separators, and other equipment to dismantle and separate IT equipment. As a first approximation, it was assumed that all data center equipment except the building shell would be shipped to this building at the end of their life. Electricity estimates were provided for the facility, and the global warming potential calculated for the end-of-life came solely from the global warming potential of the electricity used by the plant. A more thorough description of the end-of-life calculations for all equipment except the building shell is given in the more detailed analysis descriptions below. The building shell end-of-life global warming potential came from [52].

4.1.2 Detailed Analysis

All six key data center components (server, CRAC unit, chiller, PDU, UPS, and building shell) were first modeled individually. Then key assumptions were made to put together a data center from the pieces. First, the fictitious data center was assumed to be located in northern California in 2002, as that is the most recent date that enough data exists. The main design point was that data center should be able to store 540 TB. The assumed power density of the data center was $25\frac{W}{ft^2}$. To find the number of servers, the 540 TB goal was divided by the storage capabilities of each server. The electricity needed to power that number of servers was found by multiplying the number of servers by the average power use of each server. It was then assumed that the cooling load was equal to the power needed by the servers. This assumption is accurate for well insulated data centers or data centers located in cool locations. The heat was removed from the data center room by CRAC units, and the number of CRAC units needed was found by dividing the total heat load by the average cooling load of each CRAC unit. The number of chillers needed was calculated by dividing the heat that had to be moved from the CRAC units to the outside air by the average cooling load of the chiller. The number of UPS and PDUs needed was found by dividing

Table 4.1: Summary of assumptions used to create a data center from data center components.

Assumption Category	**Assumed Value**
Year of data center	2002
Data center location	Northern California
Data center size [TB]	540
Power Density $[\frac{W}{m^2}]$	25

Table 4.2: Characteristics of HP Netserver LP 2000r.

Assumption Category	**Assumed Value**
Price (year 2002 $) [21, 1]	3000
Storage size (GB)	108 (3 hard drives, each 36 GB)
Average Power (W)	265
Uptime (%)	50
Lifetime (years)	3
Mass (kg)	16.7

their respective capacities by the electrical load of the servers. Table 4.1 summarizes the assumptions used to create a data center from the six important data center components.

Server

The server modeled was an HP Netserver LP 2000r. Table 4.2 lists important information about this server. The price was inferred from other servers of that time, and the storage size and power came from the servers manual. The uptime and lifetime were assumptions that are typical of servers. Note that uptime is the percentage of the time the server is running. This value is typically around 50% as not all of the servers are always being used.

The resource extraction and manufacturing global warming potential was found using the EIO-LCA tool, the price in table 4.2, and the electronic computer manufacturing sector. The operational global warming potential came from the electricity to run the server. To determine the electricity needed to run the server over its lifetime, the average power was multiplied by the uptime and the lifetime and converted to kWh. The global warming potential was found by multiplying the electricity used by the server with carbon dioxide equivalent emissions associated with that amount of electricity. For transportation, the mass of the server was multiplied by the appropriate emissions factor and distance traveled. For end-of-life, the mass of the server was multiplied by the electricity needed by the recycling facility per unit mass and then by the global warming potential of that electricity. For more information on the global warming potential of the electricity, transportation, and end-of-life, refer to their respective sections below.

Table 4.3: 30 ton maximum capacity Stulz CRAC unit values used in global warming potential model from [63].

Assumption Category	**Assumed Value**
Total Mass (kg)	1395
Aluminum Mass (kg)	145
Copper mass (kg)	175
Steel mass (kg)	1025
Plastic mass (kg)	50
Average cooling load (tons)	15
COP	3.5
Uptime (%)	95
Lifetime (years)	10

Table 4.4: Assumed economic values of materials in table 4.3.

Assumption Category	**Assumed Value**
Aluminum ($/lb) [19]]	1
Copper ($/lb) [19]	4
Steel ($/lb) [105]	0.4
Plastic ($/lb) [78]	0.7

CRAC Unit

The CRAC unit modeled was a 30 ton unit manufactured by Stulz Air Technology Systems, Inc. Information assumed about this unit is given in table 4.3. The resource extraction and manufacturing phase global warming potential was found by using the EIO-LCA tool. In order to use the tool, economic values per unit mass were assumed for the four materials in table 4.3. These values are given in table 4.4.

The economic values of the materials in the CRAC unit were found by multiplying the price per mass by the mass. These values were then used in the EIO-LCA tool to find the global warming potential associated with their manufacturing. The electricity used by the CRAC unit in its operation was found by dividing the cooling load by the COP. Note that the average cooling load for the CRAC unit is approximately 50% of the max load of the unit. This is done to make sure that enough cooling can be provided in case of failure of a CRAC unit. Should one unit fail, a neighboring unit can be turned up higher to its full cooling capacity in an attempt to compensate. The global warming potential associated with the electricity of operation, as well as the global warming potential of the transportation and end-of-life, were found in the same method as the server.

Table 4.5: 750 ton maximum capacity chiller values used in global warming potential model.

Assumption Category	Assumed Value
Total Mass (kg)	35000
Steel mass (kg)	35000
Average cooling load (tons)	375
COP	3.5
Uptime (%)	95
Lifetime (years)	10

Table 4.6: PDU values used in global warming potential model.

Assumption Category	Assumed Value
Economic value (year 2002 $) [2]	4500
Capacity [kVA]	40
Power factor	˜1
Efficiency (%)	95
Uptime (%)	100
Lifetime (years)	10
Total Mass (kg) [2] (%)	157

Chiller

The chiller was modeled in the same manner as the CRAC unit. It was assumed that the mass of the chiller was entirely steel. This assumption was made after discussing the material composition of chillers with data center operators familiar with chillers. Other assumed values for the chiller are given in table 4.5.

PDU

Table 4.6 summarizes the assumed values needed to analyze the PDU. The global warming potential of the resource extraction and manufacturing portion of the PDU life-cycle was modeled using the EIO-LCA model. The economic sector used was the electric power and specialty transformer manufacturing sector. While a PDU is a transformer, this sector was not ideal. However, it should provide an order of magnitude estimate of the global warming potential of the PDU. For operation, the electricity consumed by the PDU was assumed to be 5% of the electricity that went through the device. This electricity was converted to heat and never reached the server. The global warming potential associated with the electricity of operation, as well as the global warming potential of the transportation and end-of-life, were found in the same method as the server.

Table 4.7: UPS values used in global warming potential model.

Assumption Category	**Assumed Value**
Economic value (year 2002 $) [70]	13000
Capacity (kVA)	20
Power factor	˜1
Efficiency (%)	75
Uptime (%)	100
Lifetime (years)	10
Total Mass (kg) [70]	275

Table 4.8: Building shell values used in global warming potential model from [52].

Values category from [52]	**Value**
Floor Area of building in [52] (ft^2)	4400
Lifetime (years)	50
Materials and construction (Mg CO_2-e)	2400
Maintenance (Mg CO_2-e)	1300
End-of-life (Mg CO_2-e)	200

UPS

The analysis of the UPS was very similar to the PDU. Table 4.7 summarizes assumed values for the UPS. In the case of the UPS, for the resource extraction and manufacturing portion of the life-cycle, the storage battery manufacturing sector was used. This is not an ideal sector, as there are many different types and sizes of storage batteries, but it is a good enough sector to give an order of magnitude estimate. The efficiency of the UPS was chosen to be similar to efficiencies from [20].

Building Shell

Global warming potential for the building shell came from [52]. Important values are summarized in table 4.8. To parallel the rest of this study, the materials and construction category was labeled as resource extraction and manufacturing and the maintenance was labeled as operation. The other portions of a normal building operation, such as HVAC, were not counted in the operation phase since they were counted separately. In order to scale this study to the fictitious data center being studied, the global warming potentials were scaled based on floor area ratio of the buildings.

Table 4.9: Global warming potential of different methods of electricity generation as well as electricity mix of PG&E.

Method of Electricity Generation	**Life Cycle Global Warming Potential (ton CO_2-e/GWh) [67]**	**Percentage of California PG & E Electricity Mix (%) [77]**
Nuclear	17	23
Hydro	18	13
Biomass	46	4
Wind	14	2
Solar PV	39	0.1
Geothermal	15	4
Coal	1041	4
Natural Gas	622	47

Electricity Generation

The global warming potential of electricity generation in northern California was needed for nearly every piece of equipment in the data center. In order to come up with this estimate, the life-cycle global warming potential was used in conjunction with percentage of PG&Es electricity mix to find the average global warming potential of electricity from PG&E. The life-cycle global warming potential of different electricity methods, as well as PG&Es energy mix, are shown in table 4.9. The average life-cycle global warming potential as a result of electricity generation by PG&E was found to be 345 g CO_2-e/kWh.

Transportation

In order to estimate the global warming potential of transportation, emission factors were taken from [27] and [65]. The ship estimate emissions came from [65], which shows that ship emissions are roughly 60% of truck emissions. These emission factors provide the mass of CO_2-e produced per mile and metric ton of payload. All of the baseline values, shown in table 4.10, assume that 25% of the distance traveled consists of empty miles as the fleet repositions itself. In addition, the values in table 4.10 also assume that the vehicle used in transportation is only 75% full on average. Using the values in table 4.10, it was determined a product being shipped by the modes of transportation and distances listed in the transportation overview would emit 930 kg CO_2-e/ton of shipped product.

End-of-Life

The global warming potential estimate was based on the electricity use of the HP computer recycling facility in Roseville, California. Based on discussions with HP personnel, this facility recycles 3 million pounds of electronics each month. It was assumed the plant operates

Table 4.10: Emissions factors for different methods of transportation from [27] as well as assumed miles traveled by each mode.

Mode of Transportation	**Emission Factor (g CO_2/ton-mile)**	**Miles Traveled**
Truck	187 [27]	500
Rail	40 [27]	400
Ship	110 [65]	7500
Air	1358 [27]	0

8 hours per day, 30 days per month. Dividing the electricity used by the plant by the mass of electronics that pass through the plant each month, it was estimated that the plant uses 0.14 kWh per kg of content that passes through it.

4.2 Life-Cycle Exergy Assessment (LCEA)

It is useful to begin with first explaining more carefully what is meant by exergy consumption. As was previously stated, exergy is the ability to do useful work. The ability to do useful work occurs when there are gradients in physical properties such as temperature, velocity, chemical potential, or even position. Using temperature as an example, work can be generated using a heat engine with a temperature difference. However, the amount of heat moved is greater than the amount of work that can be generated due to entropy generated. This loss of the ability to due work is called exergy consumption. Similar arguments could be made with other gradients. Exergy consumption is so useful because it allows for comparison of different qualities of energy (e.g. electrical vs. heat) as well as mass. Since work can be extracted from a concentration gradient, high concentration ores (relative to the Earth's crust) have an exergy value relative to the Earth's crust. Removing these ores for manufacturing results in a loss of exergy from the environment. Another way of thinking of the exergy of an ore is the minimum amount of energy that would be needed to take the Earth's crust and concentrate whatever elements were in the ore to the concentrations they are present in the ore. Since both energy transfer processes and material removal from the environment have exergy loss, the losses associated from material and energy streams can be combined into one metric. This is a very useful result.

Following the same thought process as extracting ores, putting pollution into the environment would be a positive exergy transfer into the environment (negative exergy consumption). This is because the concentration of pollutants in a pollution stream is larger than that of the reference environment of the atmosphere, ocean, or Earth's crust. This means that the concentration or thermal gradients of pollution streams could be used to generate work. Once mixed into the reference environment and equilibrated, this positive exergy value would be lost, or, in other words, the exergy in the pollution stream would be consumed. It is not impossible to envision recycling pollution streams from a data center.

For example, waste heat from a data center, which is often dumped into the environment as thermal pollution, could be used to heat a greenhouse in a cold environment instead of being dumped into the ambient outdoor air. This was done at the University of Notre Dame [29]. Since pollution streams are almost never recycled in practice (especially in regards to emissions), and are often mixed and equilibrate with the environment, these negative exergy consumption values are ignored in this study unless otherwise noted.

For a more complete discussion of life-cycle exergy consumption, the interested reader is directed to entire volumes on the subject. The author finds the book by Szargut [107] and the Ph.D. thesis by Creyts [15] to be informative and thorough works on the subject.

An LCEA can be carried out in a similar fashion to the LCA in section 4.1. The methodology for the LCEA will be laid out in the same way that it was for the LCA. First there will be a general overview, followed by a more detailed explanation of the analysis for each component. The same six components will be modeled, since the same data was available for the LCA and LCEA. In addition to the six components, air in the data center will also be modeled to add the exergy consumed due to mixing to the total life-cycle exergy consumption. The details of this calculation can be found in chapter 5.

4.2.1 Overview

The LCEA examined the same four life-cycle stages as the LCA for the same six pieces of equipment. Just as in the LCA, when addressing any of the four life-cycle stages, what is being discussed is only the activity of a particular piece of equipment in that leg. The same example as in the LCA overview about transportation in the resource extraction and manufacturing leg applies.

Resource Extraction and Manufacturing

To calculate the exergy consumed in the resource extraction and processing portion of the life-cycle, tabulated data of mass specific exergy consumption values for different materials was used in combination with a detailed listing by mass of a piece of equipment. The mass specific exergy consumptions values for resource extraction and manufacturing were taken from [107] and [22], and are given in table 4.11. These exergy consumption values account for energy needed for mining, transporting, and refining. They also account for the exergy that was removed from the environment by removing relatively highly concentrated ores or materials relative to the Earth's diffuse crust.

The manufacturing exergy consumption accounts for the energy used by the manufacturing equipment as well as the exergy lost in the material waste streams in manufacturing. A 10 % waste stream is assumed for metals, and a 50 % waste stream is assumed for the plastics [15]. Mass specific exergy consumption values for machining processes, taken from [16] and [36] for metals and plastics, respectively, are summarized in table 4.12. Area and unit specific exergy values were also found and are included in table 4.12 for printed circuit boards (PCB), integrated circuits (IC), and processors. The manufacturing exergy consump-

Table 4.11: Mass specific exergy consumption values for material extraction and processing.

Material	**Value** $\frac{kJ}{kg}$
Aluminum [107]	341,500
Steel [107]	52,100
Plastic [107]	92,300
Copper [107]	67,000
Iron [107]	51,040
Glass [107]	33,400
Epoxy [39]	20,000
Ceramics [39]	20,000
Other [39]	20,000

Table 4.12: Mass specific exergy consumption values for manufacturing.

Material	**Specific Exergy**
Metal [16] $[(\frac{kJ}{kg})]$	0.28
Plastic [36] $[(\frac{kJ}{kg})]$	14.9
PCBs [39] $[(\frac{kJ}{m^2})]$	238,400
ICs [39] $[(\frac{kJ}{unit})]$	12,500
Processors [39] $[(\frac{kJ}{unit})]$	1,242,000

tion is added to the resource extraction and processing exergy consumption to get the total resource extraction and manufacturing exergy consumption.

Operation

Each piece of equipment was assumed to be in steady-state. For a steady flow system with mass crossing its boundaries, it can be shown that the exergy consumed or destroyed is given by the following formula [68].

$$\dot{X}_d = \sum_j (1 - \frac{T_0}{T_j})\dot{Q}_j - \dot{W}_{cv} + \sum_i \dot{m}_i \phi_i - \sum_e \dot{m}_e \phi_e \tag{4.1}$$

In equation 4.1, $\dot{X}_d$ is the rate of exergy consumption (often also referred to as exergy destruction which is why it is denoted with a "d" subscript), $\dot{Q}_j$ is the rate of heat transfer through the control volume at location j, $\dot{W}_{cv}$ is the total rate of work done by the control volume that crosses the control surface, and the $\dot{m}$ and ϕ terms are the mass transfer rate and specific exergy values for the mass crossing the control surface at the inlet and exit, respectively. Note that T_0 is the reference temperature of the environment to which the system is being compared, and T_j is the temperature of the control surface where the heat,

Table 4.13: Mass specific exergy consumption values for transportation from [108].

Mode of Transportation	Specific Exergy ($\frac{kJ}{kg-km}$)
Air	22.41
Truck	2.096
Rail	0.253
Ship	0.296

$\dot{Q}_j$, is transferred. Also note that the work is considered positive when going out of the control volume. The specific exergy values for mass crossing the control surface boundaries are also derived in [68] and are given below.

$$\phi = ((h - h_0) - T_0(s - s_0) + \frac{V^2}{2} + gz) \tag{4.2}$$

Note again that the subscript "0" denotes with respect to the reference environment. The variable h denotes specific enthalpy, s denotes specific entropy, V represents velocity, z is the height relative to a set reference, and g is the gravitational constant.

Transportation

For transportation, the exergy consumed is not only a function of mass but also distance and mode of transportation. Table 4.13 summarizes the exergy consumption for different modes of transportation. Again, to obtain the total exergy consumed in this portion of the life-cycle, the total mass of the CRAC unit is multiplied by the mass specific exergy value as well as the distance traveled for the correct mode of transportation. These values are the same as in the LCA and are summarized in table 4.10. Transportation mass specific exergy values are taken from [108].

For the distances and modes of transportation discussed in subsection 4.1.2, a product being shipped would destroy 5.4 $\frac{MJ}{kg}$.

End-of-Life

The final component of the life-cycle is the recycling portion. To obtain an order of magnitude estimate of the exergy consumed in recycling, Hannemann [40] estimated that the mass specific exergy consumption for recycling is $520\frac{kJ}{kg}$.

4.2.2 Detailed Analysis

As was the case in the LCA, the six key data center components (server, CRAC unit, chiller, PDU, UPS, and building shell) were first modeled individually. The same key assumptions were made to put together a data center from the pieces. See section 4.1.2 and table 4.1

Table 4.14: Material breakdown of 2U rack mounted server.

Input Parameter	**Input Value [39]**
Aluminum [kg]	3.25
Steel [kg]	12.38
Plastic [kg]	1.41
Copper [kg]	1.56
Iron [kg]	0.85
Glass [kg]	0.11
Epoxy [kg]	0.07
Ceramics [kg]	0.04
Other [kg]	1.23
PCBs [m^2]	0.20
ICs [Number of units]	171
Processors [Number of units]	2

for a description of the assumptions used to put a data center together from the six key components.

Server

The mass breakdown of a representative server was found by Hannemann [39], and is given in table 4.14. The resource extraction and manufacturing exergy consumption was found by multiplying the masses in table 4.14 both by their respective waste stream ratio (1.10 for metals, 1.50 for plastics), then by the mass specific exergy values in tables 4.11 and 4.12 and summing the result.

The operation portion of the server was found using equation 4.1. In this equation, it was assumed that that conduction and radiation heat transfer is negligible, eliminating the $\dot{Q}_j$ term. The convective energy transport is captured in the enthalpy portion of mass specific energy terms, ϕ_i and ϕ_e, multiplied by the mass flow rate through the server. Assuming that all of the electricity into the server is converted to heat, and that the heat is transferred to the air through convective energy transport, the convective energy transport is exactly equal to but opposite in sign to the $\dot{W}_{cv}$ term. Since the mass flow rate into and out of the server are equal, this allows the these terms to cancel out. It is further assumed that the velocity and height of the air entering and exiting the server remains unchanged. The only term left is the entropy generation term. Equation 4.1, describing the operational exergy consumption of the server, simplifies to

$$\dot{X}_d = \dot{m} T_0 (s_e - s_i). \tag{4.3}$$

Note that the mass flow rate into and out of the server are identical and are represented above simply as $\dot{m}$. Table 4.15 summarizes assumed quantities for variables in equation 4.3.

Table 4.15: Assumed server operational values.

Variable	Assumed Value
$\dot{m}$ [kg/s]	0.5
T_0 [K]	298
$(s_e - s_i)[\frac{kJ}{kg*K}]$	0.018

The entropy rise in the table assumes temperature increases through the server from 290 K to 300 K.

The transportation exergy consumption is found by multiplying the total mass of the server by 5.4 $\frac{MJ}{kg}$ found in the transportation overview. The end-of-life exergy consumption is found by multiplying the server mass by the $520\frac{kJ}{kg}$ described in the end-of-life overview.

CRAC unit

To model the resource extraction and processing exergy consumption for the CRAC unit, the mass specific exergy consumption values from [107] of interest for the CRAC unit are summarized in table 4.11. To calculate the resource extraction and processing portion of the life-cycle exergy consumption, the mass values from table 4.3 are multiplied by their respective mass specific exergy consumption values in table 4.11 and summed. To calculate the manufacturing portion of the life-cycle exergy consumption, the mass values from table 4.3 are multiplied by their respective mass specific exergy consumption values in table 4.12 and summed. Mass values for a CRAC unit are summarized with other important CRAC unit modeling parameters in table 4.16.

The operational exergy consumption for a CRAC unit is more complex and is computed by using equations 4.1 and 4.2. For this analysis, the CRAC unit system will be set up as given in figure 4.1.

Depending on how a control volume is set up, different terms in 4.1 can be internalized to avoid consideration. This is helpful if terms hard to measure or estimate can be eliminated. As can be seen in figure 4.1, the control volume has been cleverly chosen so that the heat transfer in the evaporator and condenser of the CRAC unit has been internalized. As a result, the heat transfer term in equation 4.1 has been eliminated, but the mass transfer terms for the warm air and chilled water must be considered. However, it is easier for a designer to input the mass flow rate, temperature, and pressure of the input and exit streams for the air and the water than to specify the temperature at which the heat is transfered in the condenser and evaporator.

With this control volume definition, equation 4.1 has been simplified to

$$\dot{X}_d = -\dot{W}_{cv} + \sum_i \dot{m}_i \phi_i - \sum_e \dot{m}_e \phi_e. \tag{4.4}$$

At this point it is useful to summarize what information would be available to a data

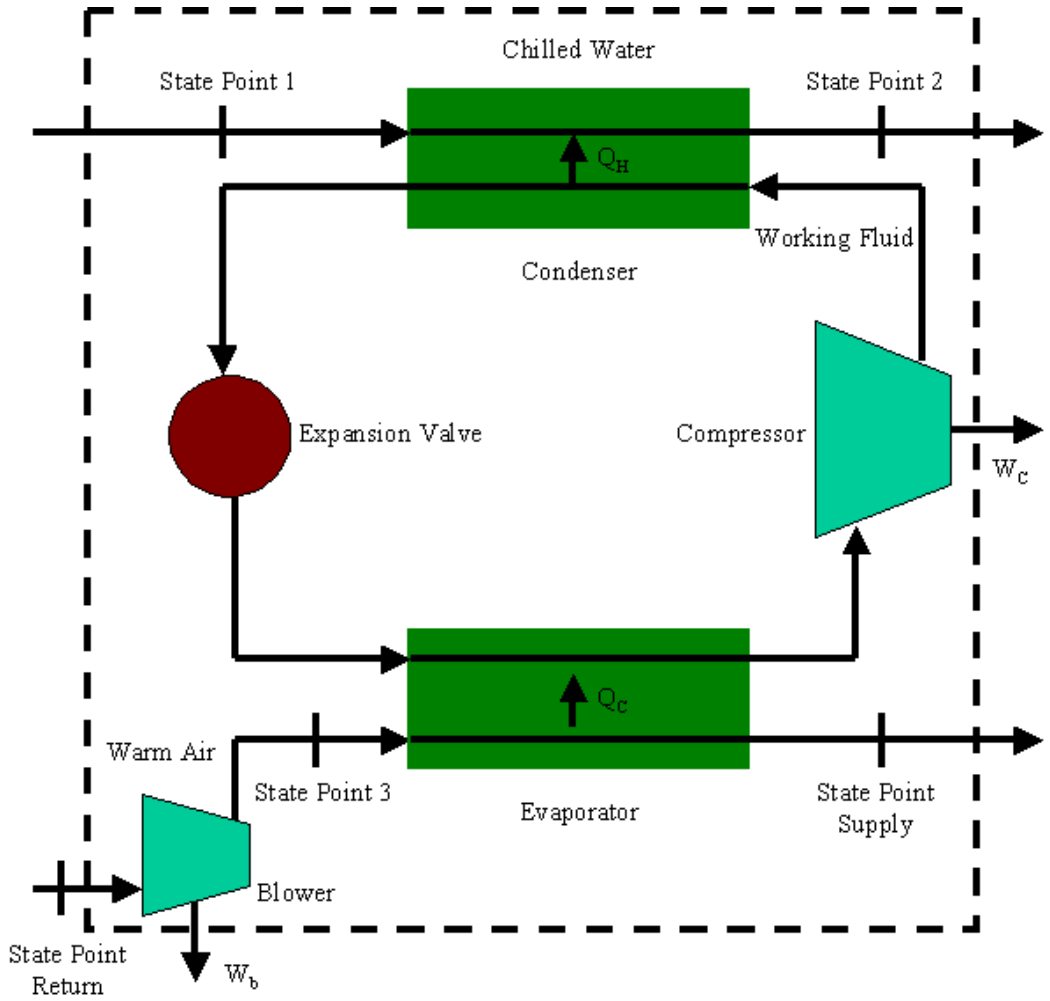

Figure 4.1: CRAC unit control volume definition.

center designer who would be analyzing this CRAC unit to find its life-cycle exergy consumption. A designer would know the following design parameters:

1. COP of the CRAC unit
2. Maximum cooling load capable by the CRAC unit, $\dot{Q}_c$
3. Temperatures of the return and supply air, T_{return} and T_{supply}
4. Pressure loss as the air travels through the CRAC unit, ΔP_b
5. Efficiency of the blowers used to provide the pressure increase for the air, η_b
6. Temperature difference of the chilled water across the condenser of the CRAC unit, ΔT_{water}

7. Inlet temperature of the cooling water, T_1.

Note that these design parameters being considered as known by the designer are somewhat arbitrary. For example, it will be shown shortly that the temperature difference of the chilled water across the condenser of the CRAC unit, combined with the input of the inlet temperature of the chilled water, will be the only information used to evaluate the thermal properties of the exiting chilled water to evaluate the specific exergy crossing that boundary of the control volume. This is not the only way to find the exit temperature of the chilled water to evaluate the specific exergy of the exiting water. Rather, the input temperature of the chilled water , the effectiveness of the heat exchanger in the condenser,the input temperature of the working fluid of the CRAC unit to the condenser, as well as the thermal properties of chilled water and the working fluid, could be used to estimate the exit temperature and thus specific exergy of the chilled water. However, these parameters are not easily known by a data center designer. The temperature difference across the condenser is an easy input for the designer. This is the reason the input parameters given in the list above where chosen.

Admitting that the list of parameters above are the correct input parameters for a designer, there are several assumptions that will be made to simplify the analysis.

1. The CRAC unit exhibits steady flow at steady state.
2. Velocity differences and gravitational potential energy differences across components are negligible when compared to enthalpy differences.
3. Air behaves like an ideal gas and thus can be approximated using the ideal gas law $P\upsilon = RT$. In addition, enthalpy differences can be approximated as $\Delta h = c_p \Delta T$.
4. Water is an incompressible substance.
5. Specific heats will be considered constant in all processes and components of the CRAC center, with the specific heat being evaluated at the average temperature of the inlet and exit of the specific component.

Given the input design parameters and assumptions, three terms must be evaluated in equation 4.4. The first quantity to be calculated is the work required by the blowers. An energy balance on a blower then becomes

$$\dot{Q} - \dot{W}_b = \dot{m}_{air} \Delta h = \dot{m_{air}} c_p (T_3 - T_{return}). \tag{4.5}$$

Assuming that the blower is adiabatic, and for the moment considering the best case scenario that the process is reversible, the process is isentropic, and equation 4.5 becomes

$$\dot{W}_{b,is} = \dot{m}_{air} c_p T_{return} (1 - \frac{T_3}{T_{return}}) = \dot{m}_{air} c_p T_{return} (1 - (\frac{P_3}{P_{return}})^{\frac{\gamma - 1}{\gamma}}). \tag{4.6}$$

Note that γ is the ratio of specific heats, $\frac{c_p}{c_v}$, and that $P_3 = P_{return} + \Delta P_b$. Equation 4.6 now becomes

$$\dot{W}_{b,is} = \dot{m}_{air} c_p T_{return} (1 - (\frac{P_{return} + \Delta P_b}{P_{return}})^{\frac{\gamma-1}{\gamma}}). \tag{4.7}$$

Recall the definition of the isentropic efficiency of a blower is $\eta_{is,b} = \frac{\dot{W}_{is}}{\dot{W}_{actual}}$, so the actual ratio of the electrical power to the mass flow rate for the blower is

$$\frac{\dot{W}_b}{\dot{m}_{air}} = \frac{c_p T_{return}}{\eta_b} (1 - (1 + \frac{\Delta P_b}{P_{return}})^{\frac{\gamma-1}{\gamma}}). \tag{4.8}$$

In order to proceed, the mass flow rate of the air through the evaporator of the CRAC unit must be known. To find this quantity, an energy balance is performed on the evaporator. Assuming there is no work interaction, the energy balance becomes

$$\dot{Q}_c = \dot{m}_{air} c_p (T_3 - T_{supply}) \tag{4.9}$$

To find T_3, an energy balance is performed on the blower and the expression for $\frac{\dot{W}_b}{\dot{m}_{air}}$ in equation 4.8 is used.

$$\dot{W}_b = \dot{m}_{air} \frac{\dot{W}_b}{\dot{m}_{air}} = \dot{m}_{air} c_p (T_{return} - T_3) \tag{4.10}$$

$$T_3 = T_{return} - \frac{1}{c_p} \frac{\dot{W}_b}{\dot{m}_{air}} \tag{4.11}$$

After rearranging, the mass flow rate of air can be solved for.

$$\dot{m}_{air} = \frac{\dot{Q}_c}{c_p [T_{return} (1 - \frac{1}{\eta_b} [1 - (1 + \frac{\Delta P_b}{P_{return}})^{\frac{\gamma-1}{\gamma}}]) - T_{supply}]} \tag{4.12}$$

The work required by the blowers can be calculated by multiplying the mass flow rate determined in equation 4.12 by equation 4.8. To determine the total work crossing the control volume to obtain the $\dot{W}_{cv}$ term in equation 4.4, the work of the blowers must be added to the work of the compressor in the CRAC unit. This total work is then

$$\dot{W}_{cv} = \dot{W}_b + \dot{W}_c, \tag{4.13}$$

where

$$\dot{W}_c = \frac{\dot{Q}_c}{COP}. \tag{4.14}$$

Note that both the blower and compressor work terms are negative because it was assumed work done by the system was positive.

At this point, the first term in equation 4.4 has been found in terms of the given input parameters. The remaining two terms in equation 4.4 may be found using equation 4.2 and the fact that there are two inlets and two outlets. Note again that the velocity and gravitational potential terms are assumed negligible compared to the enthalpy terms. The subscripts w and a denote water and air, respectively.

$$\sum_i \dot{m}_i \phi_i = \dot{m}_a[(h_{a,return} - h_{a,0}) - T_0(s_{a,return} - s_{a,0})] + \dot{m}_w[(h_{w,1} - h_{w,0}) - T_0(s_{w,1} - s_{w,0})] \quad (4.15)$$

$$\sum_e \dot{m}_e \phi_e = \dot{m}_a[(h_{a,supply} - h_{a,0}) - T_0(s_{a,supply} - s_{a,0})] + \dot{m}_w[(h_{w,2} - h_{w,0}) - T_0(s_{w,2} - s_{w,0})] \quad (4.16)$$

When equations 4.15 and 4.16 are combined and inserted into equation 4.4, the result is

$$\begin{aligned} \dot{X}_d = -\dot{W}_{cv} &+ \dot{m}_a[(h_{a,return} - h_{a,supply}) - T_0(s_{a,return} - s_{a,supply})] \\ &+ \dot{m}_w[(h_{w,1} - h_{w,2}) - T_0(s_{w,1} - s_{w,2})]. \end{aligned}$$

The mass flow rate of air has already been determined. To evaluate the enthalpy and entropy differences of air, the ideal gas approximation will again be used. Thus, the enthalpy difference between the return and the supply is simply $h_{a,return} - h_{a,supply} = c_p(T_{a,return} - T_{a,supply})$. The entropy difference can be found by plugging the ideal gas equation of state into the Tds equation.

$$ds = \frac{dh}{T} - \frac{v}{T}dP = \frac{c_p dT}{T} - \frac{RT}{T}\frac{dP}{P} \quad (4.17)$$

When this is integrated, the result is

$$s_{a,return} - s_{a,supply} = c_p \ln(\frac{T_{a,return}}{T_{a,supply}}) - R \ln(\frac{P_{a,return}}{P_{a,supply}}) \quad (4.18)$$

All of the air terms have now been solved for, leaving only the water terms. The assumption that water is an incompressible fluid means that enthalpy and temperature are related by

$$h_2 - h_1 = c(T_2 - T_1) + v(P_2 - P_1). \quad (4.19)$$

Because v for liquid water is small, and the pressure drop from state point 1 to state point 2 is also small, the second term in equation 4.19 will be assumed negligibly small. Also, the specific heat at constant pressure is equivalent to the specific heat at constant volume for an incompressible substance, and is denoted as c.

To find the mass flow rate of the water, an energy balance is performed on the water flow through the condenser. The energy balance yields

$$\dot{Q}_H = \dot{m}_w(h_2 - h_1) \quad (4.20)$$
$$= \dot{m}_w[c(T_2 - T_1) + \upsilon(P_2 - P_1)]. \quad (4.21)$$

In order to proceed, the assumption that the second term in 4.21 is negligible is used. In addition, using an alternate control volume in which only the working fluid cycle of the CRAC unit is considered, the Q_H term can be found with an energy balance.

$$\dot{Q}_H = \dot{Q}_c - \dot{W}_c = \dot{Q}_c(1 + \frac{1}{COP}) \quad (4.22)$$

Putting 4.21 together with 4.22 and after the rearranging, the mass flow rate of water becomes

$$\dot{m}_w = \frac{\dot{Q}_c(1 + COP)}{COPc(\Delta T_{water})}. \quad (4.23)$$

The final term that needs to be solved is the entropy change of the water. To do this, the Tds equation is again utilized. However, for the water, c_p is merely c, and incompressibility makes the second term identically zero.

$$s_{w,2} - s_{w,1} = c\ln(\frac{T_{w,2}}{T_{w,1}}) = c\ln(1 + \frac{\Delta T_{water}}{T_1}) \quad (4.24)$$

The rate of exergy destruction has now been determined. To calculate the total amount of exergy consumed over the life of the CRAC unit, the rate of exergy destruction must be multiplied by the amount of time the CRAC unit is run. For this calculation, equation 4.25 is used,

$$X_{d,total} = (U) * (AL) * (D) * \dot{X}_d, \quad (4.25)$$

where U is the percent uptime for the CRAC unit expressed as a fraction, AL is the average load of the CRAC unit in terms of a fraction of its peak load, and D is the operational duration of the CRAC unit.

Typical CRAC unit parameters for this case study came from two companies. Stulz Air Technology Systems, Inc., provided a typical mass breakdown for a 30 ton CRAC unit. The mass values of the different materials used to make the CRAC unit were used to estimate the material extraction, manufacturing, transportation, and recycling exergy consumptions. The operational exergy consumption was calculated using the analysis described above and typical input parameters for CRAC units from Hewlett Packard data centers. Table 4.16 summarizes typical values of all necessary input parameters necessary to predict the exergy consumption over the life-cycle of a CRAC unit. Note that the blower efficiency and static pressure drop for the blower are functions of the flow rate of the air through the CRAC unit. The COP for the compressor is a function of the desired supply side temperature achieved. Data necessary for these dependencies was provided by Hewlett Packard Laboratories.

Table 4.16: Input variables representative of CRAC unit.

Input Parameter	**Input Value**
$Q_c(ton)$	30
T_{return} (K)	311
T_{supply} (K)	289
P_{return} (atm)	1
ΔP_b (in. H_2O)	1.944
η_b (%)	85.4
COP of compressor	5.13
T_1 (K)	293
ΔT_{water} (K)	20
Operation Duration (years)	10
Estimated Uptime (%)	95
Average Device Load (%)	50

At this point, all of the thermodynamic quantities necessary to compute the exergy destroyed by the CRAC unit have been solved for in terms of the inputs. A list of design inputs was generated based on what would be convenient inputs for a designer designing a complete data center. It is important to note that this analysis has been constructed from the point of view of a data center designer, not a CRAC unit designer. Specific information for a given CRAC unit design, such as what working fluid is chosen and the flow rate of the working fluid, have not been considered directly. Rather, these specifics for a CRAC unit have been considered by specifying the inlet and outlet temperature of the warm air to be cooled as well as amount of heat the CRAC unit removes. In addition, CRAC unit specifications such as the efficiencies of the heat exchangers in the compressor and evaporator are considered by choosing the COP of the CRAC unit. From this point of view, a designer can explore the implications of varying the COP of the CRAC unit or increasing the efficiency of the blowers without having to actually design a new CRAC unit. It is left up to the CRAC unit designer to ensure that the design inputs are realistic.

One important point that a CRAC unit designer would have to consider is that the relative humidity of the air moving through the CRAC unit. The relative humidity of the air will be a function of the relative humidity of the air entering the CRAC unit and the temperature drop desired by the data center designer. If the designer selects a drop in temperature that is too large and lowers the temperature of the air below the saturation temperature, water will begin to condense out of the air in the CRAC unit. It is left up to the CRAC designer to ensure this does not occur.

To model the transportation and end-of-life exergy consumption, the total mass of the CRAC unit was multiplied by the exergy consumption per unit mass for transportation and end-of-life provided in the overview of this section. These values were 5.4 $\frac{MJ}{kg}$ and 520$\frac{kJ}{kg}$, respectively.

Chiller

A chiller was modeled very similarly to a CRAC unit. As was mentioned in the life-cycle assessment portion of this chapter, unlike the CRAC unit, detailed information about a chiller was not available. Making the same assumption as was made for the LCA, it was assumed that the mass of the chiller was entirely steel. Again, this assumption was made after discussing the material composition of chillers with data center operators familiar with chillers.

For the resource extraction and manufacturing portion of the life-cycle, the mass specific exergy consumption value from [107] for steel was used. This value is located in table 4.11. The size and mass of the chiller are summarized in table 4.5. To calculate the resource extraction and processing portion of the life-cycle exergy consumption, the mass value from table 4.5 is multiplied by the steel mass specific exergy consumption values in table 4.11. To calculate the manufacturing portion of the life-cycle exergy consumption, the steel mass value is multiplied by the mass specific exergy consumption values in table 4.12 for metal. All important values for the chiller are summarized in table 4.5.

Chiller information needed for modeling the operational portion was minimal. Since a chiller is based on the same vapor-compression refrigeration cycle as a CRAC unit, chillers achieve similar COPs as CRAC units. In this sustainability study, due to lack of information on a cooling tower, it was assumed that the chiller working fluid was cooled with air from outside the data center. Unfortunately, there was also no information on the air blown over the chiller condenser to cool the chiller working fluid. It seems reasonable to assume that the blower blowing air over the chiller condenser coils would behave similarly to the blower blowing air over the CRAC unit evaporator coils. Using this assumption, the operational exergy consumption of the chiller could be modeled almost exactly the same as the CRAC unit with two minor differences. First, figure 4.1, which shows the vapor-compression refrigeration cycle for a CRAC unit, will be exactly the same for the chiller as the CRAC unit except the evaporator now cools warm water and the condenser is now cooled by cold air. Second, the equation formed by the combination of equations 4.15 and 4.16 will have the same terms, but the second and third terms will be opposite in sign. This is because of the first difference, changing the fluid going through the condenser and evaporator. This effectively switches the direction of the working fluid if viewing 4.1 making the change of sign necessary. Finally, this is the exergy consumed by the chiller for the cooling load prescribed by the CRAC unit. However, the chiller is responsible for cooling multiple CRAC units. Therefore, the amount of exergy consumed by the chiller for each CRAC unit is scaled by the number of CRAC units being cooled by the chiller.

As was the case with the CRAC unit, the transportation and end-of-life exergy consumption was found by multiplying the mass of the chiller by the exergy consumption per unit mass for transportation and end-of-life provided in the overview of this section. These values were 5.4 $\frac{MJ}{kg}$ and 520$\frac{kJ}{kg}$, respectively.

While it may seem problematic to make all of these assumptions about a chiller, most of these assumptions do not pertain to the operational portion of the chillers life-cycle. In

Table 4.17: Important assumed properties for 208 V, 3-phase delta PDU.

Input Parameter	**Input Value**
Steel mass [kg]	9.2
Copper mass [kg]	2.9
Plastic mass [kg]	5.5
PCB area [ft^2]	1.6
Uptime [%]	100
Lifetime [years]	10

the operational portion of the life-cycle, assumptions are made about the cooling air flow rate and temperatures. The COP of the chiller, however, was not assumed and is a very realistic value. Therefore, if the exergy consumption value is dominated by the operational exergy consumption, and if the operational exergy consumption value term is dominated by the $\dot{W}_{cv}$ term, these assumptions become of negligible importance. It will be shown in the chapter 6 that this is, in fact, the case.

PDU

Information needed for the PDU analysis was again obtained from Hewlett Packard Laboratories, and is summarized in table 4.17. The resource extraction and processing, manufacturing, transportation, and end-of-life exergy consumption values were calculated using the mass breakdown as was done for the previous components. For the operational exergy consumption, it was assumed that 5% of the power flowing through the PDU was lost as heat. While this is true, the PDU does not get significantly warm. Therefore, the heat transfer term of equation 4.1 is neglected. Another way of thinking of this is that the air around the PDU is considered to be part of the PDU. The boundary that separates the PDU and the rest of the room is one such that no heat transfer is occurring across the boundary. Because the PDU does not get significantly warm, this air boundary will be very thin. The exergy that could otherwise be recovered from the warm PDU is lost as the air in this hypothetical boundary heats up. However, this amount of exergy is small because the surface temperature of the PDU is not very high.

UPS

Information needed for the UPS analysis was also again obtained from Hewlett Packard Laboratories. The total mass of a 1500 VA UPS (230 V and 980 W active power output) was 27 kg. The resource extraction, processing, and manufacturing exergy were found by multiplying the mass of the UPS by the mass specific life-cycle exergy consumption to make UPS type batteries. This value was 21 $\frac{MJ}{kg}$ taken from [22]. The transportation and end-of-life exergy consumption values were calculated using the mass breakdown as was done for the previous components.

Table 4.18: Data from [88] used to find losses in a 100 kVA, 277 V UPS as a function of load.

% Full Power	Load (kVA)	Efficiency (%)	Loss (VA)	Fixed Loss (VA)	Linear and Quadratic Losses (VA)	Current (A)
0	0	0	2310	2310	0	0
10	10	76.4	2360	2310	50	12
20	20	85.5	2900	2310	590	24
30	30	88.9	3330	2310	1020	36
40	40	90.7	3720	2310	1410	48
50	50	91.8	4100	2310	1790	60
60	60	92.4	4560	2310	2250	72
70	70	92.8	5040	2310	2730	84
80	80	93.1	5520	2310	3210	96
90	90	93.3	6030	2310	3720	108
100	100	93.4	6600	2310	4290	120

For the operational exergy consumption, equation 4.1 was once again used. It was again assumed that even though there are electrical loss mechanisms that convert electricity to heat, the UPS does not get significantly warm. Therefore, the heat transfer term of equation 4.1 is neglected. The same thought experiment can be made for the UPS that was made for the PDU to verify this assumption. In order to use equation 4.1, the electrical loss of the UPS must be known, which is the $\dot{W}_{cv}$ term. To find the electrical loss the UPS was assumed to have three loss mechanisms: fixed losses that are independent of load, losses that are linear with load, and losses that go as the square of the load [88]. Data was taken from [88] to find the fixed, linear, and quadratic losses in a 100 kVA UPS. It was assumed that the loss coefficients found would be similar for the 1.5 kVA UPS for which the mass data from Hewlett Packard was available. From data in [88], the loads and losses for a 100 kVA UPS were found and are summarized in table 4.18.

The first four columns of table 4.18 are from data in [88]. Also stated in [88] is the fact that the fixed losses in a UPS are typically on the order of 40% of the losses at 100% load. In this case, it was assumed that the fixed losses are 35% of the losses at 100% load. With this information, the losses in the 100 kVA UPS are calculated and the fixed loss is calculated to be 2310 VA. Once this is known, the linear and quadratic losses are found by subtracting the total loss from the fixed loss. The current through the UPS is calculated by dividing the apparent power, S, provided by the UPS by the line to ground voltage, 277 V, supplied by the UPS. Apparent power is related to voltage and current as shown in equation 4.26. The current is the sum of the three equal currents in the three phase UPS. Thus, the current of any one phase will be the apparent power divided by three times the voltage. The result of this calculation is the last column of table 4.18. A fit of the current through the UPS

Table 4.19: UPS values used in LCEA model.

Assumption Category	**Assumed Value**
Capacity (kVA)	1.5
Total Mass (kg)	27
Power factor	˜1
Efficiency (%)	92
Average Load [%]	70
Uptime (%)	100
Lifetime (years)	10

and the linear and quadratic losses produces constants for the linear and quadratic terms in equation 4.27.

$$S = VI \tag{4.26}$$

$$P_{loss} = C + kI + RI^2 \tag{4.27}$$

From the fit to the data, it was found that R for the UPS is $0.1013\frac{W}{A^2}$ and k is $23.54\frac{W}{A}$. The UPS with a material breakdown provided by Hewlett Packard has a max apparent power of 980 W and a voltage of 280 V. Assuming that the UPS is run at 70% of max load, which takes advantage of high efficiencies but leaves some room to ramp up power should another UPS fail, this means each of the three phases in the UPS has a current of 1.25 A. The power loss for the UPS is then 50 W. As stated in [88], nominal efficiencies for full load UPS generally fall in the range of 92%. However, with a loss of 50 W, this is only a loss of 3.3%. This leads one to conclude that assuming constant loss coefficients for different UPS sizes is not a good assumption. Therefore, it was assumed that the loss in the UPS would be 8%, or 120 W. This 120 W loss is the $\dot{W}_{cv}$ in equation 4.1 and this is equal to the rate of exergy consumption since it was reasoned that the heat transfer term was negligible. The important parameters used in duration and lifetime of the UPS are summarized in table 4.19.

4.2.3 Building Shell

For a building shell, literature was referred to for life-cycle exergy consumption values for a brick and mortar building. Biek [12] estimated that the exergy consumed in construction of a building to be approximately $4.7 - 5.8\frac{GJ}{m^2}$. It was also estimated in this work that the building decommissioning exergy consumption, or end-of-life consideration, was between $136 - 350\frac{MJ}{m^2}$. For this study, it was assumed that the construction exergy consumption is $5.3\frac{GJ}{m^2}$ and that the decommissioning exergy consumption is $240\frac{MJ}{m^2}$. To remain consistent with the rest of this study, construction was considered as resource extraction, processing,

and manufacturing. Decommissioning was counted as end-of-life. Transportation was neglected, since a building is not transported anywhere. The transportation for building the facility and decommissioning it are included in the resource extraction, processing, and manufacturing and end-of-life life-cycle legs. There also was no operational exergy consumption, since this is considered in detail through the various data center components studied. The lifetime of this building was assumed to be 50 years. To get the size of the data center, the power needed by the servers was divided by the average power per square foot listed in table 4.1.

4.3 Life-Cycle Exergy Advisor MATLAB Graphical User Interface - LCEA

The MATLAB based (GUI) developed for data center sustainability tracking is called the Life-Cycle Exergy Advisor, or LCEA. Figures 4.2 and 4.3 illustrate some of LCEA's main windows. For a more complete description, see [figure out where going to write a user manual for this].

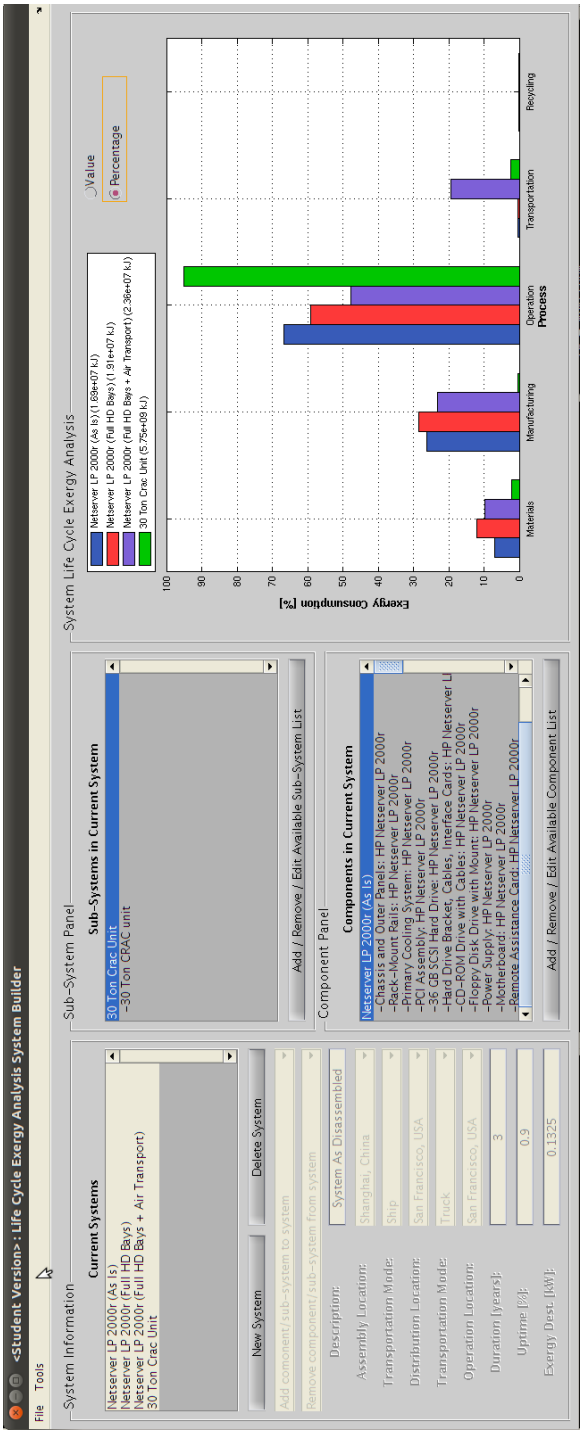

Figure 4.2: Main LCEA window for building systems.

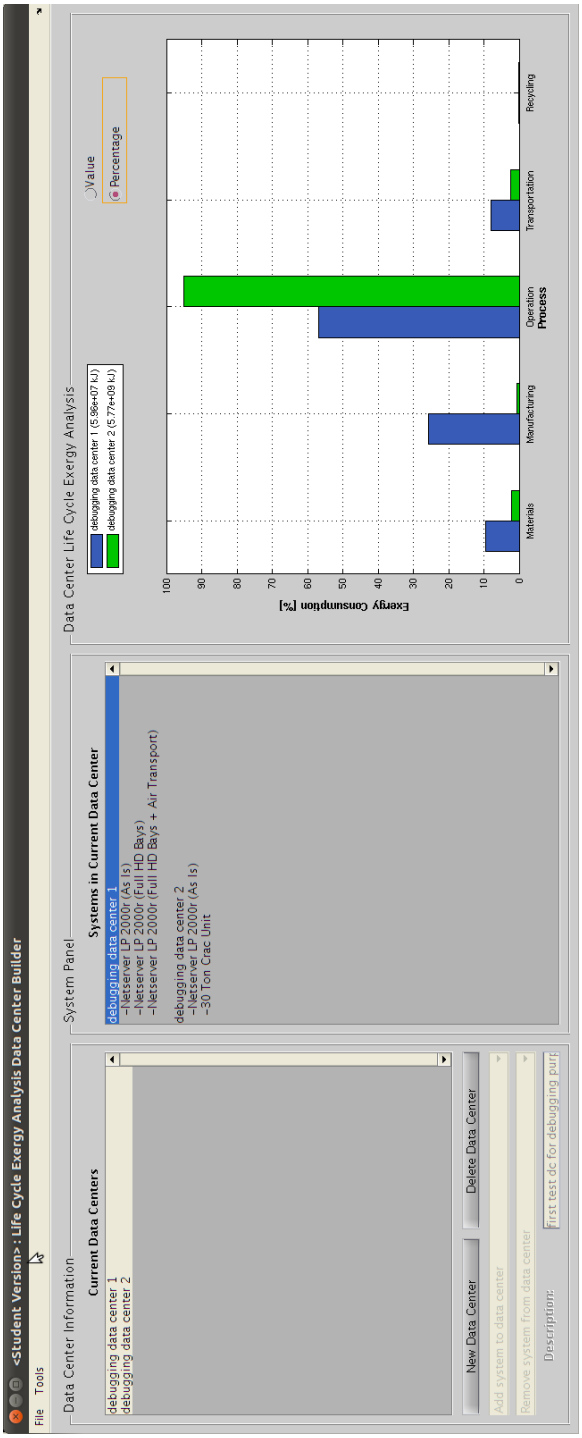

Figure 4.3: Main LCEA window for building data centers from systems.

Chapter 5

Velocity and Temperature Field Modeling Methodology

This chapter deals with the formulation needed to compare three different data sets representing the temperature field in a data center room: a potential-flow-based model output, a commercial CFD program output, and physical measurements. Previous investigations compared the potential flow model with measured temperatures [111], but adding comparisons to commercially available CFD was deemed to be better for validating the models usefulness. This is because of the reliability of model inputs, which have to be derived from physical measurements. Not all server rooms can be so thoroughly instrumented, so it would be more appropriate to compare the output from two different models (compact potential flow-based and commercial CFD) which have been given identical inputs and check their agreement with physically measured temperatures. The progression of the COMPACT model development in the Energy and Information Technologies Laboratory can be seen in 5.1:

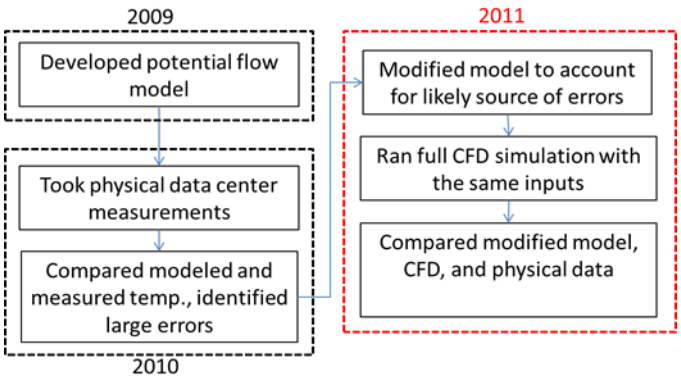

Figure 5.1: COMPACT development progression: experimental and computational validation.

5.1 Potential Flow Modeling

Development of the original potential flow model can be seen in Toulouse et al [111]. The chosen physical configuration is represented as a finite difference problem, with cubical cells filling the air in the room. All the flow boundary conditions in the room are specified and Laplaces equation is solved to find the air velocity potential field.

$$\nabla^2 \phi = 0. \tag{5.1}$$

This simplified flow solution is computationally inexpensive; more so when care is taken with the relative dimensions of air cells in each direction. Velocities can be determined by simply taking the gradient of the potential field.

To find the temperature field, it is assumed that convective energy transport is dominant. Air density, heat capacity, and flow velocity are used to balance the energy entering and exiting each air cell. Additional assumptions include full mixing, which is that air exiting the cell is at the same temperature, determined by an energy balance of incoming flows and any added temperature generated by electronics in the server racks. Below is an equation for the energy balance. Summation is over each face of the air cell.

$$(\sum C_{out})T_{cell} - \sum C_{in}T_{in} - Q_{gen} = 0. \tag{5.2}$$

C is shorthand for the specific heat capacity of the air multiplied by the mass flow rate through the cell face, and Q_{gen} is the heat generated within the cell. Since we are not modeling air within server racks but rather only in the rooms air, the heat term is added to the first cells into which server racks expel warm air.

In Toulouse et al. 2009 [111], the above equation was solved using a unique streamtube tracking approach, an approximation in which only those air cells which could be traced from the exiting face of server racks would have temperatures differing from the CRAC air temperature. However, this was not found to account for recirculation of hot air, which is a very common occurrence. Instead, MATLAB was used for a simultaneous solution of the full system of equations. These corrections are described in more detail in Toulouse et al [110]. Ultimately, earliest versions of this software package, named COMPACT 1.0 (Compact Model of Potential Flow and Convective Transport), ran in under 3 minutes on a commercially available laptop for a 4461 cell room, with later optimizations of the basic model bringing this down to under 4 seconds.

One additional feature of COMPACT, in addition to generating flow and temperature fields, is using the model output to calculate the exergy destruction field. Exergy destruction refers to the loss of usable work in a process, and in the case of a data center, is represented by the mixing of cold air from the room inlet and warmed air from the server racks. If this occurs, energy was wasted to cool some air in the CRAC unit which was not used to cool IT

equipment. Exergy destruction for COMPACT was calculated using an equation from Shah et al [99], shown below:

$$\dot{X}_d = \sum_j (1 - \frac{T_o}{T_j})\dot{Q}_j - \dot{W}_{cv} \quad + \quad \sum_{in} \dot{m}_i[(h - h_0) + \frac{V^2}{2} + g(z - z_0) - T_0(s - s_0)]_{in}$$
$$- \quad \sum_{out} \dot{m}_o[(h - h_0) + \frac{V^2}{2} + g(z - z_0) - T_0(s - s_0)]_{out}$$

It should be noted that this is a form of equation 4.1.

As the dominant form of exergy loss was due to the mixing of hot and cold flows and not the loss of kinetic or gravitational potential energy, those terms were omitted from the model. Also, since only the room airs temperature and flow modeling are within the purview of COMPACT, and we assume an adiabatic room, the Q heat generation term was omitted (the heat added to the room was only transferred inside the racks). No work is done on the boundaries of the control volume, and the nature of the temperature model in assuming convective transport as the dominant mode means that the enthalpy h terms also cancel. This leaves us with a simplified equation, seen below:

$$\dot{X}_d = \sum_{in} \dot{m}_i[-T_0(s - s_0)]_{in} - \sum_{out} \dot{m}_o[-T_0(s - s_0)]_{out} \tag{5.3}$$

The mass flow rate for each air cell is extracted from the calculated flow field, and the temperature field is used to calculate the entropy value associated with those flows. Using equation 5.3 the exergy consumption at a given location in the room can be calculated. Note that T_0 is the reference temperature, 298 K.

5.2 Vortex Superposition

Initial experimental comparisons showed a large issue with the original potential flow model [110]. Modeled temperatures near the top of the server racks were excessively high, reaching 20 K above the measured temperature in some cases. This was believed to be due to the lack of accounting for buoyancy in the potential flow model. Warm air coming out of a rack, rather than exhibiting a tendency (due to buoyant forces) to rise towards the ceiling outlets, would instead be drawn back into the front of server racks where it would be heated even further. The data center exhibited high recirculation conditions, in that the server racks as a whole possessed a larger volumetric flow rate than the CRAC units, meaning that some amount of warmed air would have to be drawn back into the racks. COMPACT was updated to include buoyancy considerations into the original potential flow model. The chosen method, as alluded to previously, was a vortex-based model of buoyancy recirculation. The updated model takes the temperature field generated by the original model, computes a modified flow field, superimposes that field on the original field, and recalculates the temperatures.

This method has the added benefit of being a non-iterative approach, which would keep computational costs low, an important factor in developing a compact model. The model works as follows: first, it calculates the average temperatures in the hot and cold aisles and the entire room (In the model GUI, locations of aisles and vortices can be automatically or manually placed). From this, it is assumed the Boussinesq approximation applies, in which the buoyancy force is an added term in the momentum equations, but incompressibility is still assumed in mass continuity. The buoyancy force is based on density variations, which is linked to differences in average temperature . δm refers to the mass of a heated parcel of air.

$$F_{\delta m} = \delta m(\Delta\rho/\rho_o)g \tag{5.4}$$

$$\Delta\rho/\rho_o = \beta\Delta T \tag{5.5}$$

Focus is given to a single row of racks at a time, consisting of a cold aisle, a hot aisle, and the row of racks itself. It is then assumed that in the hot aisle, the buoyancy force is applied over some distance on the order of the server rack height. For this model, it is assumed that height is one-half of the server rack height. Next, it is assumed that this force applied over the height is used entirely to accelerate the air upwards; in other words, the added kinetic energy from buoyancy forces, shown in equation 5.7, is equal to the added kinetic energy of vertical air flow, shown in equation 5.8.

$$\Delta KE = F_{\delta m}H = \delta m(\beta\Delta T)gH \tag{5.6}$$

$$\Delta KE = \delta m\beta(T_{H,avg} - T_{room,avg})gH \tag{5.7}$$

β is the volumetric thermal expansion coefficient of the air, which can be approximated as 1/T since air is assumed to be an ideal gas. $T_{H,avg}$ and $T_{room,avg}$ are the average hot aisle temperature and the overall average room temperature, respectively.

$$\Delta KE = \frac{1}{2}\delta m(w_B^2 - W_{H,avg}^2) \tag{5.8}$$

By equating relations 5.7 and 5.8, the added vertical air velocity due to buoyant forces is found:

$$w_B = \sqrt{w_{Havg}^2 + 2g\beta(T_{H,avg} - T_{room,avg})H} \tag{5.9}$$

w_B and $w_{H,avg}$ are the average upward hot aisle velocity with and without buoyant forces. The latter is computed from the COMPACT 1.0 model, or the COMPACT model without Rankine vortex superposition. This process is repeated for each row of server racks.

Now, for this row of server racks, we superimpose a Rankine vortex on the top of the row. A Rankine vortex is acts as a solid-body (rotational) vortex within its core, and a potential

(irrotational) vortex outside of that core. The velocity profile of a Rankine vortex can be seen in equation 5.10 below:

$$v_\theta = \begin{cases} k_v r & \text{if } r < R, \\ k_v R^2/r & \text{if } r \geq R. \end{cases} \tag{5.10}$$

A benefit of this method is that it spreads out the area of high recirculation, while adding the tendency for warm air to rise, yet preserving the potential flow model outside of the vortex core, as potential vortices satisfy Laplaces equation. Also, the effect of the vortices drops with distance from the tops of the server racks, limiting the corrective flows to the areas of greatest concern.

The distance from the vortex center is given by r. The center and R (the core radius) is set to half the depth (the distance from front to back) of the row of server racks. The center of the vortex is also centered on the top of the row of server racks, so the core covers the entire top surface. The quantity k_v is chosen so that v_θ at the edge of the vortex core (aka the cell right above the warm air outlet of the server rack) is proportional to the added velocity Δw_B previously calculated.

$$k_v = V_s \frac{\Delta w_B}{R} \tag{5.11}$$

Note the previous use of the word proportional; in equation 5.11, V_s is a vortex strength multiplier which can be chosen. Similarly, the height H over which the buoyant force is applied can be chosen. Since V_s and H can be chosen, this vortex superposition method was tuned using multiple experimental data sets to find the most accurate model configuration.

The fronts of server racks are the areas in which we desire the most model accuracy; using hot air to cool IT equipment can affect their ongoing operations and operational lifetime. Following COMPACT design goals, the vortex superposition model was optimized to minimize the errors in temperature predictions in these areas, and even more specifically on the upper halves. Those areas were the most error-prone in the original model due to the previously mentioned prevalence of recirculated warm air.

Figure 5.2 shows a result of said tuning. The height H was kept at one-half the server rack height, but the V_s multiplier was adjusted to minimize mean deviation (deviation being the absolute value of model minus measured temperature). A V_s of zero would be equivalent to the original model. It was discovered that a multiplier of 2.47 kept the mean deviation metric within 7% of its minimum in all three experimental cases, each of which had varying levels of recirculation due to varied CRAC flow rates.

5.3 Conventional Computational Fluid Dynamics

Data centers are rarely as heavily instrumented as our experimental setup was, and the potential inaccuracies in measurement meant that model inputs could not always be of

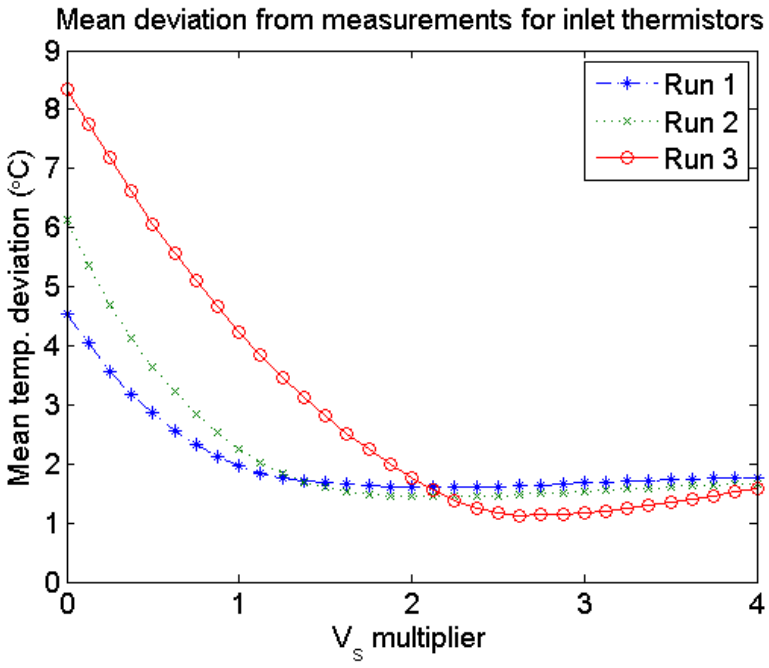

Figure 5.2: Mean deviation (at in-flowing server rack faces) of modeled temperatures from their measured values, versus the vortex strength multiplier used in vortex superposition optimization.

highest quality. Additionally, it is infeasible to fully characterize every boundary condition for all flows in a server room. Instead, much can be learned from comparing results between differing models with identical inputs.

One of the stated purposes/objectives of COMPACT is to serve as a preliminary design tool. This means that comparison to a larger conventional commercially available CFD final design tool is warranted when validating the potential flow model. Essentially, COMPACT is designed to run much faster than a full CFD package; it is worth investigating what comparative degree of accuracy is lost in the attempt.

The chosen software needed to be a previously industry- or academically-validated package, with a reasonable price tag. ANSYS FLUENT met these criteria, and was used to model the experimental server room [7]. The model was configured to solve the full set of Navier-Stokes equations, including accounting for turbulent flow. The two-equation $k-\epsilon$ method was used to model turbulence. The $k-\epsilon$ method was chosen for two reasons. First, it is the most appropriate for large, open spaces [90]. Second, the $k-\epsilon$ method is the most commonly used method, especially when modeling data centers [115]. It would therefore be useful as a benchmark with which to compare COMPACT. The Navier-Stokes and two-equation $k-\epsilon$ equations are not listed here. The interested reader is directed to [61] for a full description of these equations.

The inputs for the conventional CFD model were the same as those used in the experimental-

Table 5.1: ANSYS FLUENT CFD workstation specifications.

Specification Type	**Specification**
Processor	Intel Core i7-975 Extreme Edition
Processor Speed	3.33 GHz
Amount of RAM	18 GB
Speed of RAM	1333 MHz

COMPACT comparison, with heat generation derived from power consumption measurements and flow rate through server racks taken from the heat generation and measured temperature rise (see section 5.4 for a more detailed discussion of these inputs). The boundary conditions associated with the front and back of the servers were created in a two step process: first, the intake to each rack was treated as an air outlet exiting the room, with the corresponding air exhaust behind the rack classified as an inlet into the room. The average temperature coming into a given section of the server front was added to the measured temperature rise at that location, and the air temperature of the rear source was adjusted accordingly. ANSYS FLUENT is an iterative solver, and performed these calculations after each iteration. Flow and temperature fields were generated by FLUENT on a workstation with specification as detailed below in table 5.1.

In the FLUENT model, the turbulence intensity and length scale were specified at air inlets into the room. Turbulence intensity is the strength of the turbulent variations in velocity as compared to the free stream average, while turbulence length scale refers to the size of the turbulent eddies [8]. Both are essential quantities to specify in using a standard $k-\epsilon$ turbulence model. Since the slits in the inlet floor tiles were on the order of 1 cm, this is what the turbulence length scale was set to, with the reasoning that eddies would be of the same scale. For turbulent intensity, 1% variation from the average is considered weak and 10% is strong. With little other information to narrow these bounds, 5% was chosen. Despite best efforts, necessary decisions such as these contribute to inaccuracies in modeling data center flow. This further justifies the use of less computationally expensive models, as it lessens the appeal of more accurate but time-consuming models. For the other $k-\epsilon$ turbulence parameters, default values for FLUENT were used.

5.4 Experimental Setup

The first step taken in evaluating the model was to compare model output to experimentally gathered data. The chosen venue for gathering flow and temperature measurements for validation was a data center at Hewlett-Packard Laboratories in Palo Alto, CA. A 500 sq. foot portion of the entire data center was partitioned off, both above and below the floor plenum, and was independently served by two CRAC units, one PDU and a rack of switches,

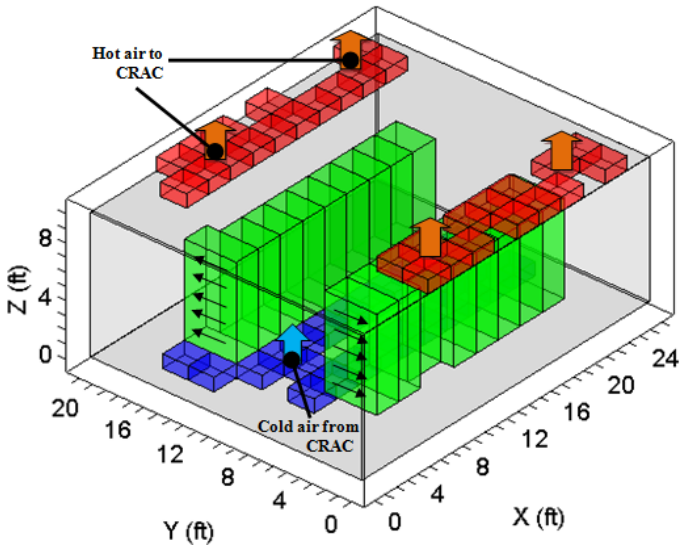

Figure 5.3: Simplified visual representation of the data center used for experimental validation, isometric view.

making it an appropriate approximation of a smaller independent server room. This server room also contained 17 racks of computer servers consuming between 100 and 115 kW of power when measured.

Figure 5.3 illustrates the room in question; floor inlets are blue, ceiling outlets are red, and server racks are green. Cool air enters from below, is drawn into the server racks by electric fans and heated, then expelled and drawn up to the ceiling plenum to return to the CRAC units.

Multiple sets of flow, temperature and power consumption measurements were recorded in this experimental data center. The volumetric flow rate through each floor inlet and ceiling outlet was measured with flow hoods and converted to flow velocities. The current through each server rack was recorded, converted to power consumption and set equivalent to heat generation. Temperature measurements in the room were recorded using thermistors on every server rack and thermocouples in the hot and cold aisles and above the racks. 170 thermistors, five in front and five in back, lined each of the 17 server racks in the room. 116 thermocouple measurements brought the total to 286 total temperature measurements per run. Initial runs omitted the above-rack thermocouples, and only had 250 temperatures; later data sets included them, however. Figures 5.4 and 5.5 below show the locations of the full set of measurements, marked by yellow dots.

COMPACT requires full characterization of flow boundary conditions, however, which includes the server rack faces. It was deemed too difficult to measure the flow rate through each rack; it was only possible for floor inlets due to a specialized flow hood with set dimensions. There is a correlation between rack fan speeds and temperature, but that is not always a standardized value readily available. Instead, the server racks are treated as a black-box

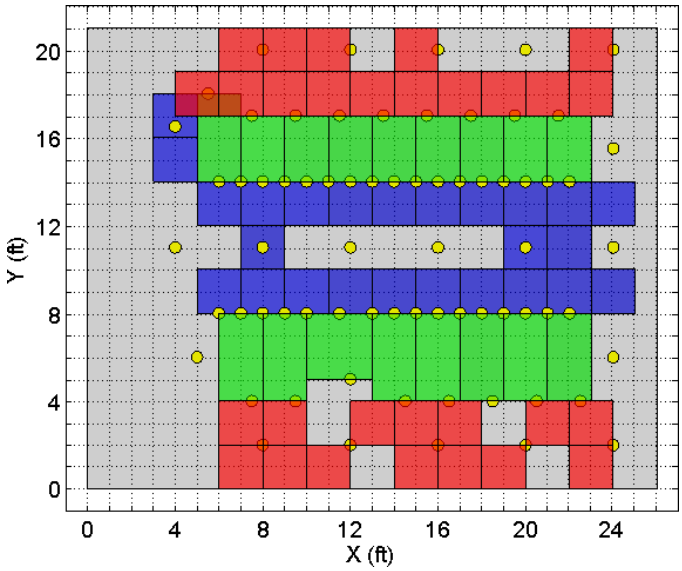

Figure 5.4: Top view of experimental data center showing location of temperature measurements.

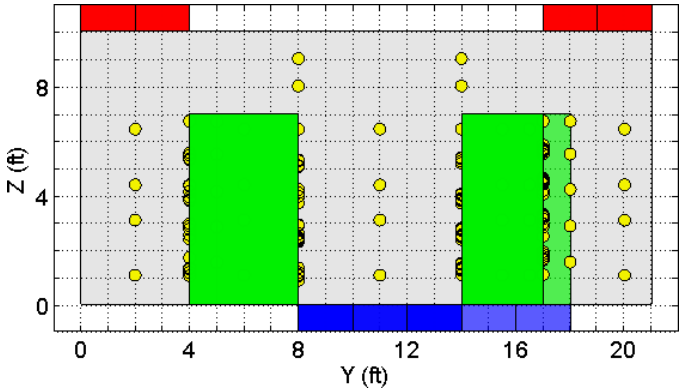

Figure 5.5: Side view of experimental data center showing location of temperature measurements.

model in which all heat generated in the rack is transferred to the air, which comes out at a higher temperature. If this assumption is made, the air flow rate through a server rack can be estimated using the heat generation and measured temperature rise from front to back.

$$V = \frac{Q_{gen}}{\rho c_p A \Delta T_R} \tag{5.12}$$

In the above equation, V is the flow velocity through a portion of the server rack with face area A, heat generation Q_gen, and measured temperature rise ΔT_R. This can be generalized to individual cell faces bordering the server rack. For a longer justification of this method, see Rambo and Joshi [81]. It should be noted that for comparing the different models and data, only temperatures were used. Measuring both magnitude and direction of mid-air flows in a non-disruptive manner was deemed too difficult and potentially inaccurate, so more attention was focused on increasing the number of locations for temperature comparisons.

5.5 Potential Flow MATLAB Graphical User Interface - COMPACT

The MATLAB based (GUI) developed for ultrafast velocity and temperature field prediction is called the Compact Model of Potential Flow and Convective Transport, or COMPACT. Figures 5.6 and 5.7 illustrate some of COMPACT's main windows. For a more complete description, see [109, 111].

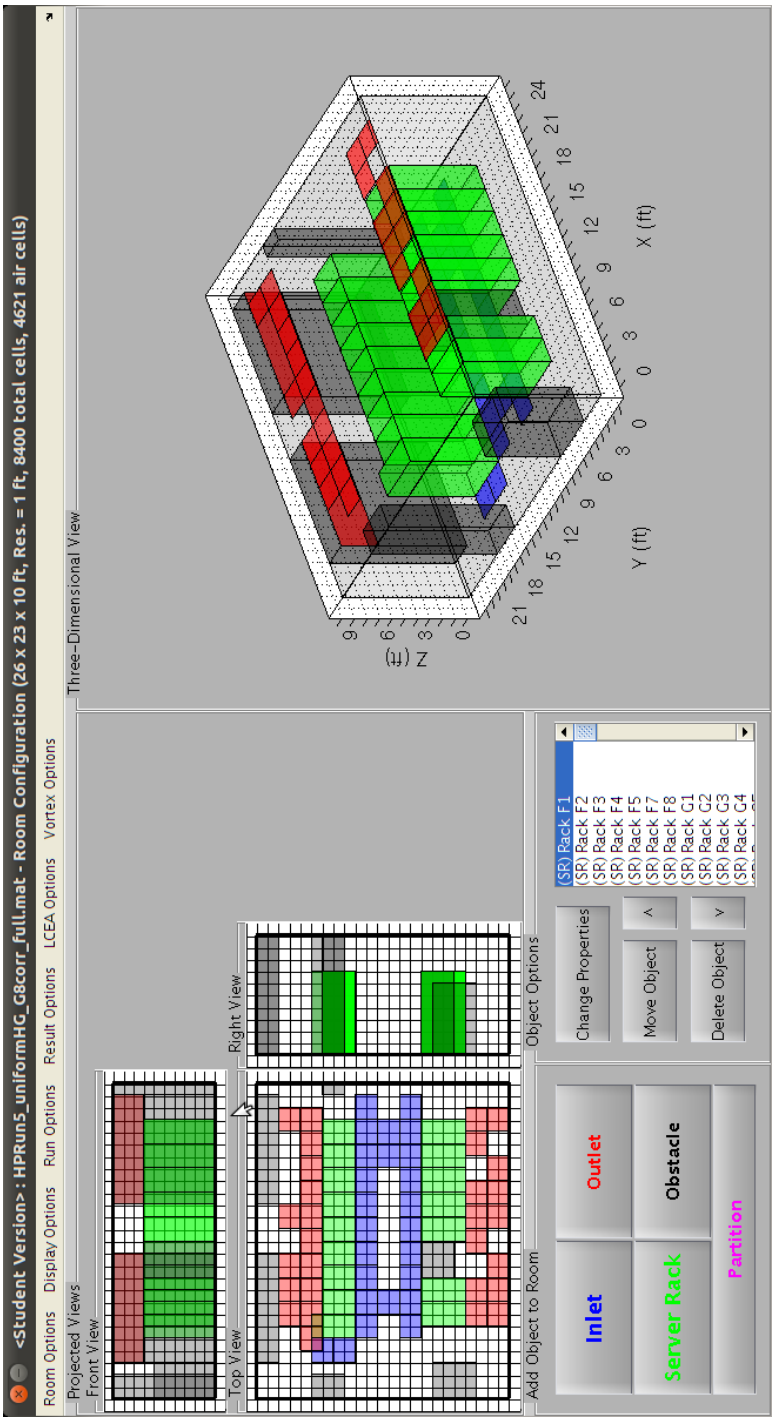

Figure 5.6: Main COMPACT window.

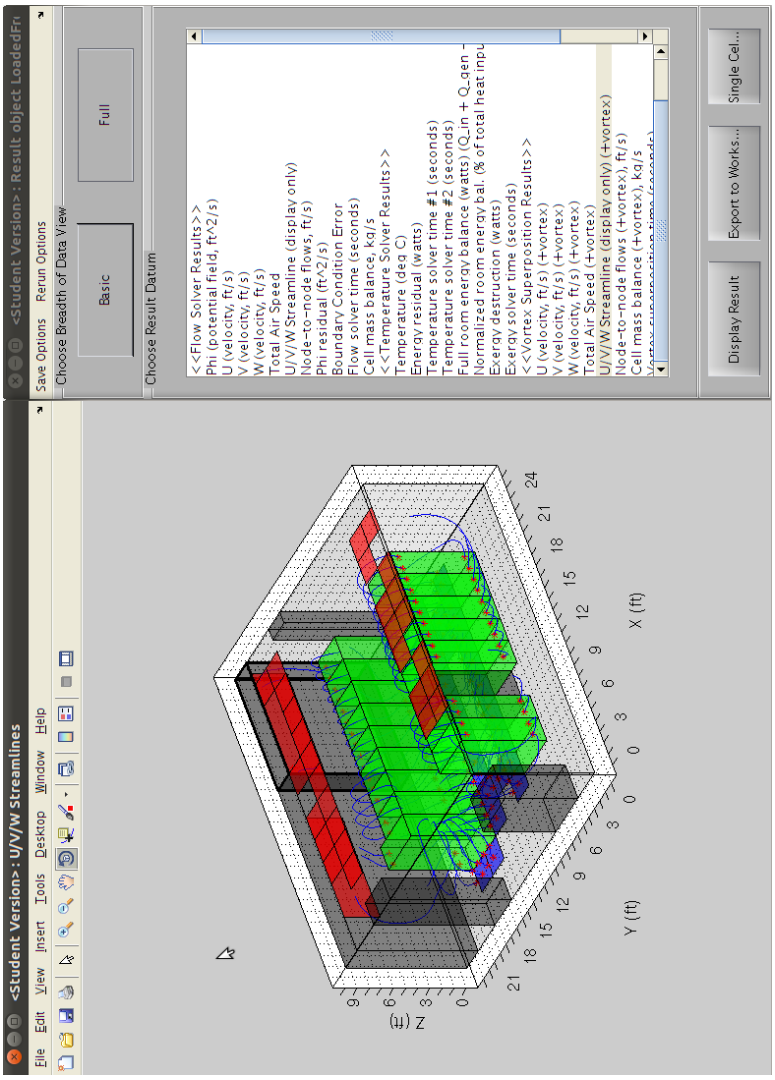

Figure 5.7: COMPACT main results window and streamline results window.

Chapter 6

Sustainability Modeling Results

6.1 Life-Cycle Assessment (LCA)

Figure 6.1 shows the results of the global warming potential of a data center created with the baseline values detailed in section 4.1 of this report. As can be seen in this figure, in terms of global warming potential, operation does in fact dominate. The global warming potential of the operation of this data center is roughly three times greater than the next largest life-cycle stage, resource extraction and manufacturing. Figure 6.1 also shows that the majority of the resource extraction and manufacturing life-cycle stage is from the servers. This is because servers are highly ordered, energy intensive equipment. The largest contributors to the operational global warming potential are the servers. The total HVAC system is the next largest contributor and would have been slightly larger if the cooling towers had been modeled, if the COP of the refrigeration cycles were slightly less, or if the data center was located in a very hot area with poor insulation. The UPS has the next largest operational global warming potential and the PDU has the least. Transportation has negligible global warming potential in comparison to the other two life-cycle stages. This is true even assuming that most of the transportation occurs via airplane, which is possible but is a conservative overestimate of a ship, the usual method of transportation across the Pacific Ocean. End of life appears to have negligible global warming potential when compared to the other life-cycle stages.

6.1.1 Sensitivity Analysis

A sensitivity analysis was performed by varying the parameters outlined in chapter 4 of this report through their ranges of possible values. Figure 6.2 shows the results of this sensitivity analysis. Table 6.1 highlights the key variables that were altered in the sensitivity analysis. Figure 6.2 shows that under the worst possible conditions, the global warming potential of resource extraction and manufacturing approaches operation. Figures 6.3 and 6.4 show the breakdown in the life-cycle global warming potentials for the best and worst case scenarios, respectively.

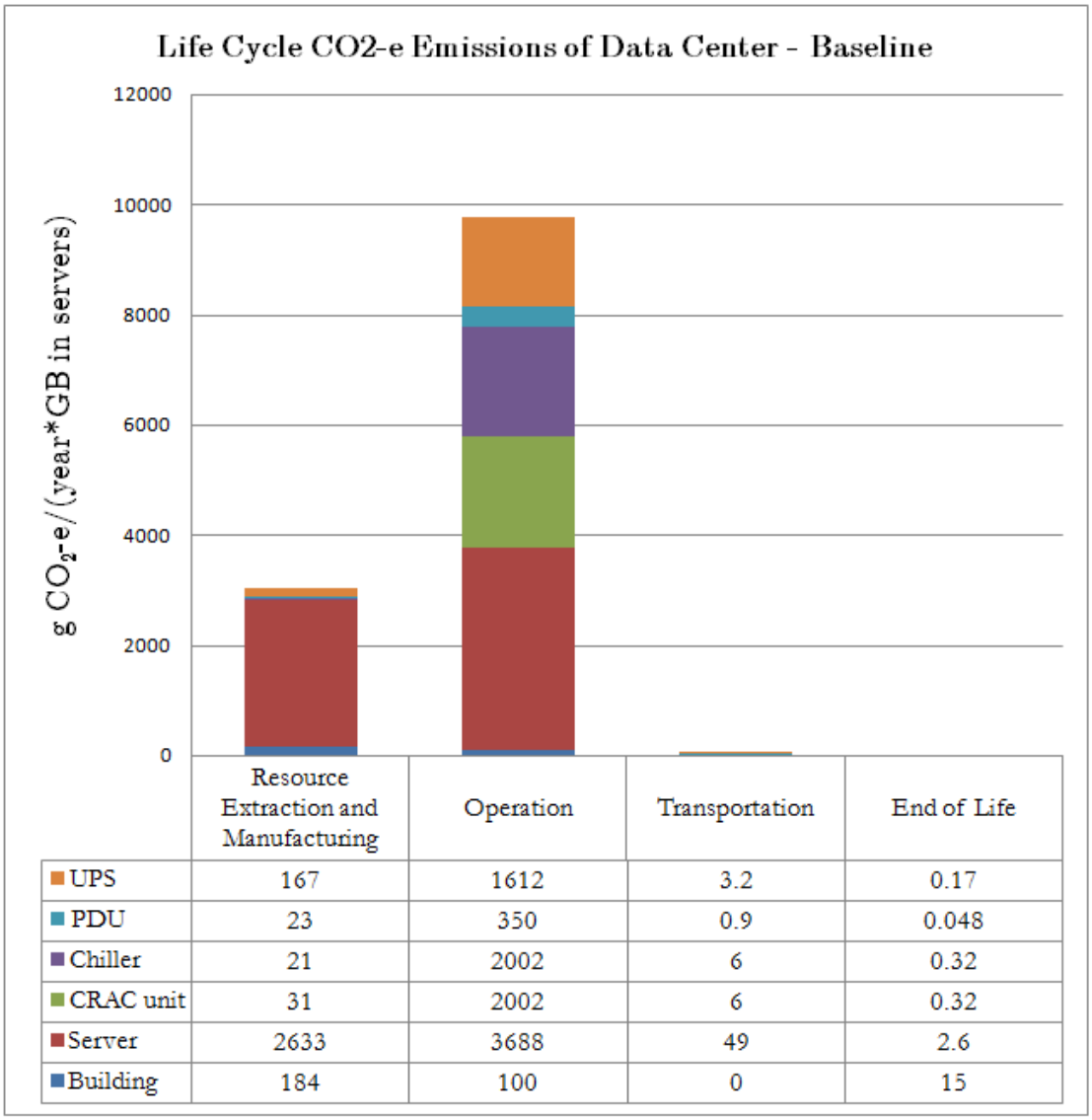

	Resource Extraction and Manufacturing	Operation	Transportation	End of Life
UPS	167	1612	3.2	0.17
PDU	23	350	0.9	0.048
Chiller	21	2002	6	0.32
CRAC unit	31	2002	6	0.32
Server	2633	3688	49	2.6
Building	184	100	0	15

Figure 6.1: Life-cycle global warming potential of data center using baseline values.

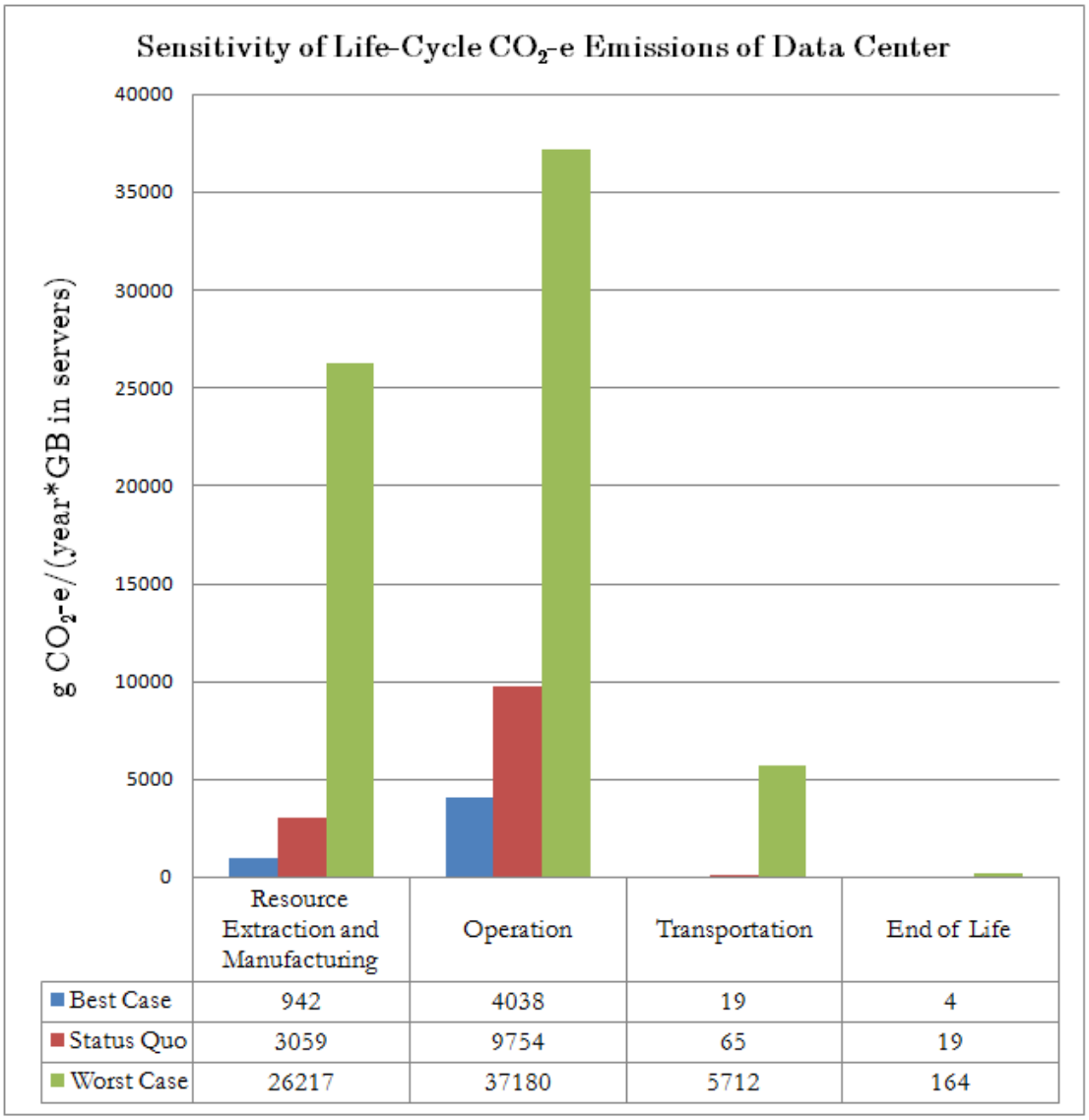

Figure 6.2: Sensitivity analysis of life-cycle global warming potential of data center.

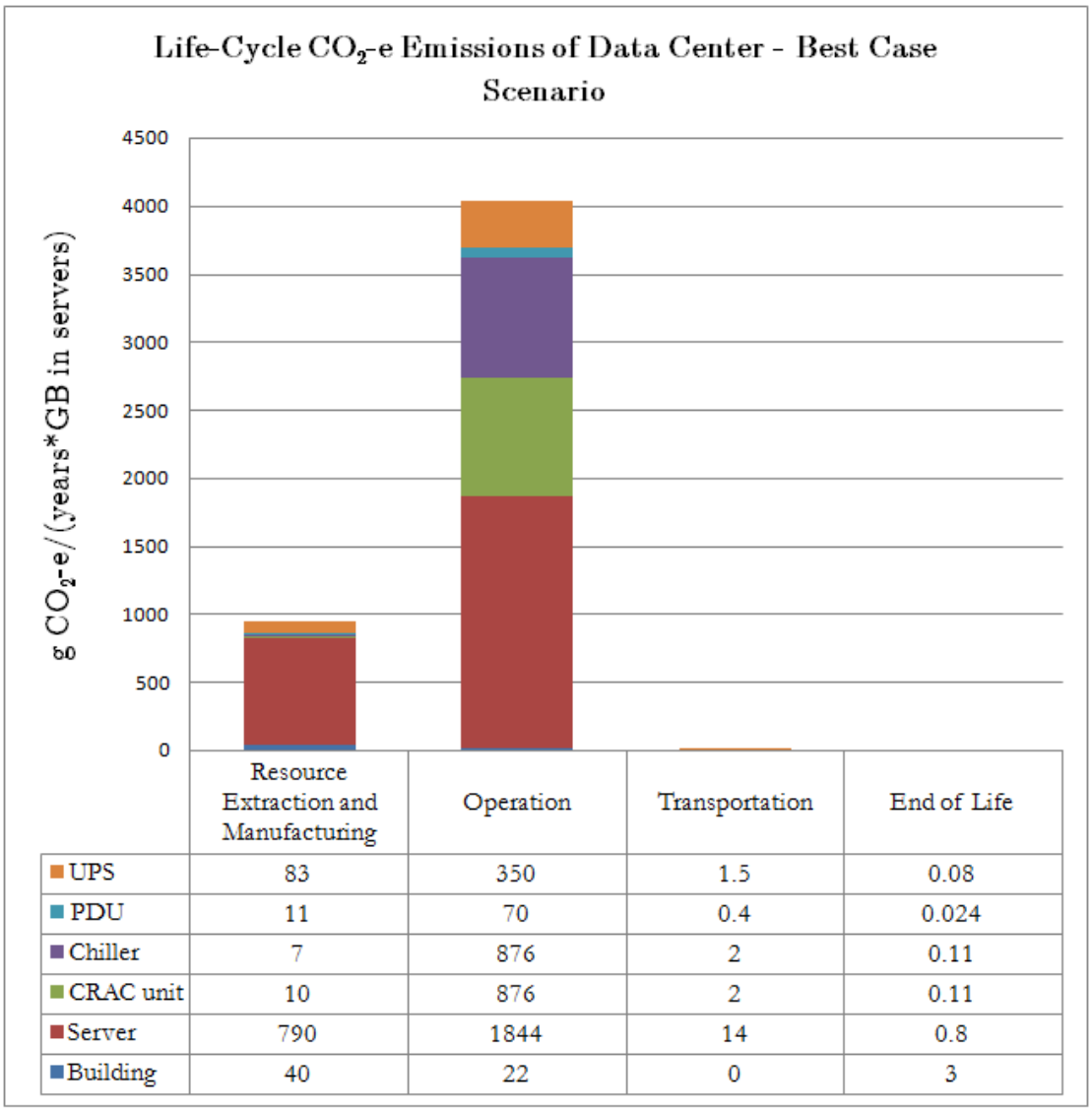

	Resource Extraction and Manufacturing	Operation	Transportation	End of Life
UPS	83	350	1.5	0.08
PDU	11	70	0.4	0.024
Chiller	7	876	2	0.11
CRAC unit	10	876	2	0.11
Server	790	1844	14	0.8
Building	40	22	0	3

Figure 6.3: Life-cycle global warming potential of data center under best case scenario.

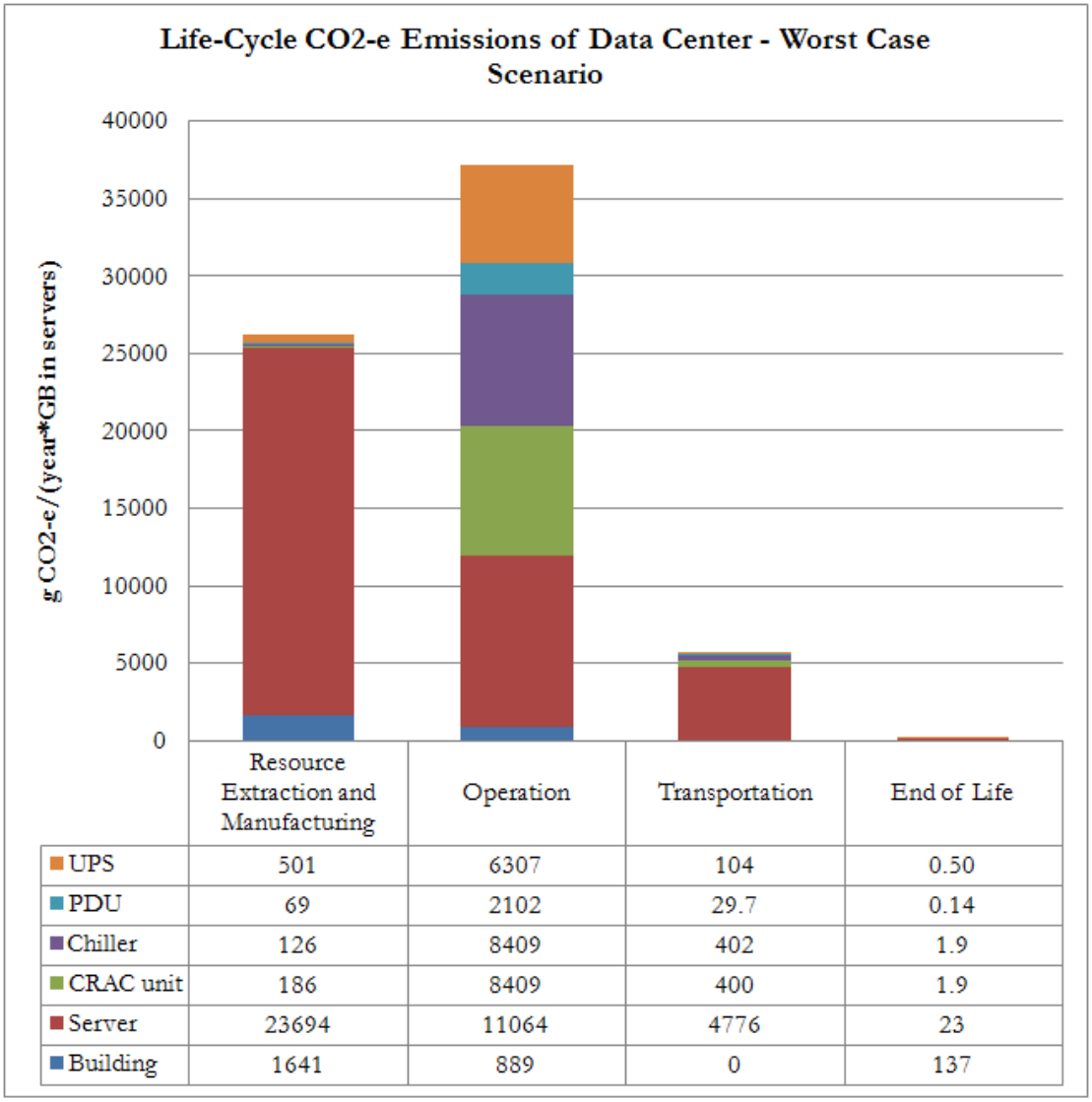

	Resource Extraction and Manufacturing	Operation	Transportation	End of Life
UPS	501	6307	104	0.50
PDU	69	2102	29.7	0.14
Chiller	126	8409	402	1.9
CRAC unit	186	8409	400	1.9
Server	23694	11064	4776	23
Building	1641	889	0	137

Figure 6.4: Life-cycle global warming potential of data center under worst case scenario.

Table 6.1: Values altered in LCA sensitivity analysis.

Data Center Component	Altered Variable	Baseline Value	Best Case Scenario Value	Worst Case Scenario Value
Server	Storage size (GB)	108	216	36
	Lifetime (years)	3	5	1
CRAC unit	COP	3.5	4	2.5
	Cooling Capacity used (% of max)	50	75	25
Chiller	COP	3.5	4	2.5
	Cooling Capacity used (% of max)	50	75	25
PDU	Efficiency	95	98	90
UPS	Efficiency	92	95	70
Building Shell	Energy Density $[\frac{W}{ft^2}]$	25	50	10
Transportation	Truck Miles	500	0	500
	Ship Miles	7500	7500	0
	Train Miles	400	900	400
	Air Miles	0	0	7500

6.1.2 Uncertainty Assessment

Table 6.2 shows the results of an uncertainty assessment of the data used in the LCA study carried out as described in [22]. The assessment shows that overall, the data was fairly good, with some data being very good, some being fair, and some data being fairly poor. The resource extraction and manufacturing had the poorest quality. This is because information on the manufacturing of data center equipment is hard to come by due to complicated supply chains, quick turnover rates, and proprietary information. The average score for this life-cycle stage was roughly 3 out of 5. While this score is not the best, it is still useful for giving an order of magnitude estimate of the the resource extraction and manufacturing. The other life-cycle stages also have minor problems, but overall average to a score of about 2.

Table 6.2: Data quality assessment of data center case study (Maximum quality = 1, minimum quality = 5), based on [53].

Category	**Resource Extraction and Manufacturing**	**Operation**	**Transportation**	**End of Life**
Acquisition Method	3	3	3	2
Independence of Data Supplier	3	3	2	4
Representativeness of Data	1	1	1	1
Temporal Correlation	3	3	3	2
Geographical Correlation	2	1	2	1
Further technological correlation	5	1	1	1

6.2 Life-Cycle Exergy Assessment (LCEA)

Figure 6.5 shows the results of the data center life-cycle exergy consumption model created with the baseline values detailed in section 4.2 of this report. As can be seen in this figure, in terms of life-cycle exergy consumption, operation does in fact dominate. Comparison of figures 6.1 and 6.5 reveal that the LCA and LCEA baseline scenarios have very similar results. The operational life-cycle exergy consumption of this data center is roughly two times greater than the next largest life-cycle stage, resource extraction and manufacturing. Figure 6.5 also shows that like in the LCA, the majority of the resource extraction and manufacturing exergy consumption is from the servers. In fact, the resource extraction and manufacturing exergy consumption of servers is larger than the operational exergy consumption. Again, this is because servers are highly ordered, energy intensive equipment. The largest contributors to the operational exergy consumption are the servers and HVAC systems. The UPS has the next largest operational life-cycle exergy consumption and the PDU has the least. Transportation has negligible life-cycle exergy consumption in comparison to the other two life-cycle stages. End-of-life appears to have negligible life-cycle exergy consumption when compared to the other life-cycle stages.

6.2.1 Sensitivity Analysis

A sensitivity analysis was performed in the exact same fashion as in the LCA study, varying the same parameters in table 6.1. The results of this analysis are shown in figure 6.6. Figure 6.6 shows that under the worst possible conditions, the exergy consumption of resource extraction and manufacturing as well as transportation exceeds operation. The reason for the high resource extraction and manufacturing term is because in the worst case scenario the servers are replaced very often and do not have much hard drive space in each server.

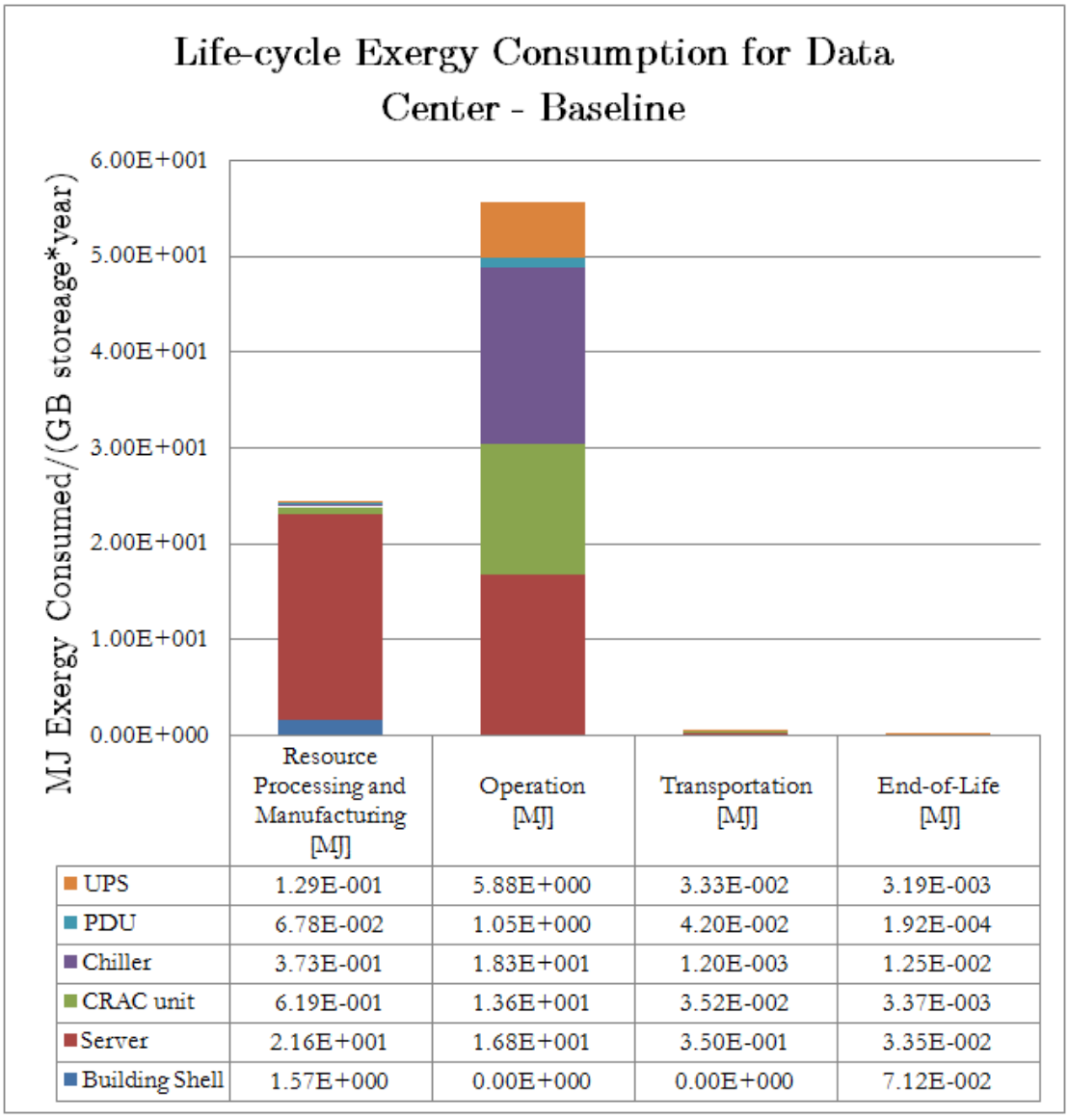

	Resource Processing and Manufacturing [MJ]	Operation [MJ]	Transportation [MJ]	End-of-Life [MJ]
UPS	1.29E-001	5.88E+000	3.33E-002	3.19E-003
PDU	6.78E-002	1.05E+000	4.20E-002	1.92E-004
Chiller	3.73E-001	1.83E+001	1.20E-003	1.25E-002
CRAC unit	6.19E-001	1.36E+001	3.52E-002	3.37E-003
Server	2.16E+001	1.68E+001	3.50E-001	3.35E-002
Building Shell	1.57E+000	0.00E+000	0.00E+000	7.12E-002

Figure 6.5: Baseline scenario for data center life-cycle exergy consumption.

The transportation is so high because in the worst case scenario the trip across the pacific is made by plane instead of ship, a much more exergy consumptive method of traveling. The worst case life-cycle carbon dioxide emissions in the LCA sensitivity analysis approach the operational emissions, but do not exceed the operational emissions. The reason that the resource extraction and manufacturing exergy emissions exceed the operational emissions is because the exergy consumed by the resource extraction and manufacturing is higher relative to operation for exergy consumption than for carbon dioxide emissions. This is apparent from comparisons of figures 6.1 and 6.5 since the ratio of operational to other life-cycle stages is less in figure 6.5 than 6.1. Figures 6.7 and 6.8 show the breakdown in the life-cycle exergy consumption for the best and worst case scenarios, respectively.

6.2.2 Uncertainty Assessment

The uncertainty assessment of the data used in the LCEA is the same as the uncertainty in the LCA since almost the entire set of data used was the same. There was different PDU and UPS data used in the two studies, but the different data sets do not change the uncertainty analysis since they have similar uncertainties.

CRAC Unit

Because the CRAC unit has an interesting operational exergy model, details of it's life-cycle exergy consumption are provided here. A chiller would have a similar analysis and is not included here to avoid redundancy. As modeled in this study, the operational exergy consumption of the rest of the data center equipment scale more or less linearly with increases in efficiency, so a detailed display of such a mundane finding is not included here.

The results of the life-cycle exergy consumption analysis are shown in figure 6.9. As can be seen in the figure, the operational exergy dominates over all other portions of the life-cycle. Plastic was chosen as the "Other" material because the life-cycle exergy consumption was slightly larger than if the "Other" material had been chosen as steel or copper, and slightly less than if the "Other" material was aluminum. However, due to the fact that over 99.99 % of the life-cycle exergy consumption is from the operational portion of the life-cycle, the assumption as to what material is constituted by "Other" is of little importance.

The large exergy consumption in the operation phase is due to the fact that it was assumed the CRAC unit runs almost continuously for 10 years. Since this portion of the life-cycle exergy consumption is so much larger than the other portions, a data center designer should focus attention on decreasing the operational exergy consumption. This can be done in several ways. The first way would be to increase the COP. Blower efficiency is already in the region where increasing efficiencies lead to small gains, but since the operational exergy is so large, even a small reduction in the rate of exergy destruction is relevant. Thus, efforts should also be focused on obtaining better blower efficiencies, but this is less important than increasing the COP. Another way in which the operational exergy could be reduced is by running the CRAC unit less. Efforts should be focused on better modeling of data center

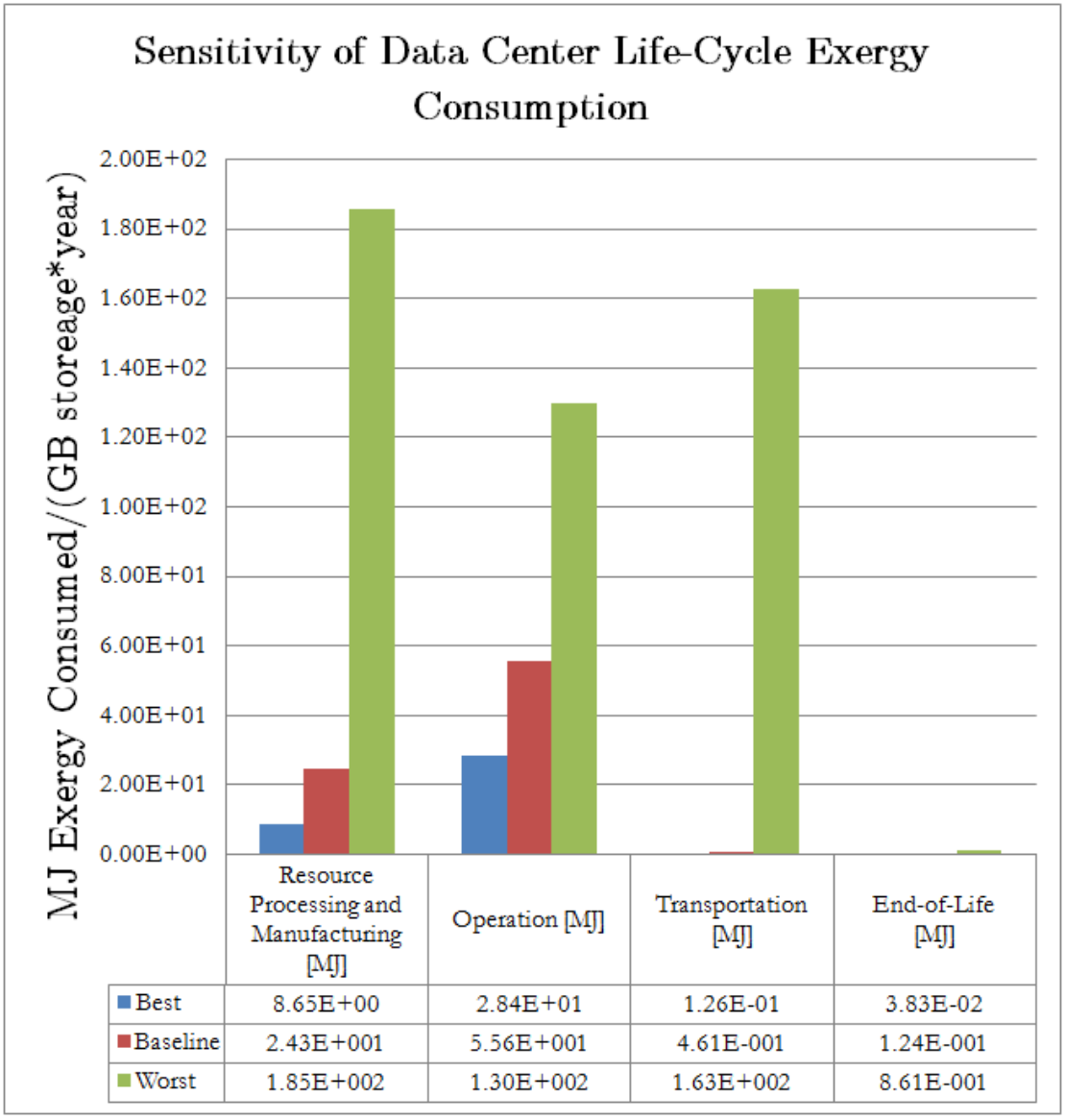

Figure 6.6: Sensitivity analysis of data center life-cycle exergy consumption.

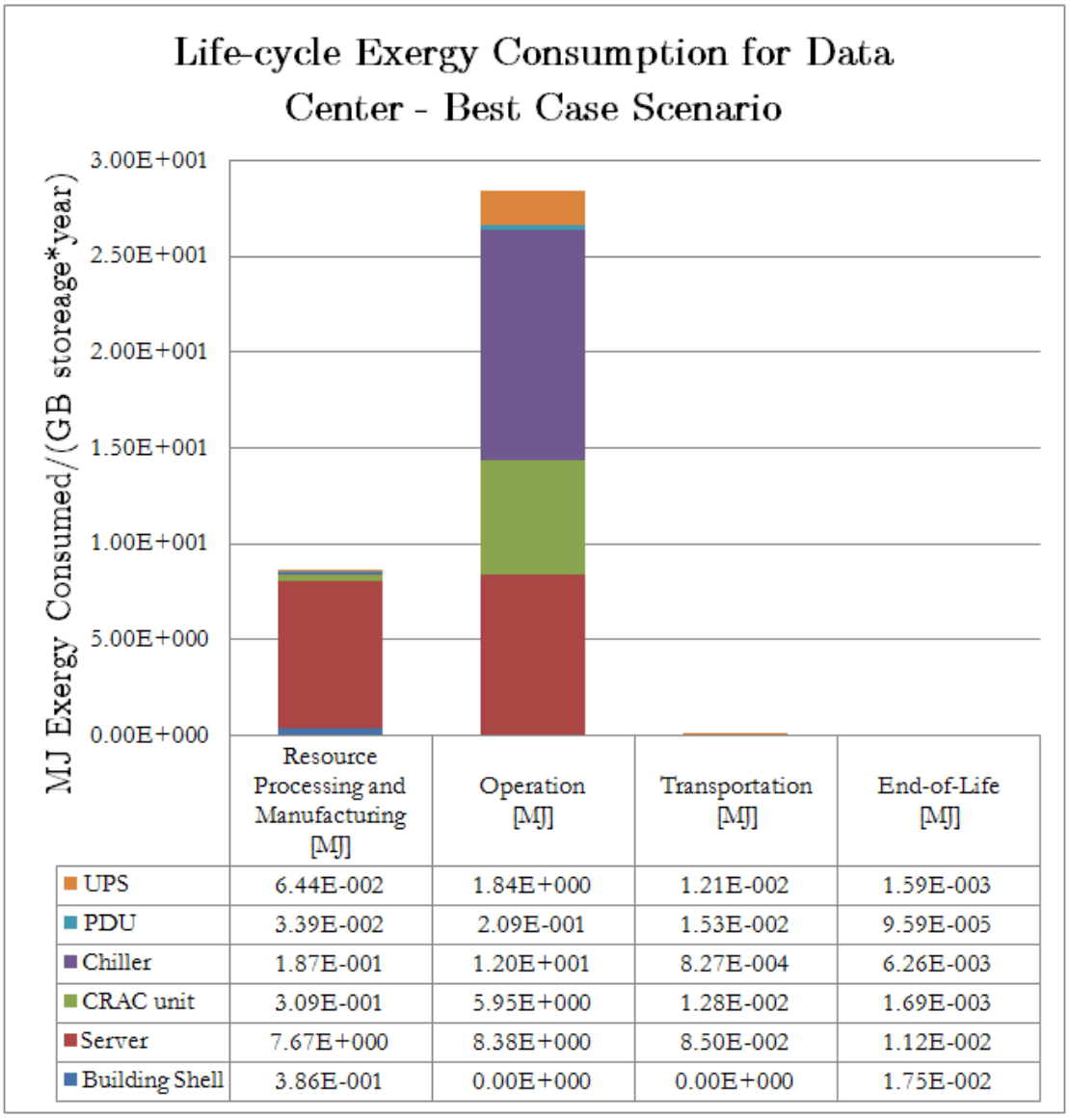

	Resource Processing and Manufacturing [MJ]	Operation [MJ]	Transportation [MJ]	End-of-Life [MJ]
UPS	6.44E-002	1.84E+000	1.21E-002	1.59E-003
PDU	3.39E-002	2.09E-001	1.53E-002	9.59E-005
Chiller	1.87E-001	1.20E+001	8.27E-004	6.26E-003
CRAC unit	3.09E-001	5.95E+000	1.28E-002	1.69E-003
Server	7.67E+000	8.38E+000	8.50E-002	1.12E-002
Building Shell	3.86E-001	0.00E+000	0.00E+000	1.75E-002

Figure 6.7: Best case scenario for data center life-cycle exergy consumption.

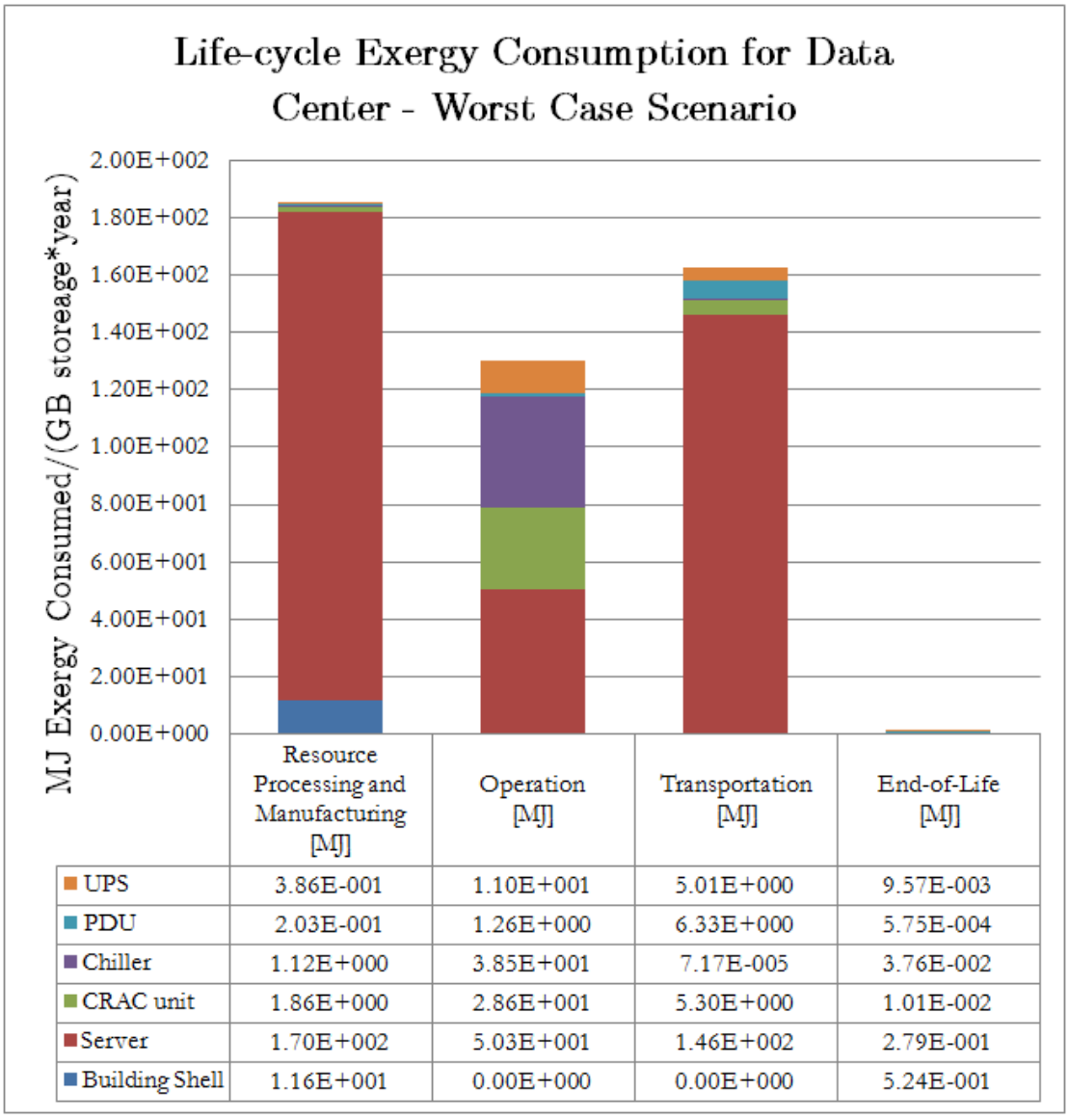

	Resource Processing and Manufacturing [MJ]	Operation [MJ]	Transportation [MJ]	End-of-Life [MJ]
UPS	3.86E-001	1.10E+001	5.01E+000	9.57E-003
PDU	2.03E-001	1.26E+000	6.33E+000	5.75E-004
Chiller	1.12E+000	3.85E+001	7.17E-005	3.76E-002
CRAC unit	1.86E+000	2.86E+001	5.30E+000	1.01E-002
Server	1.70E+002	5.03E+001	1.46E+002	2.79E-001
Building Shell	1.16E+001	0.00E+000	0.00E+000	5.24E-001

Figure 6.8: Worst case scenario for data center life-cycle exergy consumption.

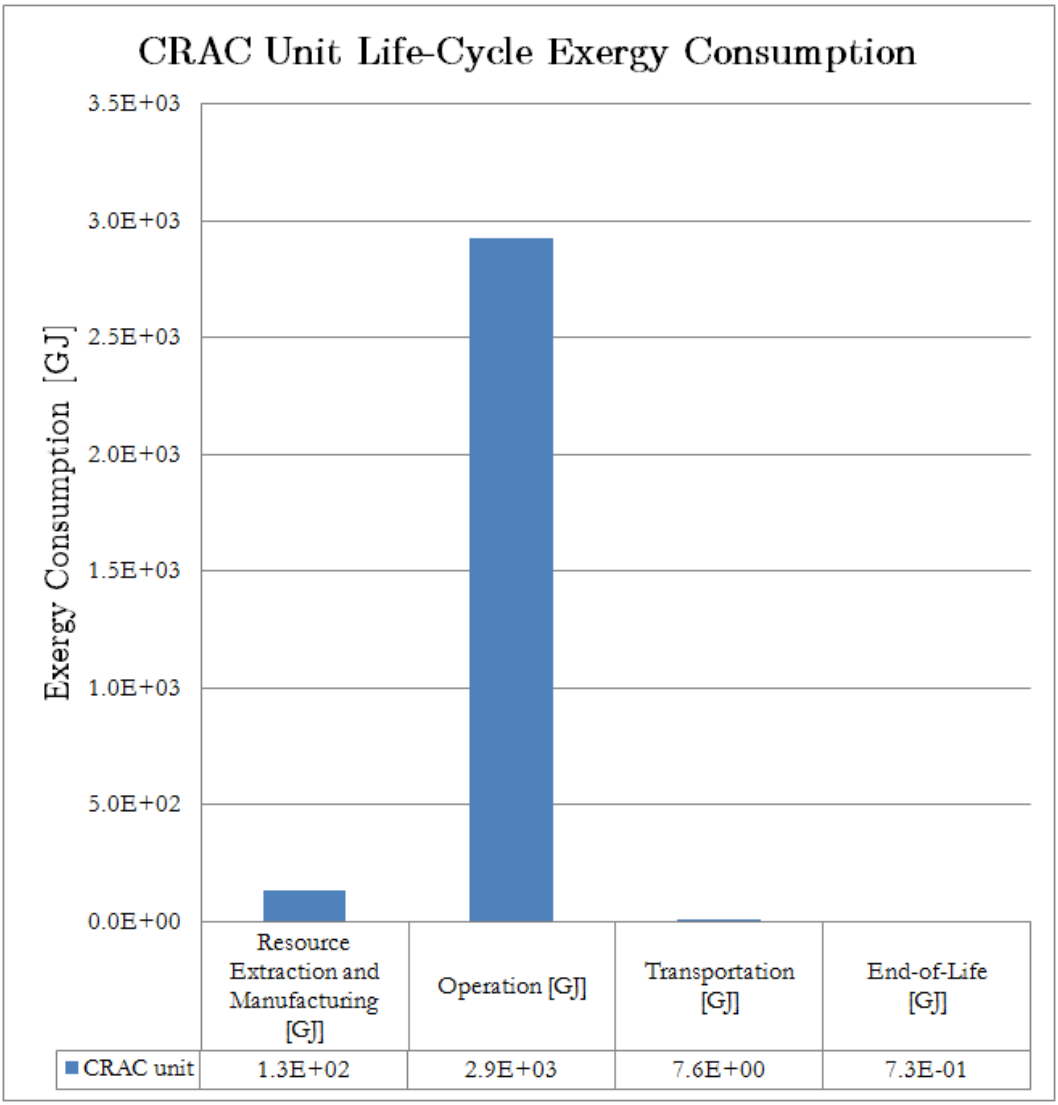

Figure 6.9: CRAC unit life-cycle exergy consumption.

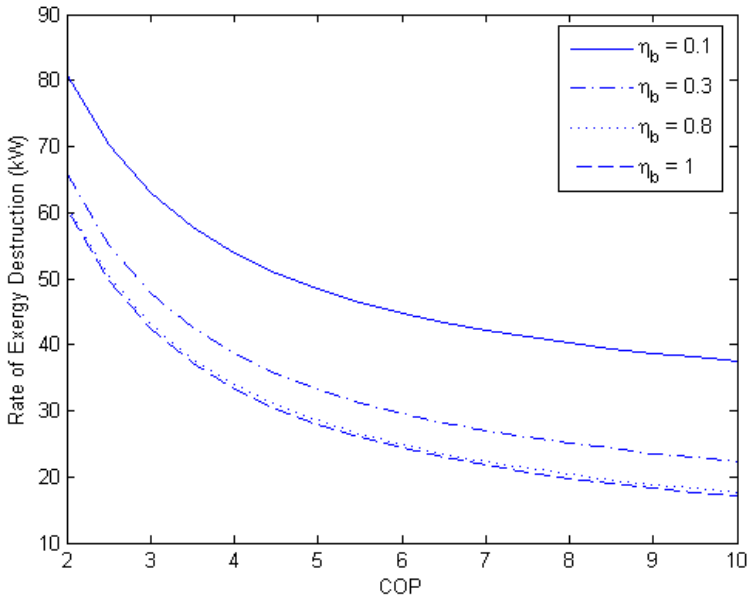

Figure 6.10: Exergy consumption rates as a function of COP for selected η_b.

cooling so that accurate estimates can be made for how much CRAC units can be turned down in times of decreased server use and thus cooling required.

Using the data in table 4.16, it was calculated that with the characteristic values of a CRAC unit, over its lifetime it will consume 2.92 TJ of exergy. In order to achieve this result, the COP, blower efficiency, and static pressure drop in the CRAC unit had to be found. From the data available, these parameters can only be found once the air flow rate is known. However, as derived in section 4.2.2, the air flow rate is dependent on COP, blower efficiency, and static pressure drop. To resolve this conflict, an iterative scheme was developed. First, an initial flow rate guess was calculated using an energy balance on the air traveling through the evaporator of the CRAC unit. This energy balance assumes that the blower is not present.

$$\dot{m}_a = \frac{\dot{Q}_c}{c_p(T_{return} - T_{supply})} \tag{6.1}$$

Using this guess, the analysis proceeds as described in section 4.2.2. When the mass flow rate of air is calculated, the guess is compared to the calculated value. If the guessed value of the air flow rate is not within $10^{-5}\%$ of the calculated airflow, the calculated airflow is used as a new guess. The iteration continues until it converges to the correct flow rate.

An analysis was performed to observe the sensitivity of the exergy destruction rate to the most interesting input parameters. In particular, the exergy destruction rate for varying COP and blower efficiencies are given in figures 6.10 and 6.11. As can be seen in figure

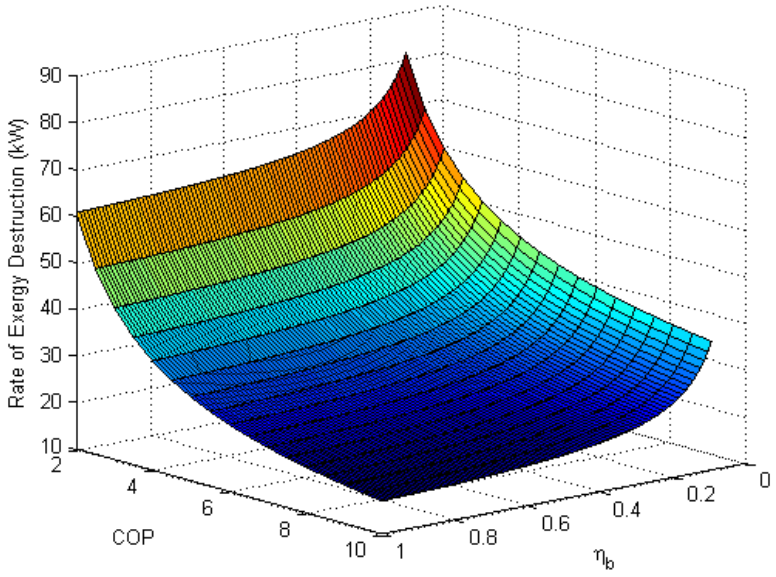

Figure 6.11: Exergy consumption rates as a function of COP and η_b.

6.10, increasing the COP results in less exergy being consumed than increasing the blower efficiency. This means it is more advantageous to increase the COP than the blower efficiency. The figure also shows that as blower efficiencies approach unity, the decrease in exergy consumption per unit increase in blower efficiency decreases drastically. Figure 6.11 suggests that increasing blower efficiencies more than 0.50 to 0.60 has little positive effect. There is a similar trend for COP values. After COP values of approximately 8 to 9, the exergy consumed levels off. Current blower technology already achieves efficiencies in the 0.50 to 0.60 range. However, current COP values are closer to 3 for the supply temperatures being considered. This suggests that a designer attempting to reduce the operational exergy consumption should focus attention on increasing the COP.

Chapter 7

Velocity and Temperature Field Modeling Results

This chapter outlines the results of the conventional CFD as well as the COMPACT predictions of temperature in a data center. Both the accuracy of the predictions as well as the speed at which the predictions were determined are analyzed. Subsequent sections show that acceptable predictions were achieved by both the ANSYS FLUENT and COMPACT models. Streamlines and temperature profiles generated by ANSYS FLUENT are shown in figures 7.1 and 7.2, and by COMPACT in figures 7.3 and 7.4. Accuracy of the predictions is quantified through three different temperature metrics: error as defined in equation 3.1, as well as maximum and mean temperature deviation. Temperature deviation is defined as

$$T_{deviation} = |T_{predicted} - T_{experiment}| \tag{7.1}$$

Two different sets of data were compared using these metrics. The first set of temperatures compare predicted and measured temperatures at the inlets of the servers only. These temperatures are the most important to predict accurately, since these temperatures must be kept below operational thresholds to ensure reliable operation. The second set of temperature data included all temperatures taken throughout the data center, including temperatures taken in front of, behind, to the side, and at the inlets and outlets of the servers.

The data center predictions were generated based on three sets of experimental data purposely constructed for different experimental conditions. Early versions of COMPACT development indicated that buoyancy and recirculation were an issue in terms of predictive accuracy. Experiments were conducted with increasing levels of recirculation to ascertain if vortex superposition could accurately predict temperature fields with different amounts of recirculation (recirculation is discussed throughout the thesis, but see sections 3.1 and 5.2 for a more thorough definition). Levels of recirculation were altered by changing the CRAC unit flow rates into the room while maintaining both the cold air supply temperature and

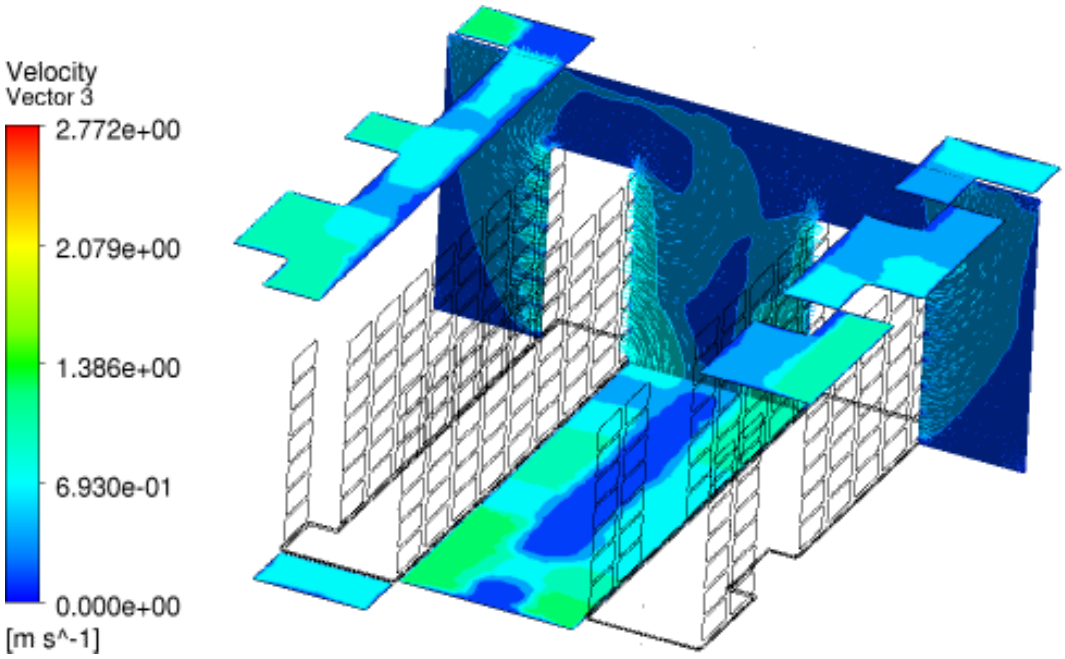

Figure 7.1: Velocity slice plot for FLUENT for experiment Run 5. Horizontal slices are flow through floor inlets and ceiling outlets; the vertical slice is a vector plot at x = 22 ft.

Table 7.1: Experiment recirculation summary.

Experimental Run Name	**Level of Recirculation**
Run 5	Lowest
Run 6	Medium
Run 7	Highest

the same level of flow through the severs. The lowest level of recirculation had high flow rates from the CRAC unit when compared to the flow rates through servers. Medium levels of recirculation were obtained by maintaining flow rates from the CRAC unit comparable to flow rates through the servers. High recirculation occurred when flow rates through the servers were larger than flow rates from the CRAC unit. Table 7.1 summarizes information about the three experimental data sets.

In additional to experimental runs, there were also different computational runs. These different computational runs had varying levels of mesh refinement. By default. FLUENT used non-uniform tetrahedral mesh elements. Therefore, there is no unique element size for a given number of elements that fill a room. The mesher was used to generate meshes of increasing number of elements. Table 7.2 summarizes the different names used in figures of this thesis to refer to different numbers of elements.

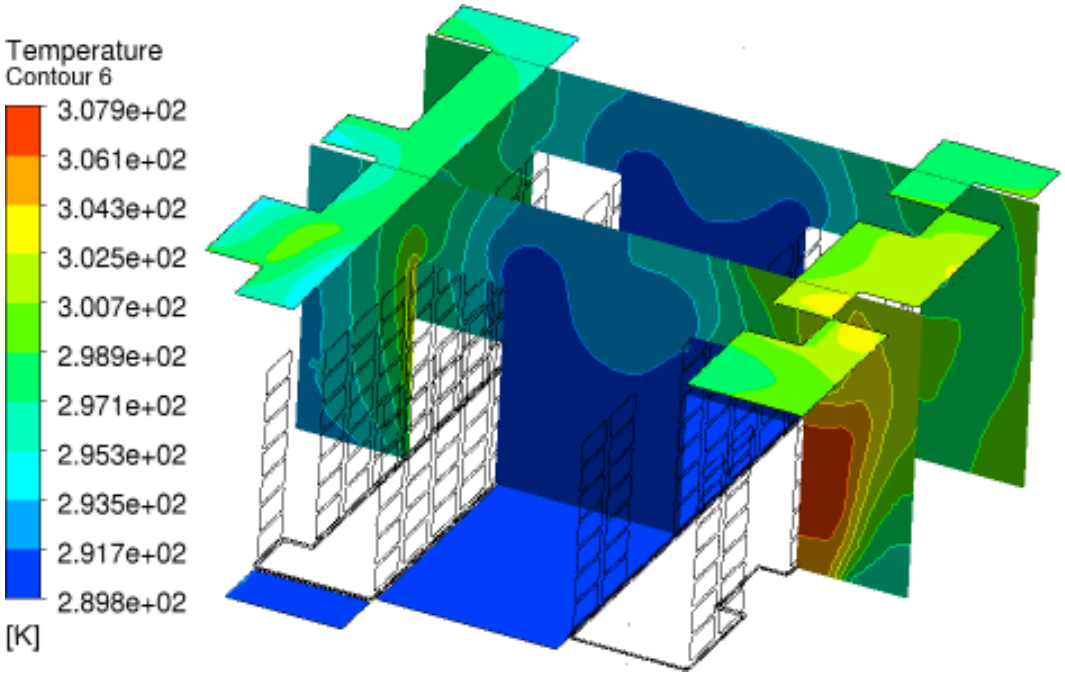

Figure 7.2: Temperature slice plot for FLUENT for experiment Run 5. Horizontal slices are air temperature at floor inlets and ceiling outlets; the vertical slices are at x = 14 ft and x = 22 ft.

Table 7.2: Name and number of elements for each computational run.

Computational Run Name	**Number of FLUENT Elements in Mesh**
Coarser3	954,606
Coarser	4,316,662
Try3	6,618,375
Finer1	8,169,179

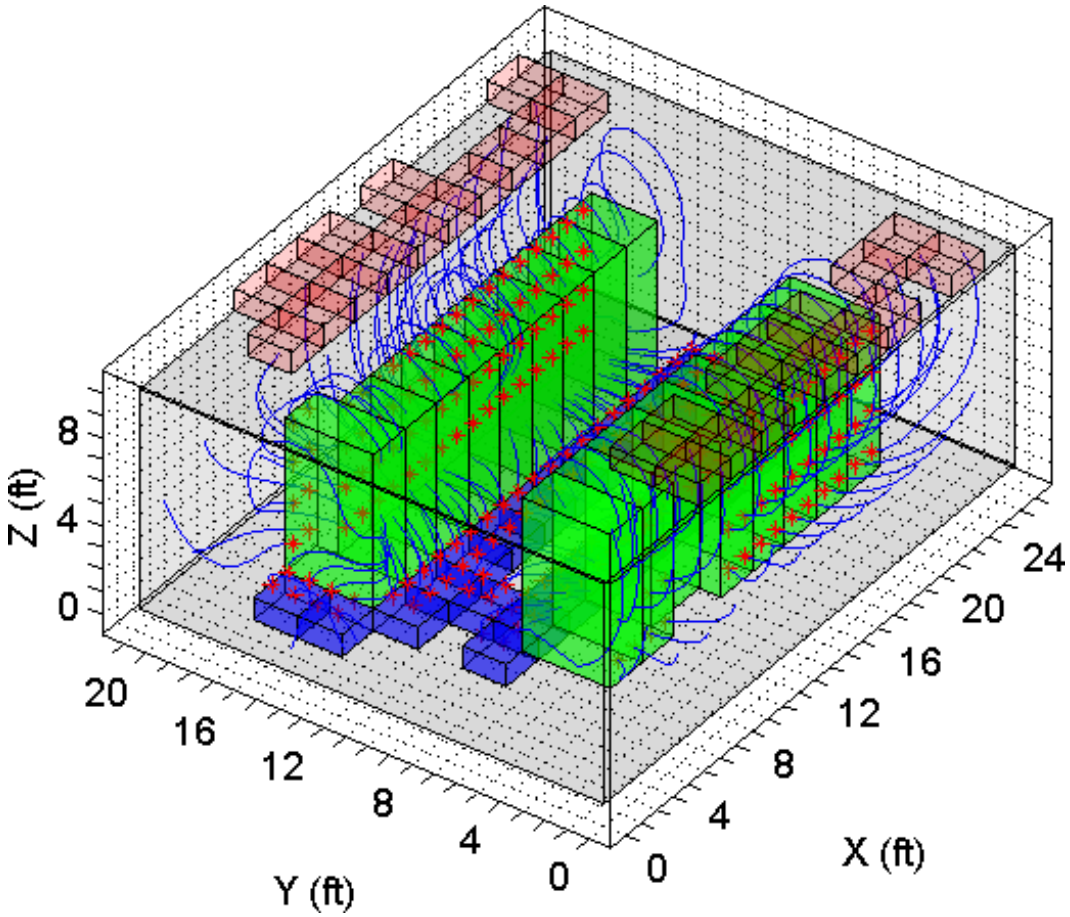

Figure 7.3: Streamline plot for optimized COMPACT for experiment Run 5. Streamlines originate from floor inlets and out-flowing server rack faces.

7.1 Conventional Computational Fluid Dynamics

7.1.1 Convergence Testing and Computational Time

It is important to ensure that FLUENT's predicted temperature field is the result of a converged simulation. This is vital since FLUENT is one standard to which COMPACT is going to be compared. ANSYS FLUENT's convergence criteria is dictated by the residuals calculated in the program. The residuals quantify the imbalance in the differential equations solved. If the solution predicted by FLUENT were the actual solution, the residuals would be zero. FLUENT seeks to drive these residuals towards zero, and when they reach an arbitrary small level, FLUENT considers the solution converged.

Since the residual limits are somewhat arbitrary, and in order to have full faith that the solutions predicted by FLUENT were indeed converged solutions, more work was done to ensure convergence. Studies were conducted to show that the temperature field solutions

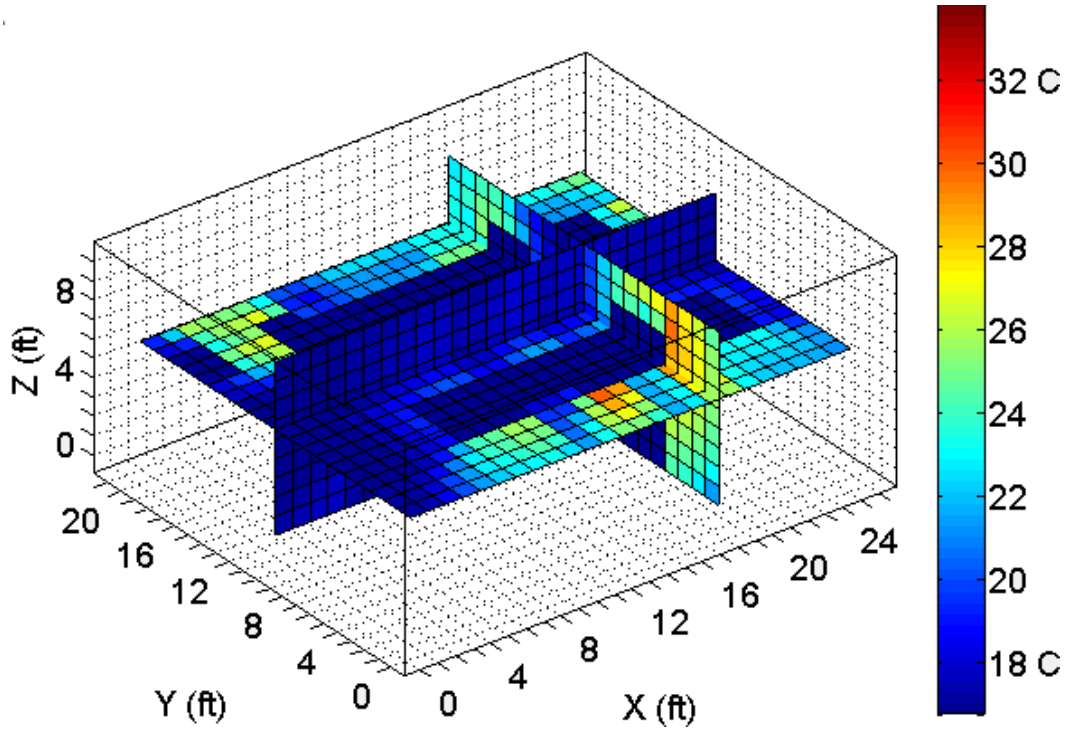

Figure 7.4: Temperature slice plot for optimized COMPACT for experiment Run 5. Slices are located at x = 18 ft, y = 10.5 ft, and z = 6 ft.

didn't deviate for lower arbitrary residuals (more iterations) or for finer mesh. A complete summary of results of the convergence study are included in the appendix of this thesis. Figures 7.5 and 7.6 are example results of the convergence study. A more thorough discussion of these figures is provided in the subsections below.

Testing Number of Iterations and Its Affect on Convergence

Figure 7.5 shows an example of a convergence study looking at number of iterations, or alternatively, residual size. The first important point to discuss is the definition of the temperature $T_{limit\ calculated}$. In order to quantify the error of a temperature predicted at a point, one could compare the predicted temperature to the true or converged temperature. Unfortunately, this true or converged temperature is not known ahead of time. Nonetheless, a temperature is still needed to compare the temperature prediction at a given point to obtain some measure of how close the temperature prediction is to being converged.

It seems reasonable that with more iterations the temperature prediction would settle down to a converged value. Ideally, as the iterations increased in number, the error between the prediction and true value would become smaller and smaller, and would decrease in magnitude for each successive iteration. If this is the case, the error would decrease as the inverse of the number of iterations. In addition, the predicted temperature would decrease

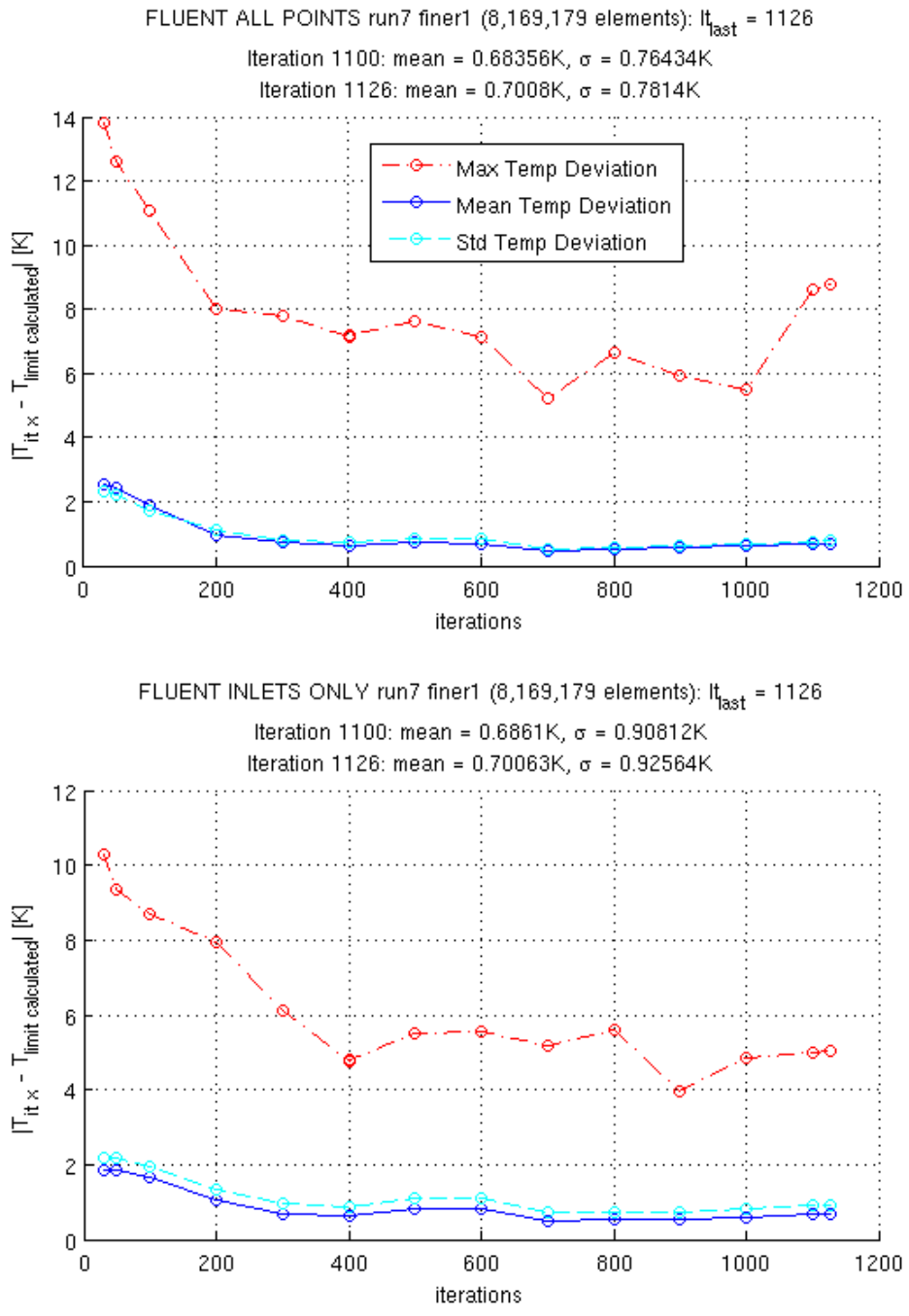

Figure 7.5: High level or recirculation case study: residual size (number of iterations convergence study) for finest mesh level.

as the inverse of the number of iterations to the final, converged temperature. This final temperature could then be described in the following equation:

$$T_{limit\ calculated} = A_1 \frac{1}{it} + A_2, \tag{7.2}$$

where A_1 and A_2 are fitting parameters and it is the iteration number. As the number of iterations goes to infinity, the first term goes to zero, and the final limiting temperature, named "limit calculated" would be the temperature the solution is heading towards. $T_{limit\ calculated}$ would then be known if A_2 were known. In order to find this constant, numerical fits were performed on the temperature predictions at each point. The entire procedure, including residual limits, went as follows:

1. FLUENT was used to solve for temperature fields in the data center. Every 100 iterations, the temperature field was saved. This was done until FLUENT reached the prescribed default residual threshold. The temperature field was also saved at the iteration number when the first residual limit was reached.

2. The residual threshold was decreased to half of the default value. The process described in step one was repeated until the new residual threshold was reached. At the final iteration, the temperature field was again saved.

3. For every point in the data center, the temperature history was constructed. A fit of the form in equation 7.2 was made for the temperature at each point. A_2 and thus $T_{limit\ calculated}$ was found for each point.

4. For each point where temperature was predicted, the temperature at every 100 iterations was compared to $T_{limit\ calculated}$. The absolute value of the temperature difference, termed "temperature deviation" in this thesis, was found for all points in the data center. There were millions of locations where this temperature deviation had been found. In order to draw conclusions about convergence from the many points, several subsets of these million points were examined. First, the average and maximum temperature deviations of all the points were found and plotted versus number of iterations. Second, a smaller subset of data was analyzed. The points within 10 cm of server inlets was given extra attention since temperature prediction in this area is most important. Figure 7.5 shows examples of plots of this form. A solution was considered converged if the average temperature deviation at all points went below and remained below 1 K.

Care must be taken when referring to every point in the data center. Traditionally, finite-volume methods (which is the method employed by FLUENT) calculate physical properties at the nodes of elements. Since different mesh configurations were used, vertices of mesh could not be used as locations to look at temperature histories since each mesh would have different node locations and thus different physical locations at which temperature was predicted. Instead, approximately 175,000 points were defined, and temperature histories were

created for the same 175,000 points for all mesh sizes and experimental runs (Runs 5, 6, and 7). The 175,000 were the vertices of the coarsest mesh, and were chosen to ensure that the locations would span the entire room and not be too spread apart. It was also computationally easiest to pick these points. 175,000 random points were also chosen in one study and it led to strikingly similar convergence plots. Since it seemed irrelevant whether totally random points or the vertices of the coarsest mesh where chosen, the 175,000 locations were chosen to be at the vertices of the coarsest mesh since this was the easiest path.

The steps in the list above were done for all four levels of mesh refinement for all three sets of experimental data. The other 11 plots analogous to figure 7.5 can be found in the appendix.

Testing Number of Elements and Its Effect on Convergence

Convergence is not only a function of the residual limit, but also the size of the mesh. A converged solution would be one in which the temperatures predicted no longer change with finer mesh. In the exact same fashion as was done for number of iterations, a convergence study was performed for number of elements. The exact same procedure was followed with one minor difference: rather than creating a temperature history as a function of iterations, a temperature history was created as a function of number of elements. Therefore, $T_{limit\ calculated}$ was calculated based on equation 7.3 for the mesh refinement study.

$$T_{limit\ calculated} = A_1 \frac{1}{M} + A_2, \tag{7.3}$$

In this equation, M is the number of elements. All of the temperatures used for a certain level of mesh resolution were from the last iteration for that mesh resolution. This was the iteration at which the residuals were twice as small as default in FLUENT.

As with the convergence study based on the number of iterations, a solution was considered converged if the average temperature deviation at all points went below and remained below 1 K for increasing number of elements. Figure 7.6 shows the results of the mesh refinement study for Run 7. The other 11 mesh refinement plots are included in the appendix.

Computational Time

Depending on the number of iterations and elements, the amount of time needed to reach a solution varies. In all cases, it was found that halving the residual size resulted in negligible changes in average temperature deviations. It was also found that increasing the number of elements above the second coarsest level, 4,316,662 elements, had negligible effect on the average temperature deviation. For this reason, table 7.3 summarizes the amount of time needed to achieve temperature predictions for the three different experimental runs with the default FLUENT residual and with 4,316,662 elements.

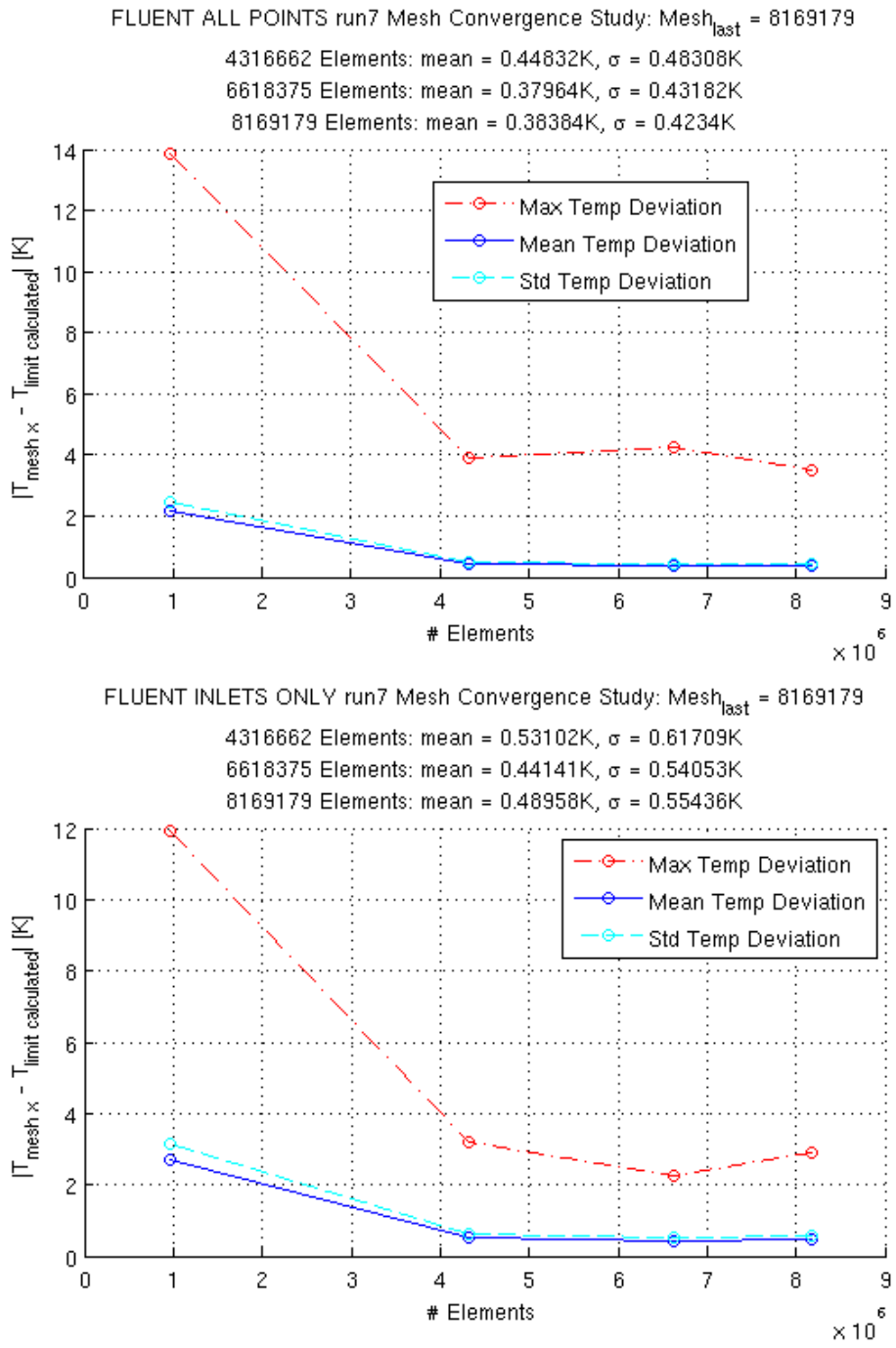

Figure 7.6: High level or recirculation case study: mesh size convergence study.

Table 7.3: Comparison between FLUENT temperature prediction and experiment as well as computational time (default FLUENT residual limit, 4,316,662 elements).

	$T_{deviation} = \lvert T_{FLUENT} - T_{experiment} \rvert$ [K]				Convergence	
Experiment	All Points		Inlets Only			
Run Name	Max	Mean	Max	Mean	Iterations	Time [S]
Run 5	13.5	3.1	5.3	1.2	369	22,000
Run 6	17.4	3.3	6.4	1.5	514	31,000
Run 7	17.8	4.6	10.6	2.9	431	26,000

7.1.2 Temperature and Flow Prediction - Comparison to experiment

Comparisons of FLUENT's temperature predictions to experimental results were satisfactory overall and better at the inlets to the servers. Temperature deviation and error, as described by equations 7.1 and 3.1, respectively, were used as metrics for predictive accuracy. Figures 7.7 and 7.8 summarize these metrics for Run 5, and figures 7.9 and 7.10 summarize these metrics for Runs 6 and 7, respectively. Table 7.3 also summarizes the highlights of the FLUENT and experiment comparison.

Figure 7.7 shows that the maximum temperature deviation for all points in Run 5 is approximately 14 K. The average error for all points is approximately 3.1 K. The predictions get better when comparing temperatures only at server inlets. In this case, the maximum temperature deviation is approximately 5.3 K, while the average deviation is approximately 1.2 K.

Figure 7.8 shows that the error metric in this thesis is unusable. The reason for this is because the uncertainty in the measurements is too large for this metric. This happens for a combination of two reasons illuminated by looking at the uncertainty equation for the error metric. Note in equation 7.4, u stands for uncertainty, u_{TC} is the uncertainty in a thermocouple reading, and $u_{temp\ variation}$ is the uncertainty due to temperature variation in a measurement. The combination of u_{TC} and $u_{tempvariation}$ is the total uncertainty in the measurement.

$$u_{error\ metric} = \sqrt{\frac{(T_{c,in} - T_{sim})^2}{(T_{exp} - T_{c,in})^4}(u_{TC}^2 + u_{temp\ variation}^2)} \tag{7.4}$$

First, the combined uncertainty in an experimental measurement was fairly high. This estimate comes from two components: one component due to the inherent inaccuracy of the thermocouples used, and the second component due to the variation in the temperatures measured. The inherent inaccuracy of the T-type thermocouples used is 1 K in the temperature range of the experiments. The temperature variation uncertainty is due to the temperature measurement varying over time. This is a result of approximating the transient data center as steady state. This uncertainty is two standard deviations of the tempera-

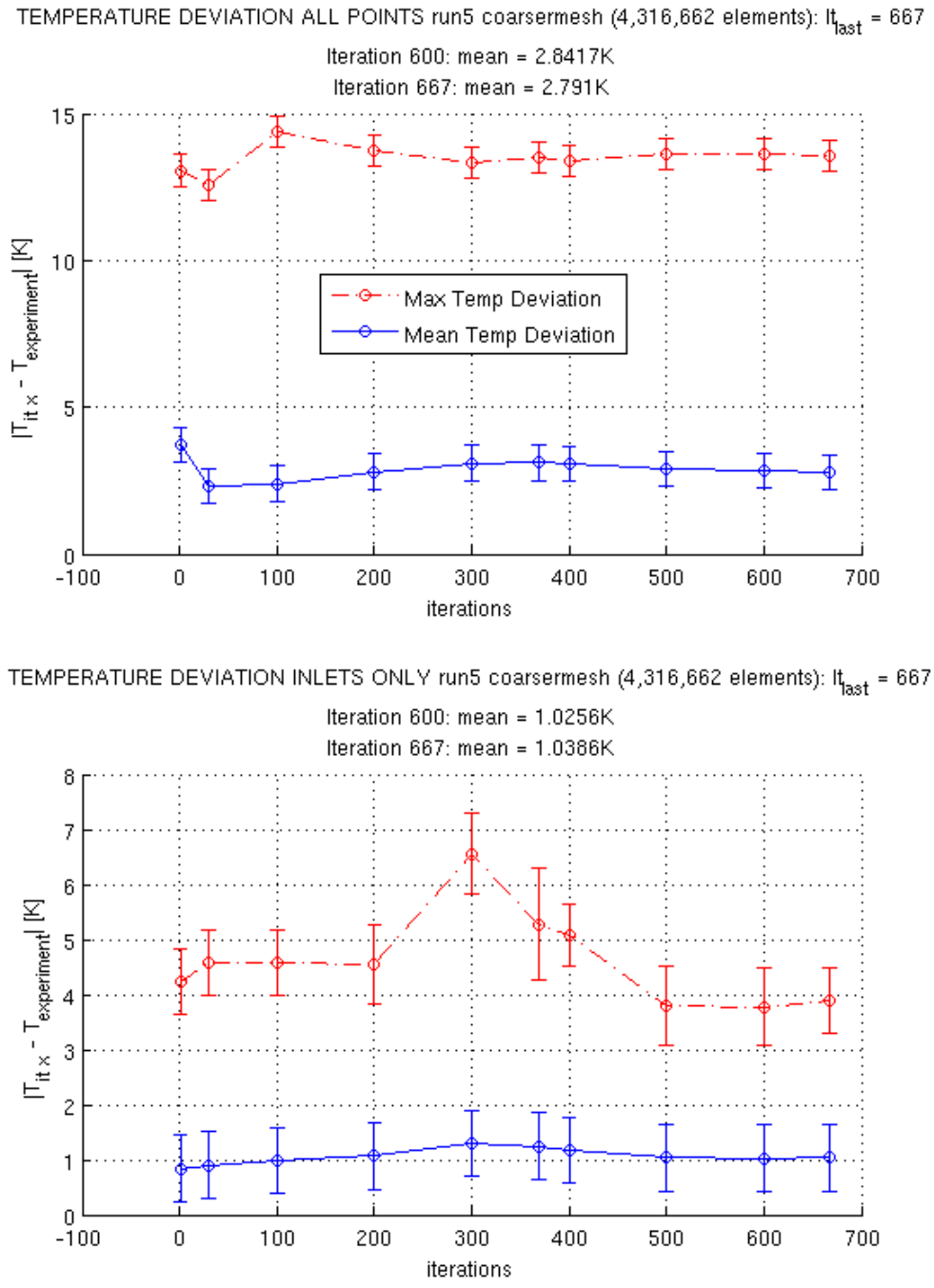

Figure 7.7: Experimental temperature deviation for Run 5.

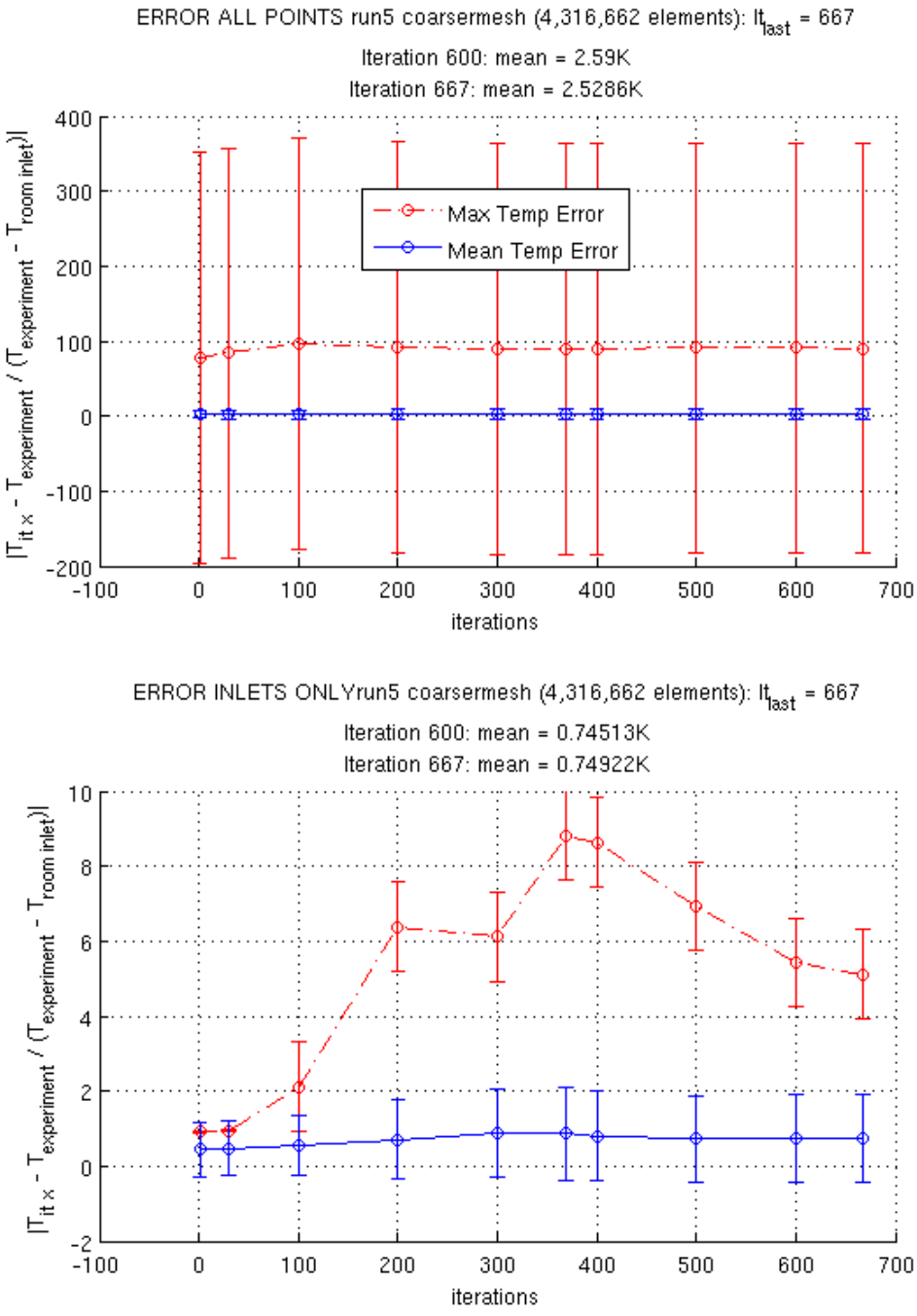

Figure 7.8: Experimental temperature error for Run 5.

ture measurement to attain 95% confidence. The temperature varying uncertainty changed depending on the measurement, but was usually around 0.4 K. The second reason that $u_{error\ metric}$ is high is because in many places $T_{exp} - T_{c,in}$ was very small. Since this term is in the denominator, and is raised to an integer power, this makes the uncertainty high. This could only be countered by a very accurate temperature reading, which as just outlined, wasn't the case. For this reason, the error metric was not used in this thesis as it was in [74] where an actual steady-state data center was modeled.

Figure 7.9 has an average temperature deviation at the inlets of 1.5 K, and figure 7.10 has an average temperature deviation at the inlets of 2.9 K. This shows that with increasing recirculation FLUENT becomes less accurate.

FLUENT has built in flow visualization tools. Strategic slice plots showing velocity contours and vector fields help to visualize the recirculation occurring in the data center. Figures 7.11 and 7.12 show such recirculation in the Run 7 simulation results. In these plots, the blank areas are something structural in the room and are blank because only the velocity field is being viewed. In figure 7.11, the semi-circular blank spots are room support columns and the rectangular blank spots are rows of server racks. In figure 7.11, the rectangular blank spots are again rows of server racks. In figure 7.11, it can be seen that a vortex is predicted above the right row of server racks. The vector field shows that air is flowing downward in the cold aisle. This is the exact opposite of what is desired, as this is a case of warm air being recirculated downward into the cold aisle. Recirculation can also occur around the sizes of the racks as is the case in figure 7.12. Towards the top of this figure, warm air is being recirculated around the ends of the server racks and flowing from the hot aisle to the cold aisle. Similar plots examining Run 5 of this study, the case with the lowest amount of recirculation possible in our experimental setup, also had recirculation occurring. These figures, and the fact that recirculation was present even in the case where it was minimized as much as possible, indicate that recirculation is indeed a phenomenon that data center designers must be concerned with.

7.2 Potential Flow Modeling

7.2.1 Convergence Testing and Computational Time

Just like FLUENT, COMPACT had to undergo analysis to ensure that convergence was achieved. COMPACT is not an iterative solver, so there were no iterations to test, but mesh sensitivity still had to be be analyzed. There were three sets of mesh analyses, and their important features are summarized in table 7.4.

As in the case of the FLUENT mesh sensitivity analyses, $T_{limit\ calculated}$ was found and used as a temperature of comparison for all points. The same 175,000 points were looked at in the COMPACT studies as in all the FLUENT studies. Figures 7.13, 7.14, and 7.15, for Runs 5, 6, and 7, respectively, show the results of the mesh refinement study.

Based on these figures, the solution generated with the lowest number of elements was

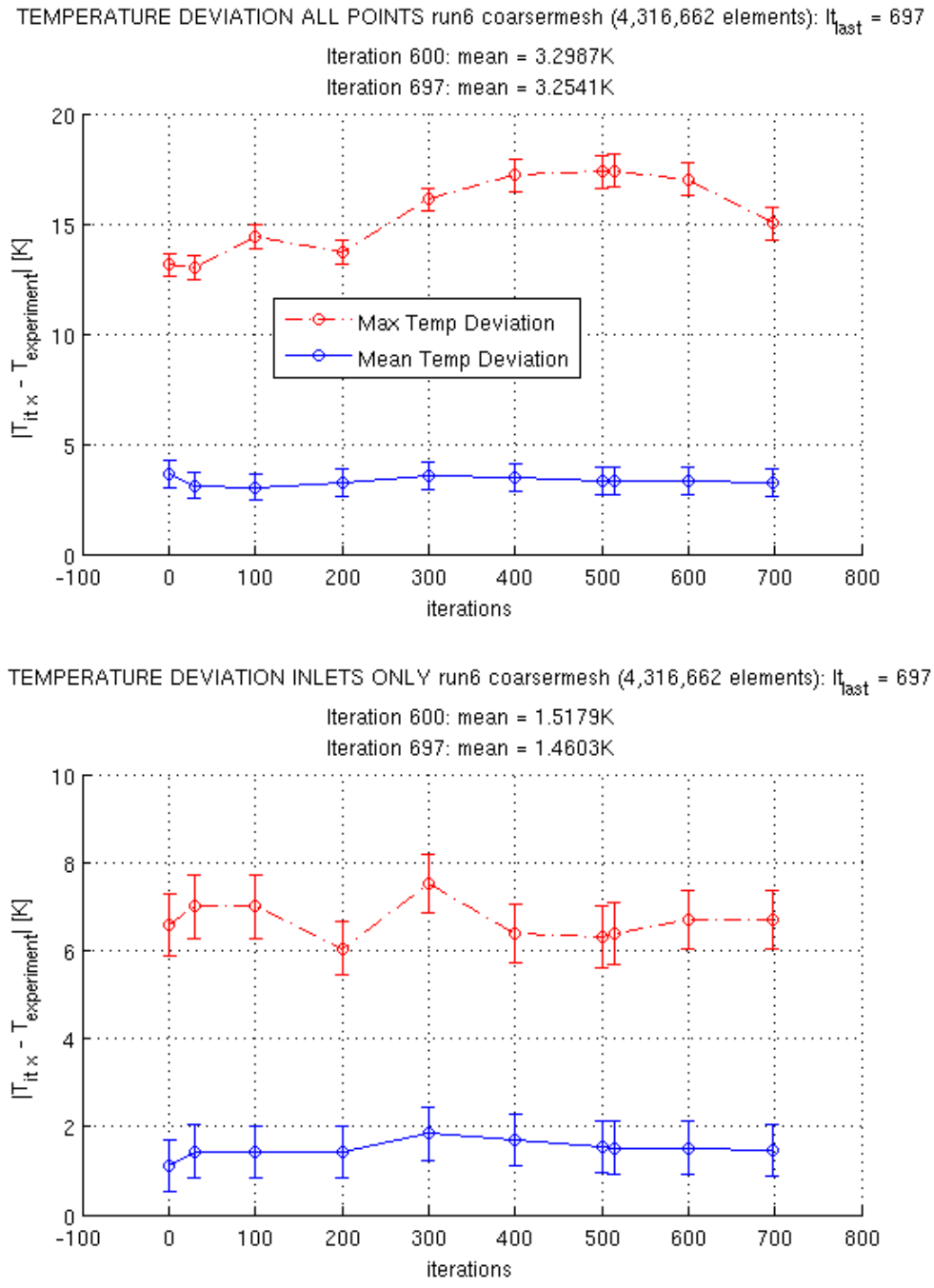

Figure 7.9: Experimental temperature deviation for Run 6.

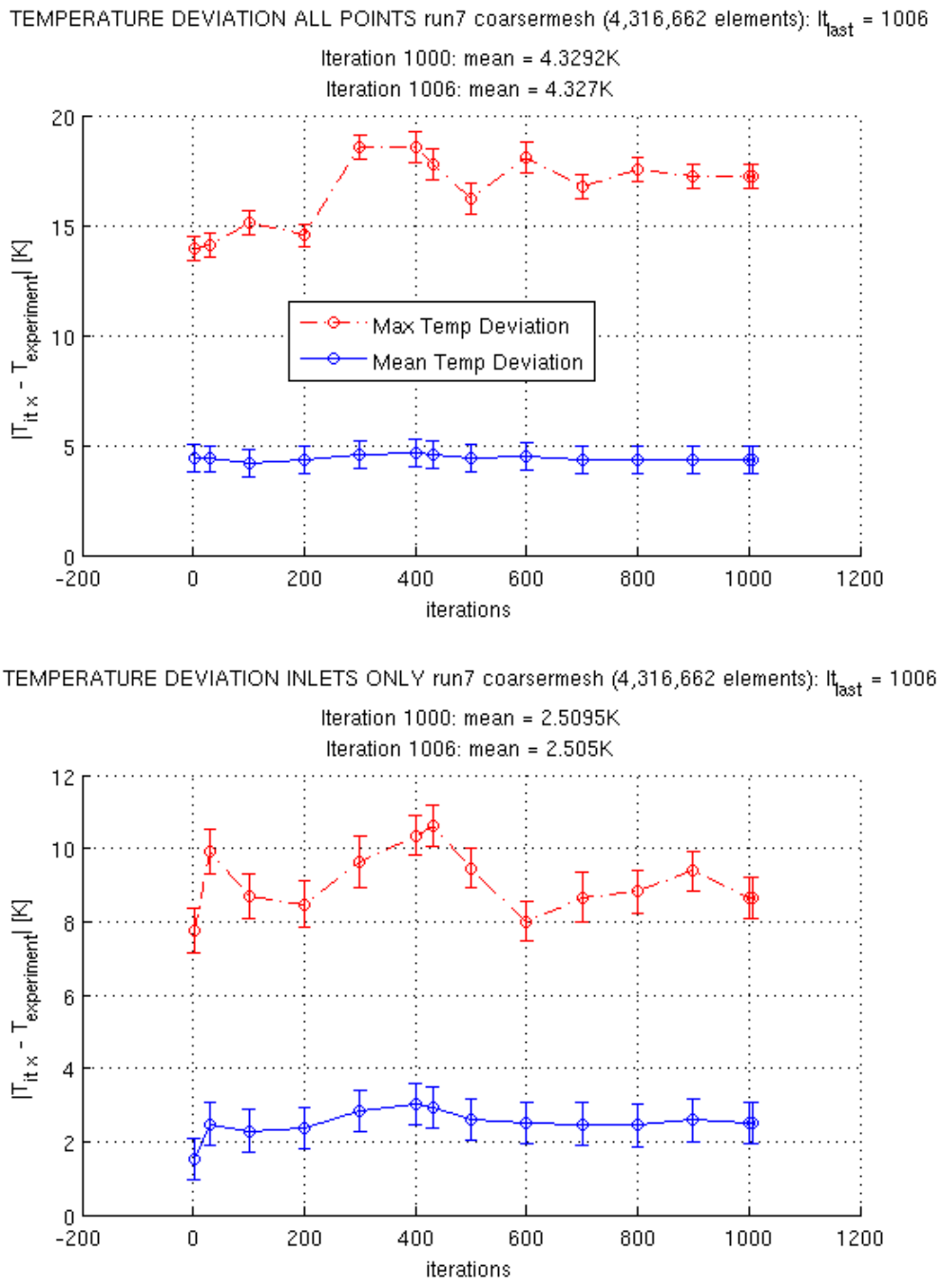

Figure 7.10: Experimental temperature deviation for Run 7.

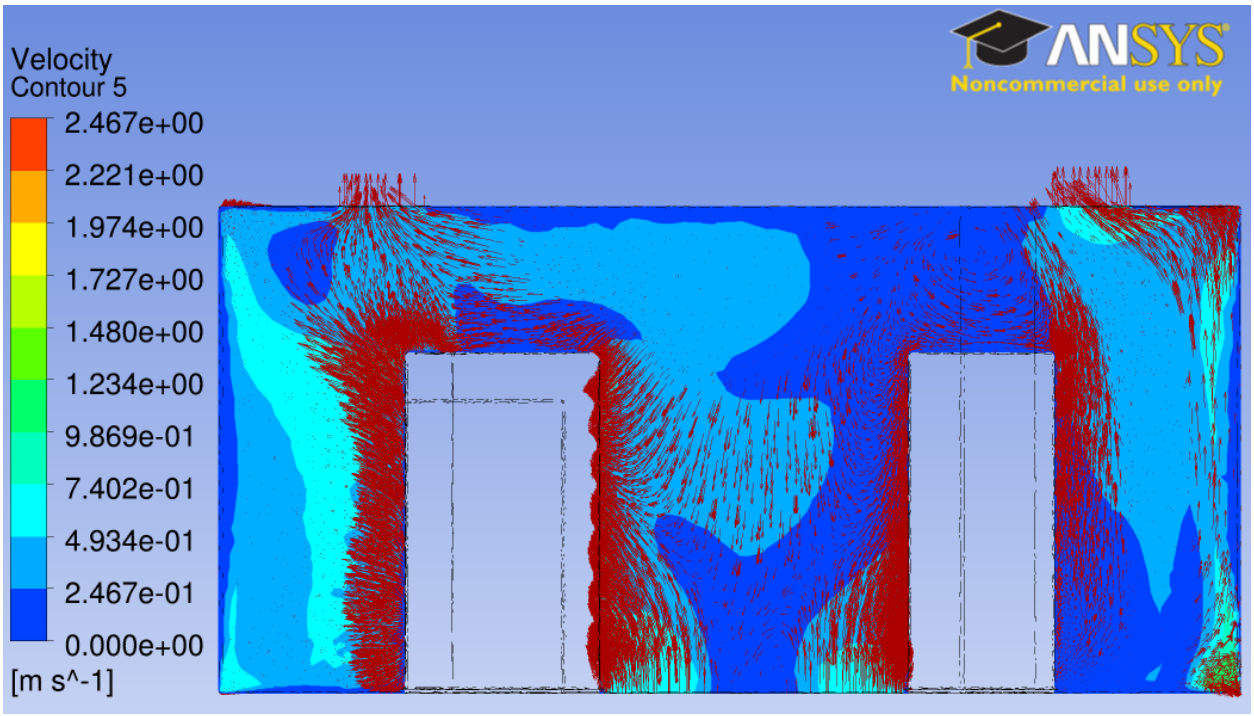

Figure 7.11: Side view of recirculation for Run 7. Slice plots are at 4 meters from data center wall.

Table 7.4: Element summary for COMPACT mesh sensitivity analysis.

Experiment Run	Mesh Fineness	Number of Elements
Run 5,6,7	Coarse	4,461
	Medium	35,688
	Fine	120,477

considered close enough to $T_{limit\ calculated}$ to be considered the converged temperature for all three experimental runs. The same criteria was used as in the FLUENT study: namely, once the mean temperature deviation went below and remained below 1 K, the solution was considered converged. In all three cases, the solution was found in approximately 4 seconds.

7.2.2 Temperature and Flow Prediction - Comparison to experiment

Table 7.5 highlights the max and mean temperature deviation between COMPACT and experiment. These values are considerable lower than the same values for FLUENT.

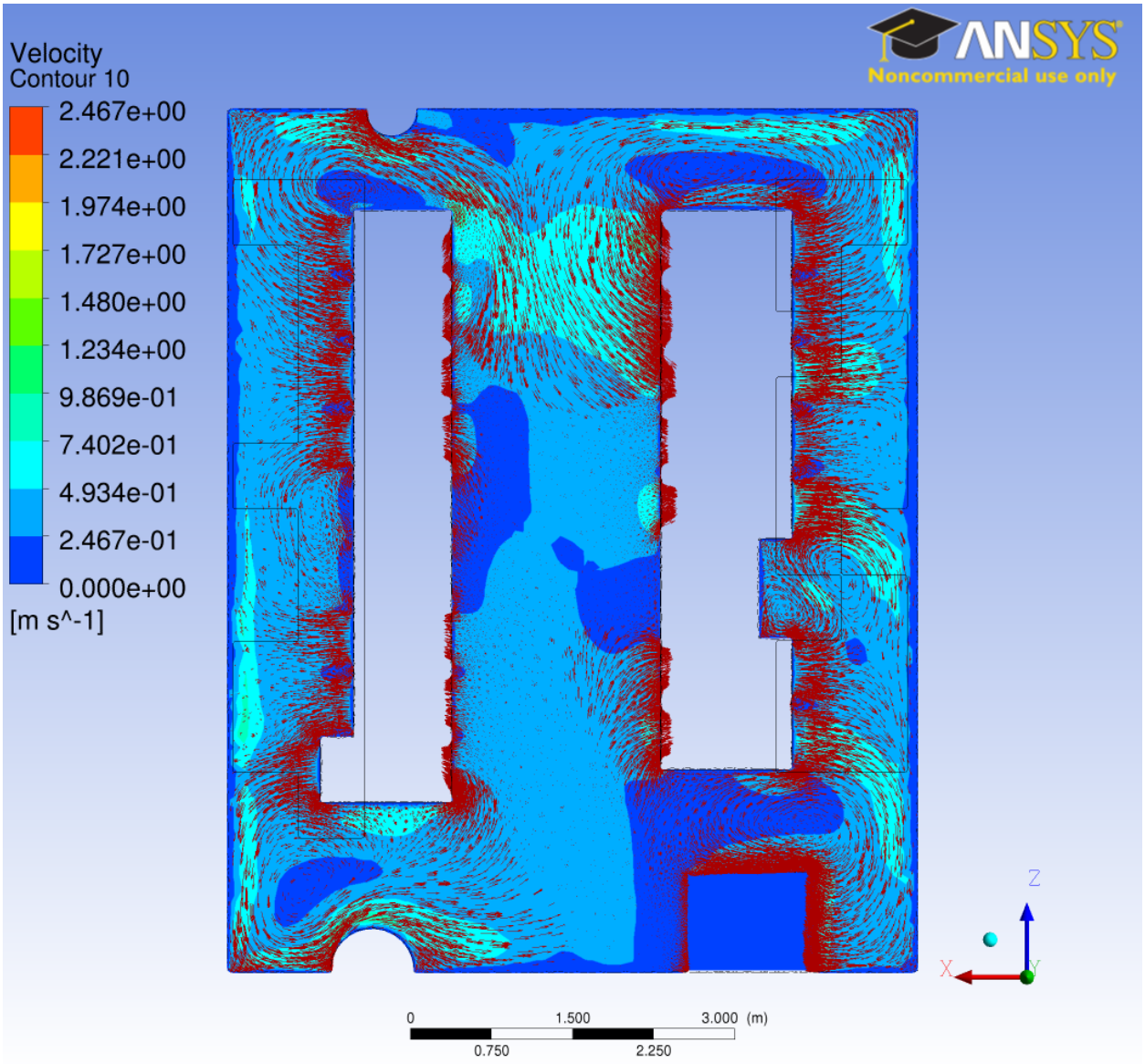

Figure 7.12: Top view of recirculation for Run 7. Slice plots are at 1.8 meters above floor of data center.

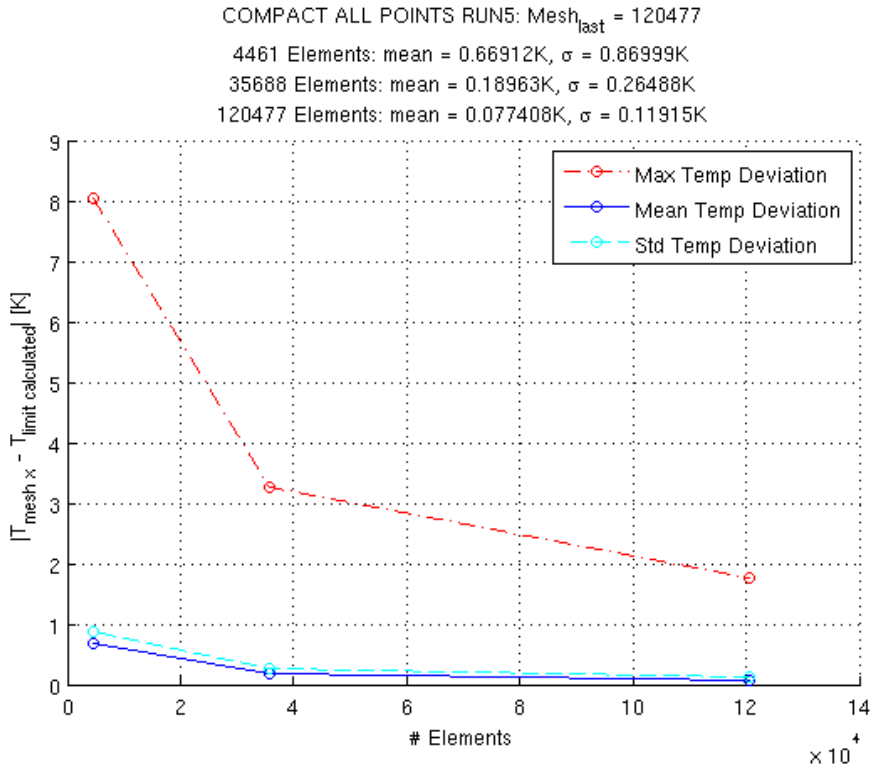

Figure 7.13: Low level or recirculation case study: mesh size convergence study.

Table 7.5: COMPACT comparison to experiment and computational time. Number of iterations is not applicable (NA) since COMPACT is not an iterative solver.

Experiment Run Name	$T_{deviation} = \lvert T_{COMPACT} - T_{experiment} \rvert$ **[K]**				**Convergence**	
	All Points		**Inlets Only**			
	Max	**Mean**	**Max**	**Mean**	**Iterations**	**Time [S]**
Run 5	5.6	1.2	2.4	0.7	NA	~4
Run 6	6.8	1.5	3.8	1.1	NA	~4
Run 7	8.1	1.7	5.3	1.5	NA	~4

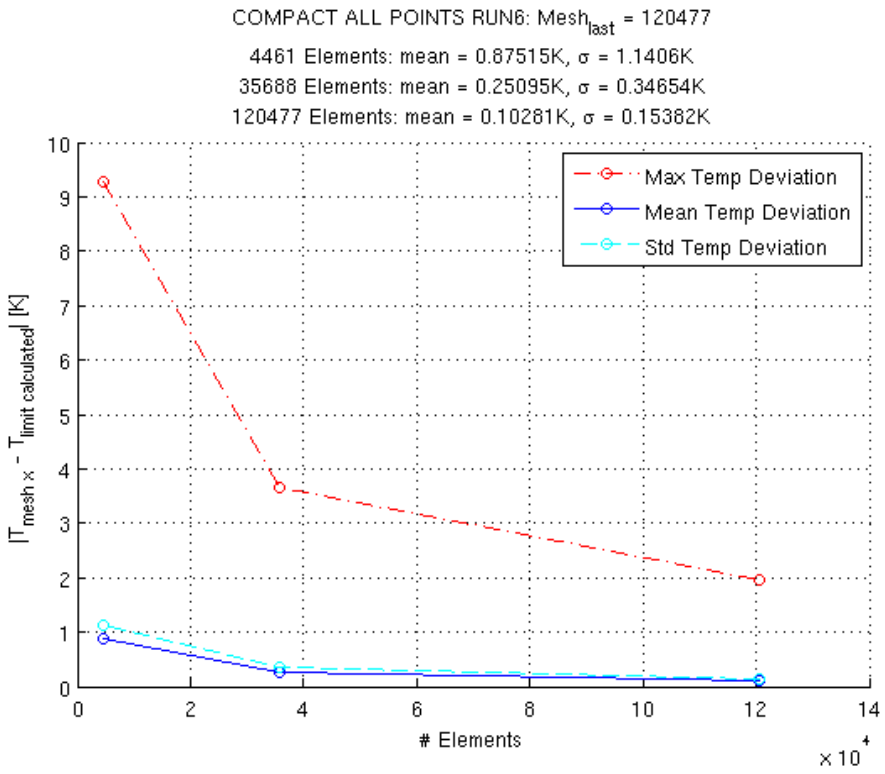

Figure 7.14: Medium level or recirculation case study: mesh size convergence study.

Table 7.6: Experimental run summary.

Experimental Run Name	**Rate of Exergy Consumption [W]**
Run 5	616
Run 6	775
Run 7	931

7.2.3 Exergy Consumption Due to Flow Mixing

The exergy consumed in the flow field due to mixing was calculated for the three runs and is shown in table 7.6. The table shows that increasing levels of recirculation result in more exergy destruction.

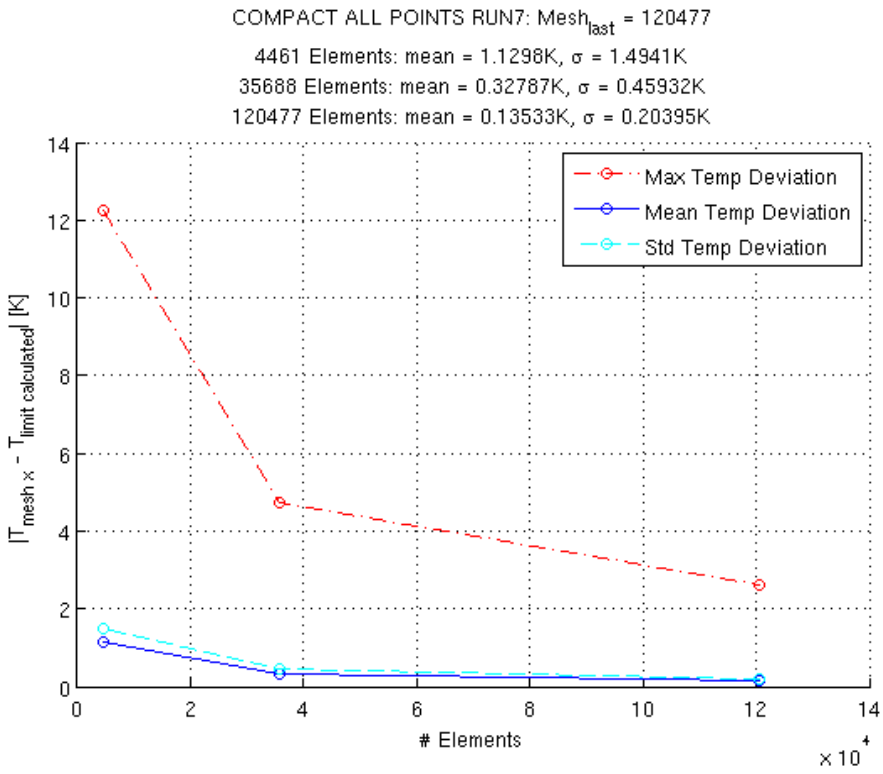

Figure 7.15: High level or recirculation case study: mesh size convergence study.

7.3 Temperature Comparison Between COMPACT and FLUENT

Table 7.7 highlights the max and mean deviations, as well as difference in computation time, between COMPACT and FLUENT at the 286 points where temperature was measured. The table shows that COMPACT and FLUENT had very large maximum deviations throughout the entire room, but average deviations at server inlets were acceptable.

Table 7.7: COMPACT comparison to FLUENT ($T_{deviation}$ and computation time).

Experiment Run Name	$T_{deviation} = \lvert T_{FLUENT} - T_{COMPACT} \rvert$ **[K]**				**Convergence**
	All Points		**Inlets Only**		**Computation Time Ratio** $\frac{TimeFLUENT}{TimeCOMPACT}$
	Max	**Mean**	**Max**	**Mean**	
Run 5	15.1	3.9	6.5	1.1	5,500
Run 6	19.9	4.2	7.6	1.4	7,750
Run 7	20.9	5.8	11.5	3.2	6,500

Chapter 8

Discussion of Results

8.1 Sustainability Discussion

The fictitious data center constructed matches well with traditional data centers. The power distribution in the fictitious data center is given in figure 8.1, and the total power usage of the data center is approximately 2.5 MW. Both the power distribution and the total power usage are in the range of typical data centers of its size and location. A measure of data center efficiency, the power usage effectiveness, was also in the correct range for a data center of this size. Power usage effectiveness (PUE) is defined as the total power used to run the data center divided by the powers of the computers in the data center. Typical PUE values are in the range of 1.5 - 2.5 [34]. The PUE for this fictitious data center is 1.9, which is slightly more efficient than typical data centers but within the range of normal. It is believed this fictitious data center is slightly more efficient than average due to the stated omissions in the HVAC system, namely the cooling towers.

As is often assumed but not necessarily quantified, in terms of both global warming potential and life-cycle exergy consumption, operation is much more influential than other life-cycle stages. When a sensitivity analysis was performed, under worst case scenario, the resource extraction and manufacturing life-cycle leg approaches or exceeds the operation leg, depending on whether the LCA or LCEA results are used. It is clear from figures 6.4 and 6.8 that the cause for large increase in the resource extraction and manufacturing is the short life-time assumed for the server. This new shorter lifetime is perhaps possible if server technology advances at a rapid pace. Computer servers are very energy intensive pieces of equipment made from highly ordered materials, and the large amounts of energy and relatively rare materials used to make the servers corresponds to a large global warming potential but an even larger life-cycle exergy consumption. Since, under the worst case scenario, servers are being replaced every year, there is a large global warming potential and exergy consumption incurred every year as new servers are being manufactured. While it is true that computer technology is advancing at a rapid pace compared to HVAC, transportation, and end-of-life equipment, it is unlikely that servers would be replaced every year. Figure 6.3 shows that

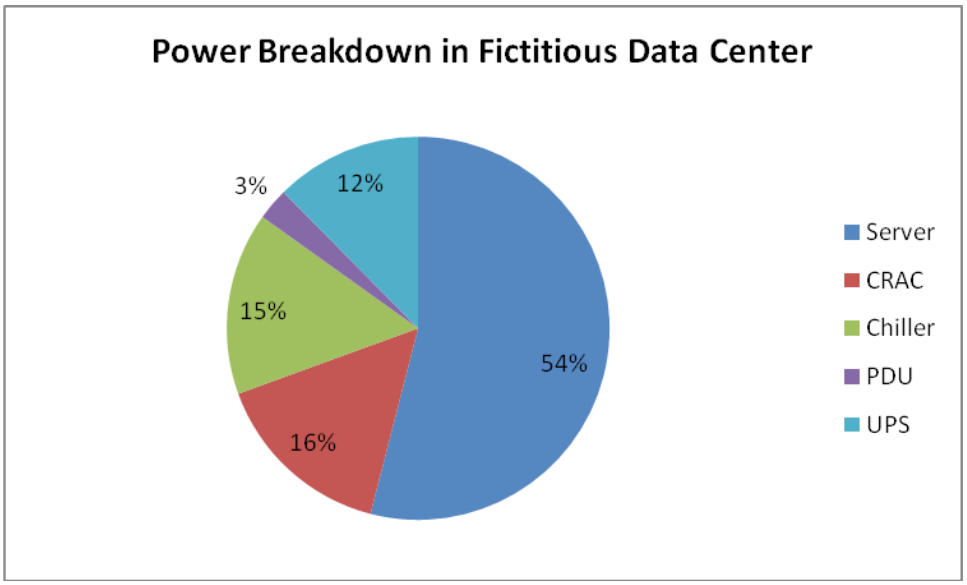

Figure 8.1: Power breakdown in fictitious data center.

under the best case scenario, the operational global warming potential still exceeds resource extraction and manufacturing, the next closest life-cycle leg, by a factor of four. A similar trend is shown for life-cycle exergy consumption in figure 6.7. The reason for the difference in transportation for the worst case scenarios between the LCA and LCEA studies has to do with the global warming potential and life-cycle exergy consumption environmental factors used for air travel. For global warming potential, the global warming potential is roughly one order of magnitude worse for air than ship. For life-cycle exergy consumption, the difference is two orders of magnitude. Based on the LCA and LCEA results, it is recommended that a data center designer or operator focus on the operational leg of the life-cycle, while at the same time ensuring that servers are used for several years rather than a single year, to improve environmental performance. This will likely not only reap environmental benefits but also monetary savings.

Table 6.2 shows that some data in this study was not as strong as it could be. Also, as discussed throughout the report, some data center equipment was omitted. For example, switches, ducting, piping, cable, and cooling towers as well as general data center maintenance were not modeled. The largest reason for these model weaknesses was lack of good, available data. Efforts should continue to be made to obtain better and more data to obtain a more accurate and complete analysis of the life-cycle exergy consumption or global warming potential of a data center. However, while some data is missing and other data is not particularly strong, the results of this study are still useful. It is unlikely that future, better data will change the trends found in this study. The largest components of the data center were analyzed and they all showed the same trend of having by far the largest global warming potential from the operation leg.

8.2 Velocity and Temperature Field Prediction Discussions

The goal of the temperature prediction portion of this study is to compare the accuracy and computational expense of a commercial CFD code with full physics modeling to a simpler potential flow based model. Tables 7.3 and 7.5 show that COMPACT was most accurate predictive tool overall. COMPACT performed very well, better than FLUENT considering mean deviation in temperature prediction at all points measured. COMPACT still has large deviation when looking at the temperature deviation with experimental measurements throughout the room. The largest deviation for optimized COMPACT was approximately 8 K. However, the maximum deviation for FLUENT was approximately 18 K. Error in prescribing boundary conditions could be contributing to the deviation in both COMPACT and FLUENT. One such example of boundary condition error was observed cold air leakage from the under floor plenum below one of the racks. Since the leakage was below one of the racks, it was nearly impossible to quantify. However, this rack was one of the racks with the largest temperature deviation.

Temperature deviation for both COMPACT and FLUENT is much smaller at inlet faces as compared to the entire room. This is a promising result, as predicting temperature at the inlet faces of the servers is the ultimate goal of data center designers and operators. When looking just at inlet temperature predictions, tables 7.3 and 7.5 show that the optimized COMPACT prediction has a smaller temperature deviation than FLUENT. It is important to note that the COMPACT prediction was tuned to minimize this error, so these results are not surprising. The superposed Rankine vortex strength is roughly based on theory, but has a vortex strength factor that was tuned to minimize errors. Future work could ascertain if the tuned potential flow will perform as well under different data center geometries and configurations. Irrespective of what future studies may find, this study shows that a properly tuned COMPACT model can accurately predict temperatures at inlets of server racks to within 0.7 K on average or 5.3 K at worst. Even if future work reveals this is the extent of COMPACTs capabilities, COMPACT will still be useful as a real time controller. After being tuned or calibrated, this work shows that COMPACT will be able to predict temperatures in the event of dynamic IT loading or cooling equipment failure.

The comparison of the COMPACT and FLUENT temperature predictions with each other showed very close agreement in some areas. COMPACT predictions were within 1-3 K of FLUENT predictions at server rack inlets. When considering the entire room, rather than just the temperatures at the inlets of the racks, COMPACT did not compare as well to FLUENT. However, the results shows that COMPACT can produce similar estimates to FLUENT in the areas of a data center that matter the most, and more importantly, is better at predicted temperatures than FLUENT. These conclusions are true for all levels or recirculation in the data center. It was found that increasing recirculation levels led to larger temperature deviations for both FLUENT and COMPACT, but in all cases COMPACT had smaller temperature deviations than FLUENT.

The total rate of exergy consumption calculated by COMPACT is not necessarily useful by itself. The exergy consumption field can be used to visualize where mixing is occurring in the data center. Eliminating these areas of mixing will lead to more efficient cooling. In addition, when combined with other life-cycle exergy consumption calculations, exergy consumption in the room can be compared to other instances of life-cycle exergy destruction. This is desirable because it will aid in identifying the most inefficient stages of a data centers life-cycle. Table 7.6 lists the rate of exergy consumption for the different experiments. The exergy consumption values show that exergy consumption due to mixing in the room is negligible when compared to the entire life-cycle, since the 600-1000 W of exergy consumption is less exergy consumption than by a couple servers.

COMPACT had a much lower computational expense than FLUENT. For Run 5, the optimized COMPACT model predicted the temperature and velocity fields for in approximately 6 seconds on a 2008 Dell laptop with a 2.16 GHz Core 2 DUO processor and 3 GB of ram. The FLUENT model took approximately 6 hours to converge on a 2010 workstation with better specifications in every category, most notably a faster processor and RAM. COMPACT was also run on the 2010 workstation for a more fair comparison, resulting in a reduced run-time of 4 seconds. Table 7.7 shows that depending on the experiment run number, COMPACT was 5,500-7,500 times faster than FLUENT.

8.3 Sustainability Case Study Example: Brick and Mortar vs. Shipping Container Data Center

A simple example shows the utility of these two modeling tools. Someone interested in building a new data center could be confronted with two choices: build a traditional bricks and mortar data center or building a modular shipping container data center. A shipping container data center is a modular data center where shipping containers are recycled as housing units for IT and HVAC equipment. Advantages of this type of data center include increased mobility of equipment when company requirements change, "shorter deployment times, higher system and power densities, and lower cooling and manufacturing costs [35]." In addition, it gives data center designers flexibility to grow a data center if only a small data center is needed now but a larger data center will be needed in the future. This can lead to more efficient data center design and operation, since someone designing the cooling strategy won't have to guess at future IT cooling needs. A mismatch in predicted and actual cooling needs is often a source of inefficiency.

Using the two modeling tools developed in this thesis, as was done in chapters 6 and 7, a designer could put desired IT equipment in a virtual shipping container, use the compact modeling tool to ensure IT equipment remained below design thresholds, and use the sustainability tool to analyze the system and make more efficient design decisions. This will not be done here, since there are many, many design choices that have to be made, resulting in an extensive analysis. This example is just being presented to show the two tools developed

in this utility.

Design choices would have important sustainability ramifications which could be captured with a LCEA. For example, each shipping container has its own CRAC unit. If the shipping container doesn't need the full cooling load of the CRAC unit, the extra embodied exergy consumed to make a CRAC unit past the size needed would be wasted. This would show up in extra resource extraction and manufacturing exergy consumption due to more CRAC units being needed. In addition, the building shell exergy would differ. If shipping containers were truly recycled, rather than being made from virgin steel, there would likely be less exergy consumed in the building shell than a traditional brick and mortar data center. This is because the life-cycle exergy would be amortized over the data center portion of the shipping containers life-cycle as well as its previous use. If a new shipping container was constructed purely for the purpose of being used as part of a modular data center, the building shell life-cycle exergy consumption would increase. This is because making a steel building shell consumes more than a traditional building shell per area. An estimate of the steel shell could be found by multiplying the weight of the shipping container steel [26] by the exergy consumed for resource extraction and processing as well as manufacturing, and then normalizing by area of the shipping container [26]. The result is an exergy consumption value of $9.6\frac{GJ}{m^2}$ for a steel shipping container versus $5.3\frac{GJ}{m^2}$ as was assumed for a brick and mortar building, or an 80 % increase in building shell exergy consumption. This may or may not be important in the entire life-cycle of a data center, but the results from chapter 6 indicate that it is likely not vital in the life-cycle perspective.

Chapter 9

Conclusions

This dissertation has two main groups of goals: one set for sustainability modeling, one for fast predictive modeling. The first goal of the first group was to quantify the industry wide, commonly accepted idea that more sustainable data centers will be achieved by minimizing the environmental footprint of operation. Both global warming potential and life-cycle exergy consumption show this to be true under both standard and best case operation conditions. Under both standard and best case scenario operating conditions, the global warming potential of operation was approximately 70-80% of the total global warming potential, and resource use and manufacturing was the second largest contributor with 20-30% of the total. Under these operating conditions, it is recommended that operational electricity use be minimized even at the expense of more greenhouse gas emissions or exergy consumption in the resource extraction and manufacturing phase. Under the worst case scenario, the global warming potential for resource extraction and manufacturing and operation were roughly equivalent, due almost entirely to a 1 year turnover of server equipment. For life-cycle exergy consumption, resource extraction and transportation exceeded operational exergy consumption. It is recommended that a 1 year turnover of equipment be avoided due to the large global warming potential and life-cycle exergy consumption that it causes. Future work could focus on modeling equipment left out of this study or in obtaining better information to model equipment in this study.

The second sustainability goal of was to evaluate life-cycle exergy consumption as a sustainability metric. When compared to the life-cycle global warming potential found through a LCA, life-cycle exergy consumption seems to be an appropriate metric. Similar conclusions are reached in the worst, baseline, and best case scenarios studied. There were some differences, most notably whether operation is more or less than both resource extraction and transportation in the worst case, but the general trends were all exactly the same. Given the rough approximation of life-cycle analyses, both in terms of an LCEA or LEA, the two modeling tools were considered to be in agreement.

The second group of goals centered around investigating the accuracy and computational speed of a reduced-order predictive tool when compared to a conventional CFD tool. The main objective of compact modeling is to achieve an acceptable balance of computational

speed and accuracy. A simplified potential flow model was created, which, when compared to commercially available CFD code, generated temperature predictions in seconds rather than hours. Previous work with the simplified potential flow model showed that while it generated predictions very rapidly, it was too inaccurate to be useful [110]. Through experimental validation, this thesis shows that when augmented with vortices that have been correctly tuned, potential flow modeling can generate predictions more accurately than full CFD modeling but in a fraction of the time. Comparisons of the vortex superposition potential flow model and experiments, as well as ANSYS FLUENT and experiments, showed that both numerical techniques differed from the experimental results throughout the room. It was concluded that this may be in part caused by differences between measured boundary conditions and true conditions in the room. Despite these temperature deviations, both the vortex superposed potential flow model and FLUENT predicted the temperature at the inlet of servers accurately. This study shows that the vortex superposed code achieves drastically reduced run time without the loss of accuracy, since the tuned potential flow model predicted temperatures in the data center better than FLUENT. It is concluded that future work could investigate the optimization method outlined in this study and determine if it will hold up under different server room or flow configurations.

Bibliography

[1] Last Accessed December 5, 2010. URL: http://www.tpc.org/results/individual_results/IBM/ibm.m80.v5.062201.es.pdf.

[2] *3-Phase Distribution Cabinet System*. Last Accessed December 2010. URL: http://www.tripplite.com/en/products/product-series.cfm?txtSeriesID=873.

[3] *About SimaPro*. Last Accessed March 2012. URL: http://www.pre-sustainability.com/content/simapro-lca-software/.

[4] US Environmental Protection Agency. *EPA Report on Server and Data Center Energy Efficiency*. Aug. 2007. URL: http://www.energystar.gov/ia/partners/prod_development/downloads/EPA_Datacenter_Report_Congress_Final1.pdf.

[5] J. E. Ahern. "The Exergy Method of Energy Systems Analysis". In: New York: John Wiley & Sons, 1980.

[6] O.M. Al-Rabghi and D.C. Hittle. "Energy simulation in buildings: overview and BLAST example". In: *Energy conversion and Management* 42.13 (2001), pp. 1623–1635.

[7] *ANSYS FLUENT Flow Modeling Simulation Software*. Last Accessed November 2011. URL: http://www.ansys.com.

[8] *ANSYS FLUENT Users Guide*. Release 13.0. Nov. 2010.

[9] R. U. Ayres, L. W. Ayres, and K. Martinas. "Exergy, waste accounting, and life-cycle analysis". In: *Energy* 23.5 (1998), pp. 355–363.

[10] A. Azapagic. "Life cycle assessment and its application to process selection, design, and optimisation". In: *Chemical Engineering Journal* 73.1 (Apr. 1999), pp. 1–21.

[11] A.H. Beitelmal and C.D. Patel. "Thermo-fluids provisioning of a high performance high density data center". In: *Distributed and Parallel Databases* 21.2 (2007), pp. 227–238.

[12] D. Biekša, V. Martinaitis, and A.A. Šakmanas. "An estimation of exergy consumption paterns of energy-intensive building service systems". In: *Journal of Civil Engineering and Management* 12.1 (2006), pp. 37–42.

[13] T.D. Boucher et al. "Viability of dynamic cooling control in a data center environment". In: *Journal of electronic packaging* 128 (2006), p. 137.

[14] R. Cornelissen and G. G. Hirs. "The value of the exergetic life cycle assessment besides the LCA". In: *Energy Conversion and Management* 43.9-12, special issue (June 2002), pp. 1417–1424.

[15] J.C. Creyts. "Extended Exergy Analysis: A Tool for Assessment of the Environmental Impact of Industrial Processes". PhD thesis. University of California, Berkeley, 1998.

[16] JC Creyts and VP Carey. "Use of extended exergy analysis to evaluate the environmental performance of machining processes". In: *Proceedings of the Institution of Mechanical Engineers, Part E: Journal of Process Mechanical Engineering* 213.4 (1999), pp. 247–264.

[17] E. Cruz et al. "Comparison of Numerical Modeling to Experimental Data in a Small Data Center Test Cell". In: ASME. 2009.

[18] E. Cruz et al. "Comparison of numerical modeling to experimental data in a small, low power data center test cell". In: *Proceedings of ASME IMECE conference, Paper number IMECE2009-12860*. Nov. 2009.

[19] *Current primary and scrap metal prices – LME (London metal exchange)*. Last Accessed December 2010. URL: `http://www.metalprices.com/`.

[20] *Data Centers: Facilities: High-performance buildings for high-tech industries*. Last Accessed December 2010. URL: `http://hightech.lbl.gov/datacenters`.

[21] *Determining deployment costs for windows 2000 server*. Last Accessed December 5, 2010. URL: `http://articles.techrepublic.com.com/5100-10878_11-1059131.html`.

[22] J. Dewulf et al. "Recycling rechargeable lithium ion batteries: Critical analysis of natural resource savings". In: *Resources, Conservation and Recycling* 54.4 (2010), pp. 229–234.

[23] J. Elkington. "Towards the sustainable corporation: Win-win-win business strategies for sustainable development". In: *California Management Review* 36.2 (1994), pp. 90–100.

[24] World Commission on Environment and Development. *Our Common Future, Report of the World Commission on Environment and Development*. Published as Annex to General Assembly document A/42/427, Development and International Co-operation: Environment August 2, 1987. URL: `http://www.un-documents.net/wced-ocf.htm`.

[25] D. C. Esty et al. "2005 Environmental Sustainability Index: Benchmarking National Environmental Stewardship". In: New Haven: Yale Center for Environmental Law & Policy, 2005.

[26] *Evergreen Marine Corp.* Last Accessed April 30, 2012. URL: `http://www.evergreen-marine.com/tei1/jsp/TEI1_Containers.jsp`.

[27] C. Facanha and A. Horvath. "Evaluation of Life-Cycle Air Emission Factors of Freight Transporation". In: *Environmental Science & Technology* 41 (2007), pp. 7138–7144.

[28] *Facilities: High Performance Buildings for High-Tech Industries*. Last Accessed May 2011. URL: `http://hightech.lbl.gov/benchmarking-dc-charts.html`.

[29] Mark Fontecchio. *Data center air recyling saves cash-strapped greenhouse*. May 2009. URL: `http://searchdatacenter.techtarget.com/news/1356439/Data-center-air-recycling-saves-cash-strapped-greenhouse`.

[30] S. Gondipalli et al. "Effect of isolating cold aisles on rack inlet temperatures". In: *11th Intersociety Conference on Thermal and Thermomechanical Phenomena in Electronic Systems (ITHERM)*. optional. optional. Orlando, FL, May 2008, pp. 1247–1254.

[31] S. Gondipalli et al. "Optimization of cold aisle isolation designs for a data center with roofs and doors using slits". In: *ASME 2009 InterPACK Conference collocated with the ASME 2009 Summer Heat Transfer Conference and the ASME 2009 3rd International Conference on Energy Sustainability (InterPACK2009)*. Vol. 2. San Francisco, California, USA, July 2009.

[32] M. Gong and G. Wall. "On exergetics, economics and optimization of technical processes to meet environmental conditions". In: *TAIES'97*. Beijing, China, June 1997.

[33] R. Goodland and H. Daly. "Environmental sustainability: Universal and non-negotiable". In: *Ecological Applications* 6.4 (Nov. 1996), pp. 1002–1017.

[34] A. Greenberg et al. "The cost of a cloud: research problems in data center networks". In: *ACM SIGCOMM Computer Communication Review* 39.1 (2008), pp. 68–73.

[35] C. Guo et al. "BCube: a high performance, server-centric network architecture for modular data centers". In: *ACM SIGCOMM Computer Communication Review*. Vol. 39. 4. ACM. 2009, pp. 63–74.

[36] T. Gutowski et al. "A thermodynamic characterization of manufacturing processes". In: *Electronics & the Environment, Proceedings of the 2007 IEEE International Symposium on*. IEEE. 2007, pp. 137–142.

[37] T. Hak, B. Moldan, and A. Dahl. "Sustainability Indicators: A Scientific Assessment". In: Washington, D.C.: Island Press, 2007.

[38] H.F. Hamann, V. López, and A. Stepanchuk. "Thermal zones for more efficient data center energy management". In: *Thermal and Thermomechanical Phenomena in Electronic Systems (ITherm), 2010 12th IEEE Intersociety Conference on*. IEEE. 2010, pp. 1–6.

[39] C. R. Hannemann. "Lifetime Exergy Consumption Analysis of Data Centers". Masters thesis, Dept. of Mechanical Eng., The University of California at Berkeley, Berkeley, CA. 2006.

[40] C. R. Hannemann et al. "Lifetime exergy consumption as a sustainability metric for enterprise servers". In: *Proceedings of the ASME 2nd International Conference on Energy Sustainability*. Jacksonville, Florida, Aug. 2008.

[41] J. L. Hau. "Toward environmentally conscious process systems engineering via joint thermodynamic accounting of industrial and ecological systems". Ph.D. thesis, Dept. of Chem. Eng., The Ohio State University, Columbus, OH. 2005.

[42] J. L. Hau and B. R. Bakshi. "Promise and Problems of Emergy Analysis". In: *Ecological Modeling* 178.1-2 (Oct. 2004), pp. 215–225.

[43] M. Herrlin and C. Belady. "Gravity-assisted air mixing in data centers and how it affects the rack cooling effectiveness". In: *Proceedings of the tenth intersociety conference on thermal and thermo-mechanical phenomena in electronic systems (ITHERM)*. San Diego, CA, 2006, pp. 434–438.

[44] E. G. Hertwich, W. S. Pease, and C. P. Koshland. "Evaluating the environmental impact of products and production processes: A comparison of six methods". In: *Science of the Total Environment* 196.1 (Mar. 1997), pp. 13–29.

[45] V. H. Hoffmann, K. Hungerbuhler, and G. J. McRae. "Multiobjective screening and evaluation of chemical process technologies". In: *Industrial and Engineering Chemistry Research* 40.21 (Oct. 2001), pp. 4513–4524.

[46] A. Horvath and A. Shehabi. "Improving Energy Performance of Data Centers". In: *University of California Energy Institute*. 2008.

[47] M. Ibrahim et al. "Effect of thermal characteristics of electronic enclosures on dynamic data center performance". In: *IMECE conference*. Vancouver, Canada, 2010.

[48] M. Ibrahim et al. "Numerical modeling approach to dynamic data center cooling". In: *Thermal and Thermomechanical Phenomena in Electronic Systems (ITherm), 2010 12th IEEE Intersociety Conference on*. IEEE. 2010, pp. 1–7.

[49] Carnegie Mellon University Green Design Institute. *Economic Input-Output Life Cycle Assessment (EIO-LCA), US 2002 Industry Benchmark model [Internet]*. 2012. URL: `http://www.eiolca.net/`.

[50] "ISO/DIS 14040, Environmental Management Life Cycle Assessment Part 1: Principles and Framework". In: 1997.

[51] M. Iyengar et al. "Comparison between Numerical and Experimental Temperature Distributions in a Small Data Center Test Cell". In: ASME. 2007.

[52] S. Junnila, A. Horvath, and A. Guggemos. "Life-cycle Assessment of Office Buildings in Europe and the U.S. J. of Infrastructure Systems". In: *ASCE* 12.1 (2006), pp. 10–17. DOI: `10.1061/(ASCE)1076-0342(2006)12:1(10)`.

[53] S. Junnila et al. "Life-cycle environmental effects of an office building". In: *Journal of Infrastructure Systems* 9 (2003), p. 157.

[54] S. Kang et al. "A methodology for the design of perforated tiles in raised floor data centers using computational flow analysis". In: *IEEE Transactions on Components and Packaging Technologies* 24.2 (June 2001), pp. 177–183.

[55] S. Kang et al. "A methodology for the design of perforated tiles in raised floor data centers using computational flow analysis". In: *IEEE Transactions on Components and Packaging Technologies* 24l.2 (June 2001), pp. 177–183.

[56] K. Karki and S. Patankar. "Techniques for controlling airflow distribution in raised-floor data centers". In: *Proceedings of the Pacific Rim/ASME international electronic packaging techni cal conference and exhibition (IPACK03)*. Kauai, Hawaii, 2003.

[57] K. Karki, A. Radmehr, and S. Patankar. "Use of computational fluid dynamics for calculating flow rates through perforated tiles in raised-floor data centers". In: *International Journal of Heating, Ventilation, Air-Conditioning, and Refrigeration Research* 9.2 (2003), pp. 153–166.

[58] K.C. Karki and S.V. Patankar. "Airflow distribution through perforated tiles in raised-floor data centers". In: *Building and environment* 41.6 (2006), pp. 734–744.

[59] A. Kumar. "Use of air side economizer for data center thermal management". PhD thesis. Georgia Institute of Technology, 2008.

[60] N. Kumari et al. "Optimization of Outside Air Cooling in Data Centers". In: *Proceedings of the 2011 Pacific Rim Technical Conference and Exposition on Packaging and Integration of Electronic and Photonic Systems*. Portland, OR, July 2011.

[61] PK Kundu and IM Cohen. *Fluid Mechanics. 2004*.

[62] D. Lettieri. "Life-Cycle Exergy Consumption as Metric for Data Center Sustainability". MA thesis. U.C. Berkeley, May 2009.

[63] D. Lettieri, A.J. Shah, and V.P. Carey. "Exergy-Based Environmental Design of a Computer Room Air Conditioning Unit". In: *Proceedings of the 2009 International Congress and Exposition*. paper IMECE2009-11461. Orlando, FL, Nov. 2009.

[64] D. Lettieri et al. "Lifetime Exergy Consumption as a Sustainability Metric for Information Technologies". In: *Proceedings, International Symposium on Sustainable Systems and Technology (ISSST)*. Phoenix, AZ, 2009, pp. 1–5.

[65] C.H. Liao, P.H. Tseng, and C.S. Lu. "Comparing carbon dioxide emissions of trucking and intermodal container transport in Taiwan". In: *Transportation Research Part D: Transport and Environment* 14.7 (2009), pp. 493–496.

[66] V. López and H.F. Hamann. "Measurement-based modeling for Data Centers". In: *Thermal and Thermomechanical Phenomena in Electronic Systems (ITherm), 2010 12th IEEE Intersociety Conference on*. IEEE. 2010, pp. 1–8.

[67] P.J. Meier. "Life-Cycle Assessment of Electricity Generation Systems and Applications for Climate Change Policy Analysis". Accessed Dec. 2010. PhD thesis. University of Wisconsin, 2002. URL: `http://fti.neep.wisc.edu/pdf/fdm1181.pdf`.

[68] M. J. Moran and H. N. Shapiro. "Fundamentals of Engineering Thermodynamics". In: Fifth. New York: John Wiley & Sons, 2004, p. 292.

[69] M. Nakao, H. Hayama, and M. Nishioka. "Which cooling air supply system is better for a high heat density room: underfloor or overhead". In: *Proceedings of the international telecommunications energy conference (INTELEC)*. Kyoto, Japan, 1991, pp. 393–400.

[70] *Network/Server UPS System*. Last Accessed December 2010. URL: `http://www.tripplite.com/en/products/product-series.cfm?txtSeriesID=744`.

[71] H. Noh, K. Song, and S. Chun. "The cooling characteristic on the air supply and return flow system in the telecommunication cabinet room". In: *Proceedings of the international telecommunications energy conference (INTELEC)*. San Francisco, CA, 1998, pp. 777–784.

[72] H. T. Odum. "Environmental Accounting: Emergy and Environmental Decision Making". In: New York: John Wiley & Sons, 1996.

[73] S. Patankar and K. Karki. "Distribution of cooling airflow in a raised-floor data center." In: *ASHRAE Transactions* 110.2 (2004), pp. 629–635.

[74] C. Patel et al. "Computational fluid dynamics modeling of high compute density data centers to assure system inlet air specification". In: *Proceedings of the Pacific Rim/ASME international electronic packaging technical conference and exhibition (InterPACK)*. Maui, Hawaii, 2001.

[75] C.D. Patel et al. "Thermal considerations in cooling large scale high compute density data centers". In: *Thermal and Thermomechanical Phenomena in Electronic Systems, 2002. ITHERM 2002. The Eighth Intersociety Conference on*. Ieee. 2002, pp. 767–776.

[76] T. D. Patzek. "Thermodynamics of the corn-ethanol biofuel cycle". In: *Critical Reviews in Plant Sciences* 23.6 (2004), pp. 519–567.

[77] *PG&E Corporate Responsibility Report*. Last Accessed December 2010. URL: `http://www.pgecorp.com/corp_responsibility/reports/2007/environment/energy-future.html`.

[78] *Price - World Scrap - Scrap Plastic, metal, paper, rubber, electric, make your scrap trade easy*. Last Accessed April 20, 2012. URL: `http://www.worldscrap.com/modules/price/index.php`.

[79] *Product Sustainability Software: GaBi Software*. Last Accessed March 2012. URL: `http://www.gabi-software.com/america/index/`.

[80] J. Rambo and Y. Joshi. "Convective transport processes in data centers". In: *Numerical Heat Transfer, Part A: Applications* 49.10 (2006), pp. 923–945.

[81] J. Rambo and Y. Joshi. "Modeling of data center airflow and heat transfer: state of the art and future trends". In: *Distributed and Parrallel Databases* 21.2 (2007), pp. 193–225.

[82] J. Rambo and Y. Joshi. "Reduced order modeling of steady turbulent flows using the POD". In: *Proceedings of ASME Summer Heat Transfer Conference, San Francisco, CA*. 2005.

[83] J. Rambo and Y. Joshi. "Thermal modeling of technology infrastructure facilities: A Case Study of Data Centers". In: *Handbook of Numerical Heat Transfer* (2006), pp. 821–849.

[84] J. Rambo, G. Nelson, and Y. Joshi. "Airflow distribution through perforated tiles in close proximity to computer room air conditioning units". In: *ASHRAE Trans* 113.2 (2007), pp. 124–135.

[85] J.D. Rambo. "Reduced-order modeling of multiscale turbulent convection: Application to data center thermal management". PhD thesis. Citeseer, 2006.

[86] A. D. Sagar and A. Najam. "The human development index: a critical review". In: *Ecological Economics* 25.3 (June 1998), pp. 249–264.

[87] E. Samadiani, J. Rambo, and Y. Joshi. "Numerical Modeling of Perforated Tile Flow Distribution in a Raised-Floor Data Center". In: *Journal of Electronic Packaging* 132 (2010), p. 021002.

[88] R.L. Sawyer. *Sawyer, R.L., Increasing the Efficiencies of UPS Systems – and Proving It!* Last Accessed April 23, 2012. URL: `http://www.commissioning.org/downloads/Increasing%20the%20Efficiency%20of%20UPS%20Technology%20-%20Sawyer.ppt`.

[89] R. Schmidt. "Effect of data center characteristics on data processing equipment inlet temperatures, Advances in Electronic Packaging 2001". In: *Proceedings of the Pacific Rim/ASME international electronic packaging technical conference and exhibition (IPACK01)*. Vol. 2. 2001, pp. 1097–1106.

[90] R. Schmidt and E. Cruz. "Raised floor computer data center: effect on rack inlet temperatures of chilled air exiting both the hot and cold aisles". In: *Proceedings of the eighth intersociety conference on thermal and thermo-mechanical phenomena in electronic systems (ITHERM)*. San Diego, CA, 2002, pp. 580–594.

[91] R. Schmidt and E. Cruz. "Raised floor computer data center: effect on rack inlet temperatures when high powered racks are situated amongst lower powered racks". In: *ASME 2002 International Mechanical Engineering Congress and Exposition (IMECE2002)*. New Orleans, Louisiana, USA, Nov. 2002, pp. 297–309.

[92] R. Schmidt and E. Cruz. "Raised floor computer data center: effect on rack inlet temperatureswhen adjacent racks are removed". In: *Proceedings of the Pacific Rim/ASME international electronic packaging technical conference and exhibition (IPACK03)*. Maui, Hawaii, 2003, pp. 481–493.

[93] R. Schmidt and M. Iyengar. "Comparison between Underfloor Supply and Overhead Supply Ventilation Designs for Data Center High-Density Clusters". In: *ASHRAE Transactions* 113.1 (2007).

[94] R. Schmidt and H. Shaukatullah. "Computer and telecommunications equipment room cooling: a review of literature." In: *IEEE transactions on components and packaging technologies,* 26.1 (Mar. 2003), pp. 89–98.

[95] R. Schmidt et al. "Measurements and predictions of the flow distribution through perforated tiles in raised-floor data centers". In: *Proceedings of the Pacific Rim/ASME international electronic packaging technical conference and exhibition (IPACK01)*. Kauai, Hawaii, 2001.

[96] R.R. Schmidt et al. "Measurements and predictions of the flow distribution through perforated tiles in raised floor data centers". In: *The Pacific Rim/ASME International Electronics Packaging Technical Conference and Exhibition*. 2001.

[97] A. Shah, C.E. Bash, and C.D. Patel. "Optimizing Data Center Cooling Infrastuructures Using Exergothermovolumes". In: *ITherm*. Las Vegas, NV, June 2010.

[98] A. Shah et al. "An Exergy-Based Figure of Merit for Electronic Packages". In: *Journal of Electronic Packaging* 128.4 (2006), pp. 360–369.

[99] A. Shah et al. "Exergy Analysis of Data Center Thermal Management Systems". In: *Journal of Heat Transfer* 130.2 article no. 021401 (2008).

[100] A. Shehabi. "Energy Implications of Economizer Use in California Data Centers". In: (2008).

[101] S. Shrivastava et al. "Comparative analysis ofdifferent data center airflow management configurations". In: *Proceedings of InterPACK*. San Francisco, CA, July 2005.

[102] S.K. Shrivastava, J.W. VanGilder, and B.G. Sammakia. "A statistical prediction of cold aisle end airflow boundary conditions". In: *Thermal and Thermomechanical Phenomena in Electronics Systems, 2006. ITHERM'06. The Tenth Intersociety Conference on*. IEEE. 2006, 9–pp.

[103] S.K. Shrivastava, J.W. VanGilder, and B.G. Sammakia. "Prediction of Cold Aisle End Airflow Boundary Conditions Using Regression Modeling". In: *Components and Packaging Technologies, IEEE Transactions on* 30.4 (2007), pp. 866–874.

[104] L. Stahl and C. Belady. "Designing an alternative to conventional room cooling". In: *Telecommunications Energy Conference, 2001. INTELEC 2001. Twenty-Third International*. IET. 2001, pp. 109–115.

[105] *Steel Price Per pound*. Last Accessed April 20, 2012. URL: `http://steel-prices.net/steel-price-per-pound.html`.

[106] S. Suh et al. "System boundary selection in life-cycle inventories using hybrid approaches". In: *Environmental Science & Technology* 38.3 (2004), pp. 657–664.

[107] J. Szargut, D. R. Morris, and F. R. Steward. "Exergy Analysis of Thermal, Chemical, and Metallurgical Processes". In: New York: Hemisphere, 1988.

[108] R.L. Thayer Jr. "The Word Shrinks, the World Expands". In: *Landscape Journal* 27.1 (2008), pp. 9–22.

[109] Michael Toulouse. "Exploration and validation of a potential-flow-based compact model of air-flow transport in data centers". MA thesis. U.C. Berkeley, 2010.

[110] M.M. Toulouse et al. "Experimental Validation of the COMPACT code in Data Centers". In: *Proceedings of the 2010 International Mechanical Engineering Congress and Exposition, Vancouver, BC, Canada*. Nov. 2010.

[111] M.M. Toulouse et al. "Exploration of a Potential-Flow-Based Compact Model of Air-Flow Transport in Data Centers". In: *Proceedings of the 2009 International Mechanical Engineering Congress and Exposition, Orlando, FL*. Nov. 2009.

[112] W.F. Tschudi et al. "High Performance Data Centers: A Research Roadmap". In: *Lawrence Berkeley National Laboratory, Berkeley, CA, Report LBNL-53483* (2003).

[113] UNDP. "Human Development Report". In: New York: Oxford University Press, 1990.

[114] J.W. VanGilder and S.K. Shrivastava. "Real-time prediction of rack-cooling performance". In: *ASHRAE transactions* (2006), pp. 151–162.

[115] P. Kumar et. al Y. Joshi. *Energy Efficient Thermal Management of Data Centers*. Ed. by Y. Joshi and P. Kumar. Springer Science+Business Media, 2012. DOI: 10.1007/978-1-4419-7124-1_1. URL: http://www.springerlink.com/content/978-1-4419-7123-4/contents/.

Appendix A

Convergence Plots for All FLUENT Simulations

This appendix has all of the residual and mesh refinement convergence studies for Runs 5, 6, and 7. The plots are ordered starting with Run 5 and ending with Run 7. Within each experimental run, the plots are ordered with the residual refinement first, from the coarsest mesh to the finest mesh, and then the mesh refinement study. The Run 7 residual refinement for the finest mesh as well as the Run 7 mesh refinement plots are not in this appendix, since they were included in the body of this thesis.

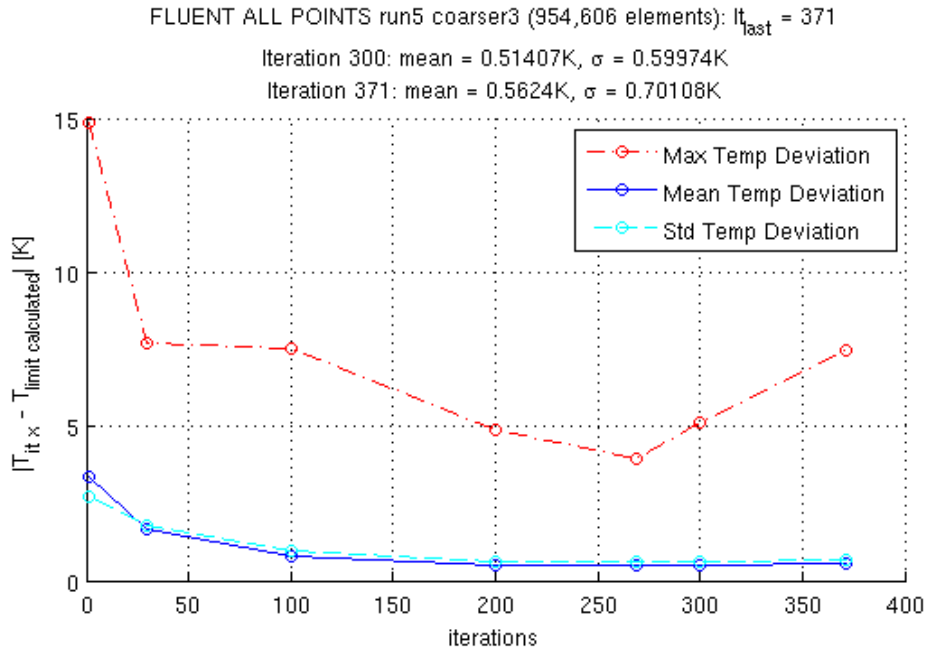
FLUENT ALL POINTS run5 coarser3 (954,606 elements): It$_{last}$ = 371
Iteration 300: mean = 0.51407K, σ = 0.59974K
Iteration 371: mean = 0.5624K, σ = 0.70108K
Max Temp Deviation
Mean Temp Deviation
Std Temp Deviation
|T$_{it\ x}$ - T$_{limit\ calculated}$| [K]
iterations
0
5
10
15
0
50
100
150
200
250
300
350
400

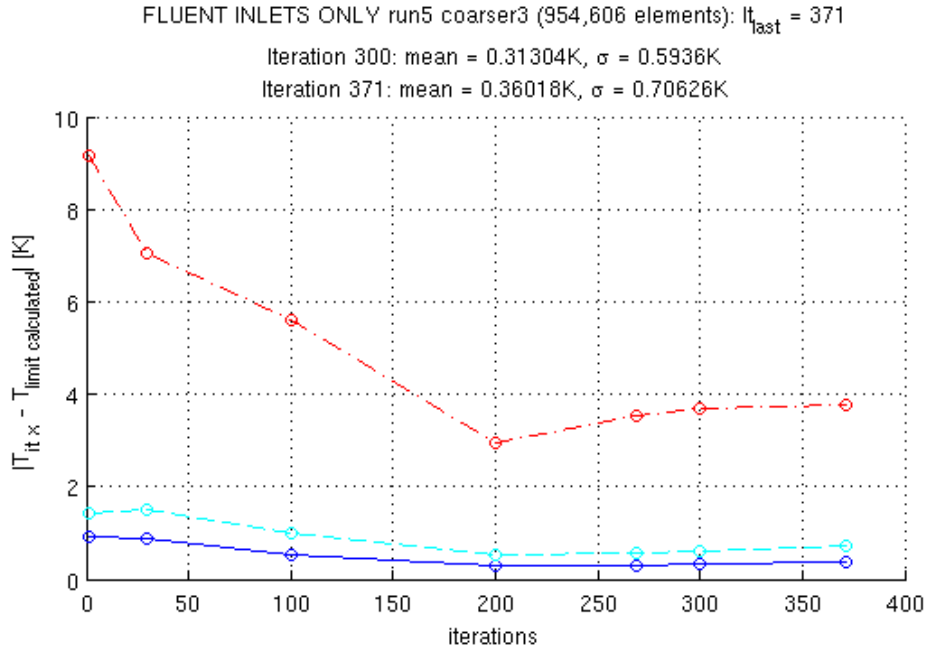
FLUENT INLETS ONLY run5 coarser3 (954,606 elements): It$_{last}$ = 371
Iteration 300: mean = 0.31304K, σ = 0.5936K
Iteration 371: mean = 0.36018K, σ = 0.70626K
|T$_{it\ x}$ - T$_{limit\ calculated}$| [K]
iterations
0
2
4
6
8
10
0
50
100
150
200
250
300
350
400

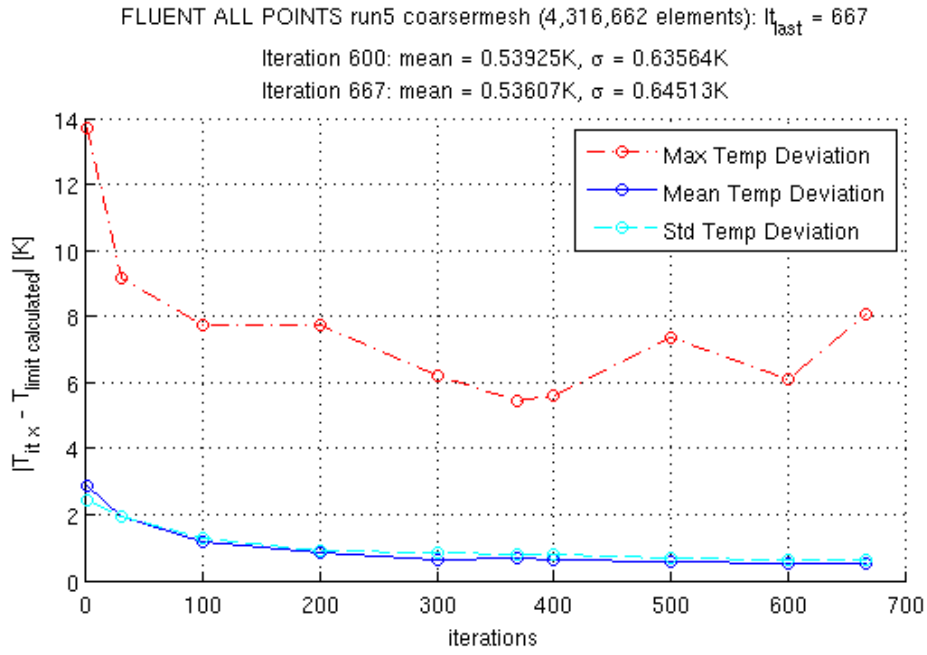
FLUENT ALL POINTS run5 coarsermesh (4,316,662 elements): It$_{last}$ = 667
Iteration 600: mean = 0.53925K, σ = 0.63564K
Iteration 667: mean = 0.53607K, σ = 0.64513K
Max Temp Deviation
Mean Temp Deviation
Std Temp Deviation
|T$_{it\ x}$ - T$_{limit\ calculated}$| [K]
iterations
0
2
4
6
8
10
12
14
0
100
200
300
400
500
600
700

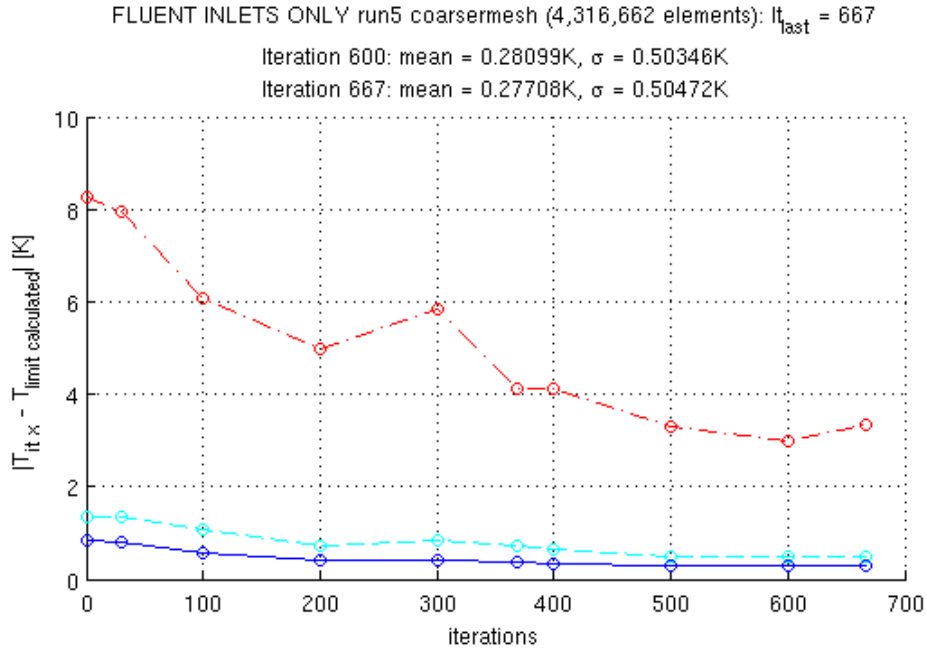
FLUENT INLETS ONLY run5 coarsermesh (4,316,662 elements): It$_{last}$ = 667
Iteration 600: mean = 0.28099K, σ = 0.50346K
Iteration 667: mean = 0.27708K, σ = 0.50472K
|T$_{it\ x}$ - T$_{limit\ calculated}$| [K]
iterations
0
2
4
6
8
10
0
100
200
300
400
500
600
700

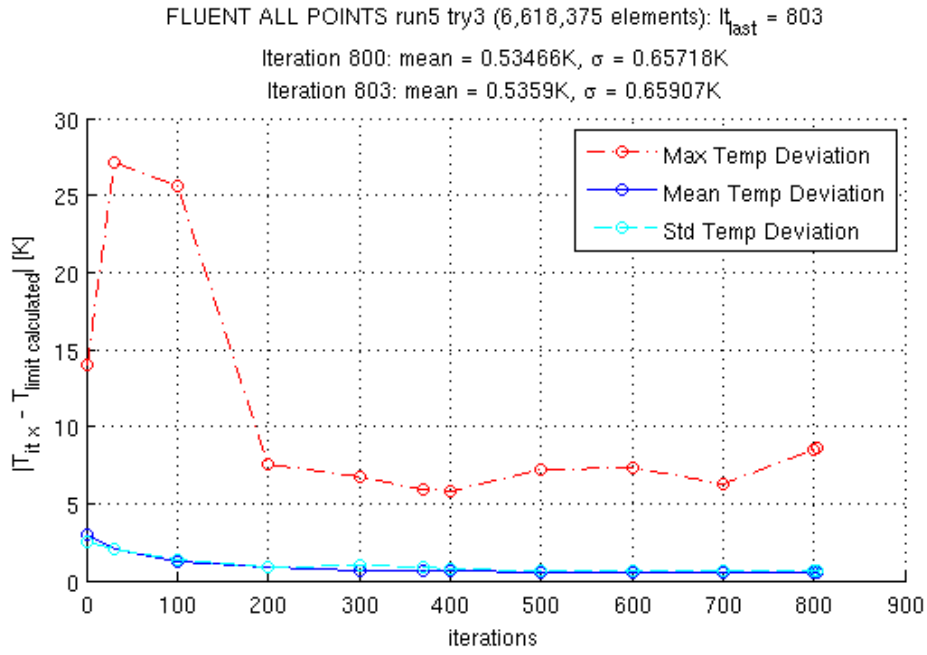
FLUENT ALL POINTS run5 try3 (6,618,375 elements): It$_{last}$ = 803
Iteration 800: mean = 0.53466K, σ = 0.65718K
Iteration 803: mean = 0.5359K, σ = 0.65907K
Max Temp Deviation
Mean Temp Deviation
Std Temp Deviation
|T$_{it\ x}$ - T$_{limit\ calculated}$| [K]
iterations
0
5
10
15
20
25
30
0
100
200
300
400
500
600
700
800
900

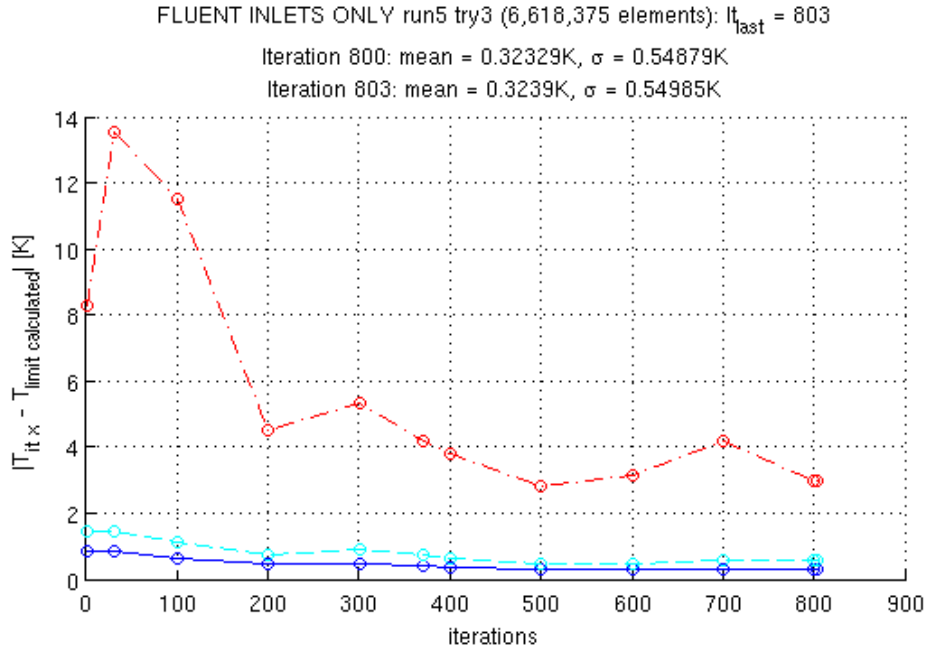
FLUENT INLETS ONLY run5 try3 (6,618,375 elements): It$_{last}$ = 803
Iteration 800: mean = 0.32329K, σ = 0.54879K
Iteration 803: mean = 0.3239K, σ = 0.54985K
|T$_{it\ x}$ - T$_{limit\ calculated}$| [K]
iterations
0
2
4
6
8
10
12
14
0
100
200
300
400
500
600
700
800
900

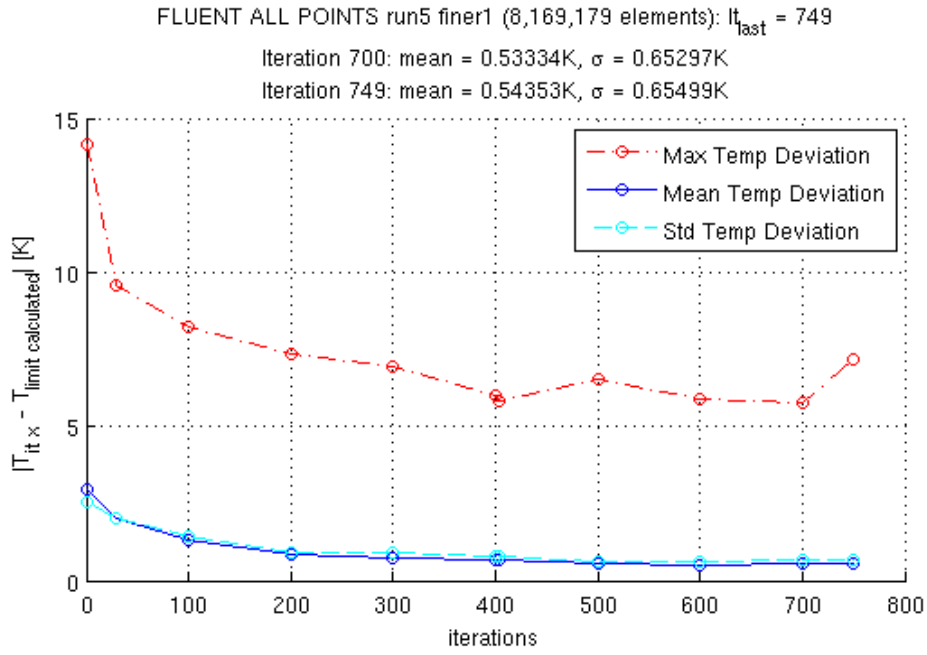
FLUENT ALL POINTS run5 finer1 (8,169,179 elements): It$_{last}$ = 749
Iteration 700: mean = 0.53334K, σ = 0.65297K
Iteration 749: mean = 0.54353K, σ = 0.65499K
Max Temp Deviation
Mean Temp Deviation
Std Temp Deviation
|T$_{it\ x}$ - T$_{limit\ calculated}$| [K]
iterations
0
5
10
15
0
100
200
300
400
500
600
700
800

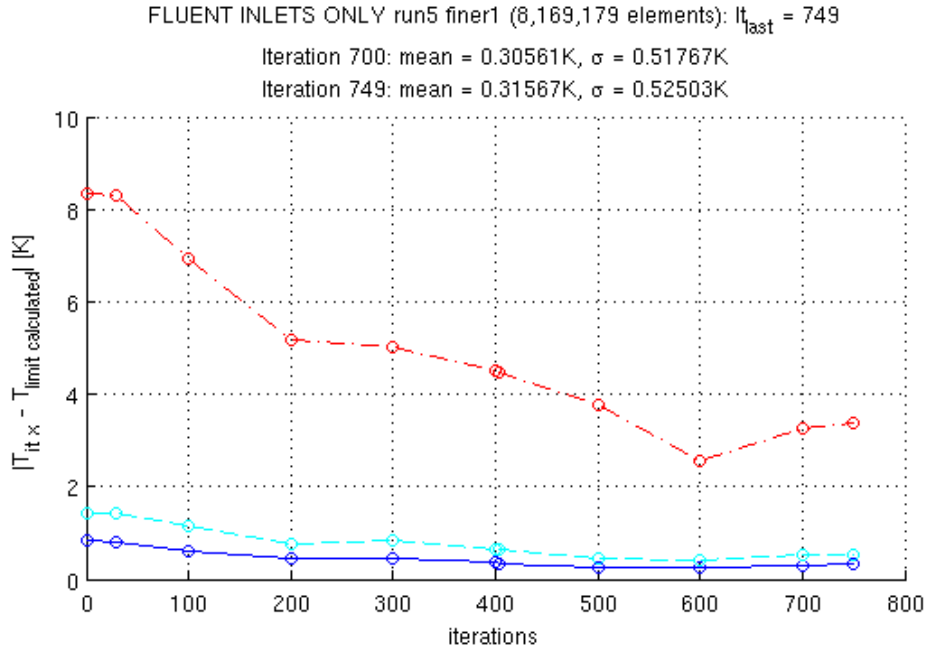
FLUENT INLETS ONLY run5 finer1 (8,169,179 elements): It$_{last}$ = 749
Iteration 700: mean = 0.30561K, σ = 0.51767K
Iteration 749: mean = 0.31567K, σ = 0.52503K
|T$_{it\ x}$ - T$_{limit\ calculated}$| [K]
iterations
0
2
4
6
8
10
0
100
200
300
400
500
600
700
800

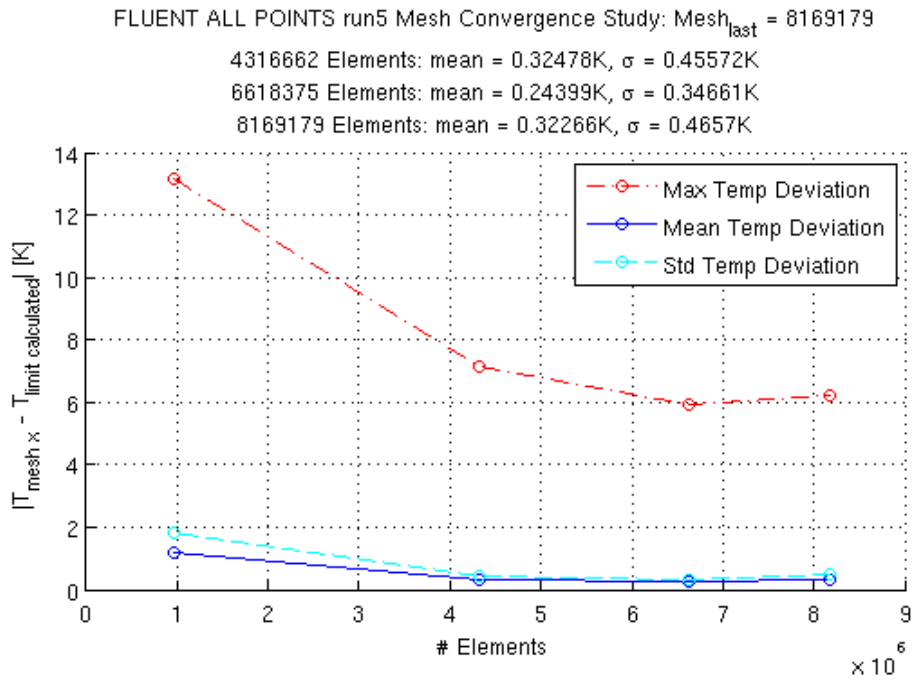
FLUENT ALL POINTS run5 Mesh Convergence Study: Mesh$_{last}$ = 8169179
4316662 Elements: mean = 0.32478K, σ = 0.45572K
6618375 Elements: mean = 0.24399K, σ = 0.34661K
8169179 Elements: mean = 0.32266K, σ = 0.4657K
Max Temp Deviation
Mean Temp Deviation
Std Temp Deviation
|T$_{mesh\ x}$ - T$_{limit\ calculated}$| [K]
Elements
x 10^{6}

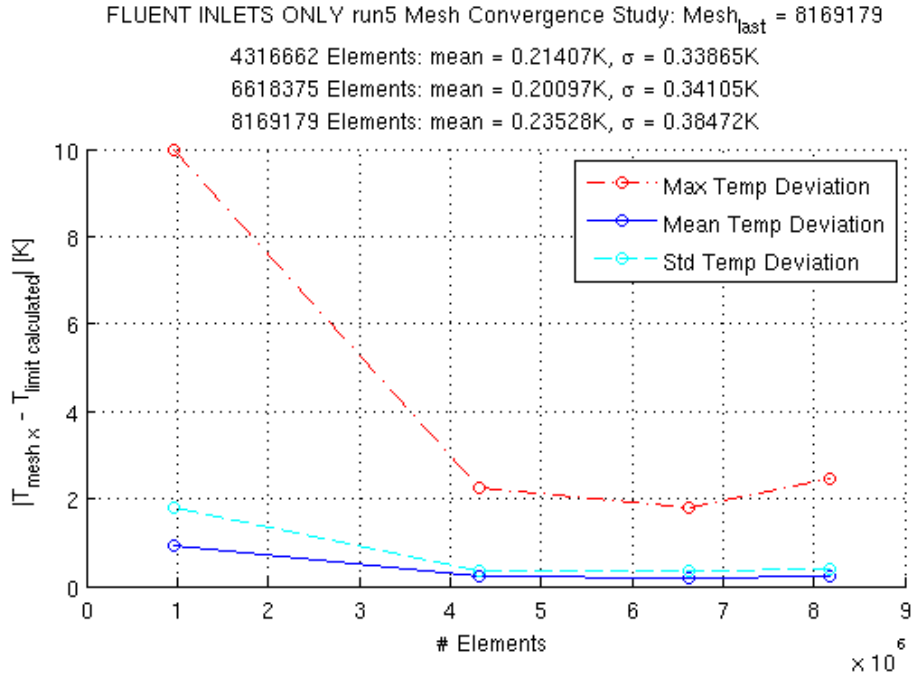
FLUENT INLETS ONLY run5 Mesh Convergence Study: Mesh$_{last}$ = 8169179
4316662 Elements: mean = 0.21407K, σ = 0.33865K
6618375 Elements: mean = 0.20097K, σ = 0.34105K
8169179 Elements: mean = 0.23528K, σ = 0.38472K
Max Temp Deviation
Mean Temp Deviation
Std Temp Deviation
|T$_{mesh\ x}$ - T$_{limit\ calculated}$| [K]
Elements
x 10^{6}

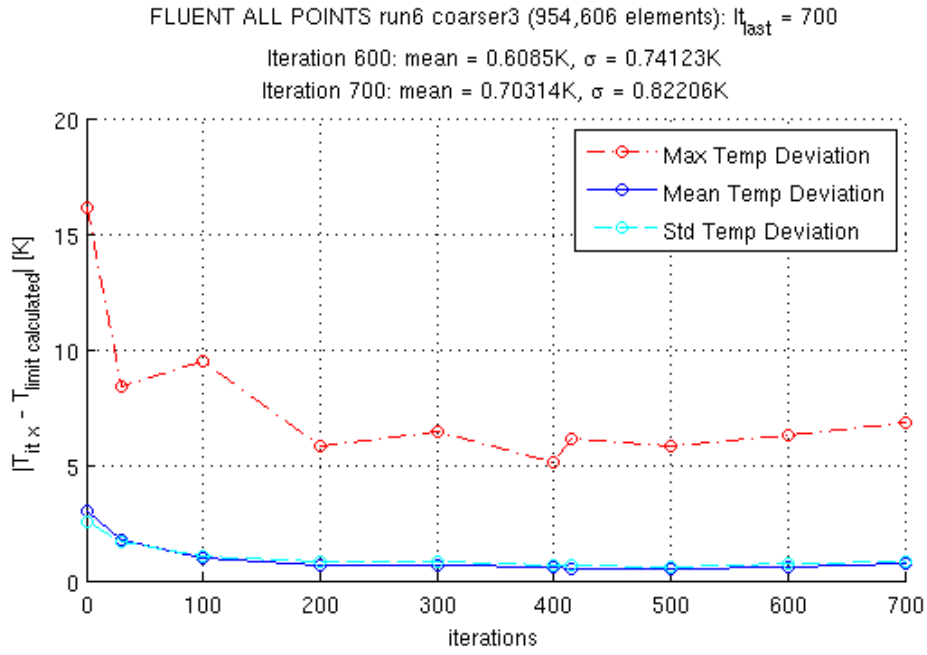
FLUENT ALL POINTS run6 coarser3 (954,606 elements): It$_{last}$ = 700
Iteration 600: mean = 0.6085K, σ = 0.74123K
Iteration 700: mean = 0.70314K, σ = 0.82206K
Max Temp Deviation
Mean Temp Deviation
Std Temp Deviation
|T$_{it\ x}$ - T$_{limit\ calculated}$| [K]
iterations
0
5
10
15
20
0
100
200
300
400
500
600
700

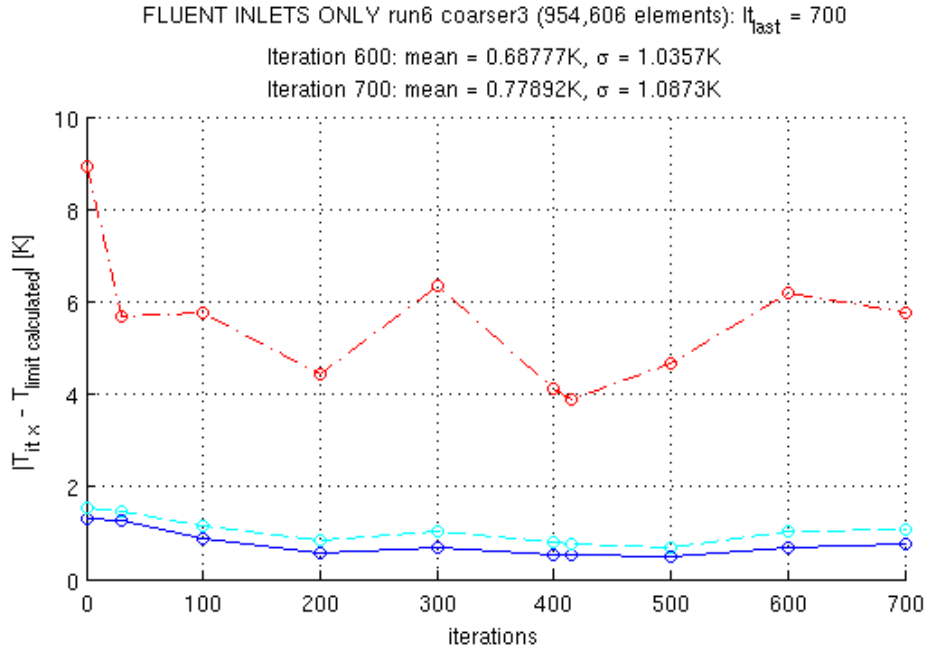
FLUENT INLETS ONLY run6 coarser3 (954,606 elements): It$_{last}$ = 700
Iteration 600: mean = 0.68777K, σ = 1.0357K
Iteration 700: mean = 0.77892K, σ = 1.0873K
|T$_{it\ x}$ - T$_{limit\ calculated}$| [K]
iterations
0
2
4
6
8
10
0
100
200
300
400
500
600
700

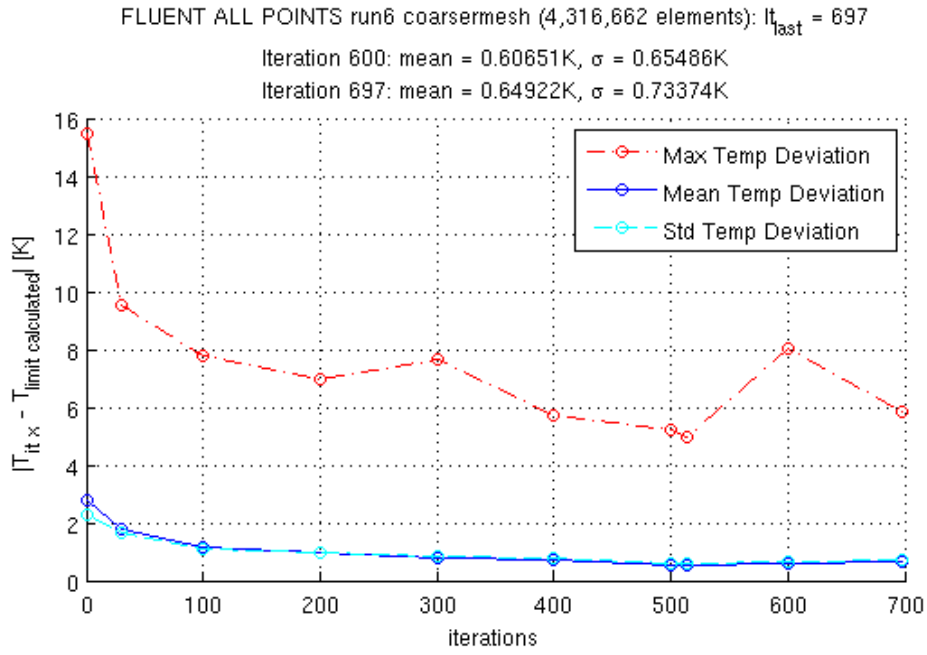
FLUENT ALL POINTS run6 coarsermesh (4,316,662 elements): It$_{last}$ = 697
Iteration 600: mean = 0.60651K, σ = 0.65486K
Iteration 697: mean = 0.64922K, σ = 0.73374K
Max Temp Deviation
Mean Temp Deviation
Std Temp Deviation
|T$_{it\ x}$ - T$_{limit\ calculated}$| [K]
iterations
0
2
4
6
8
10
12
14
16
0
100
200
300
400
500
600
700

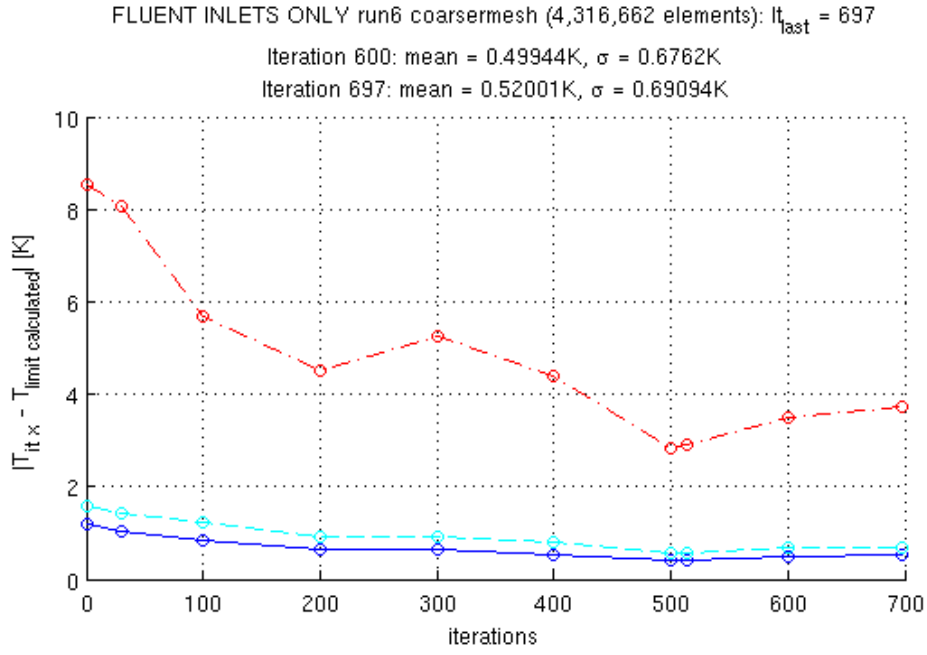
FLUENT INLETS ONLY run6 coarsermesh (4,316,662 elements): It$_{last}$ = 697
Iteration 600: mean = 0.49944K, σ = 0.6762K
Iteration 697: mean = 0.52001K, σ = 0.69094K
|T$_{it\ x}$ - T$_{limit\ calculated}$| [K]
iterations
0
2
4
6
8
10
0
100
200
300
400
500
600
700

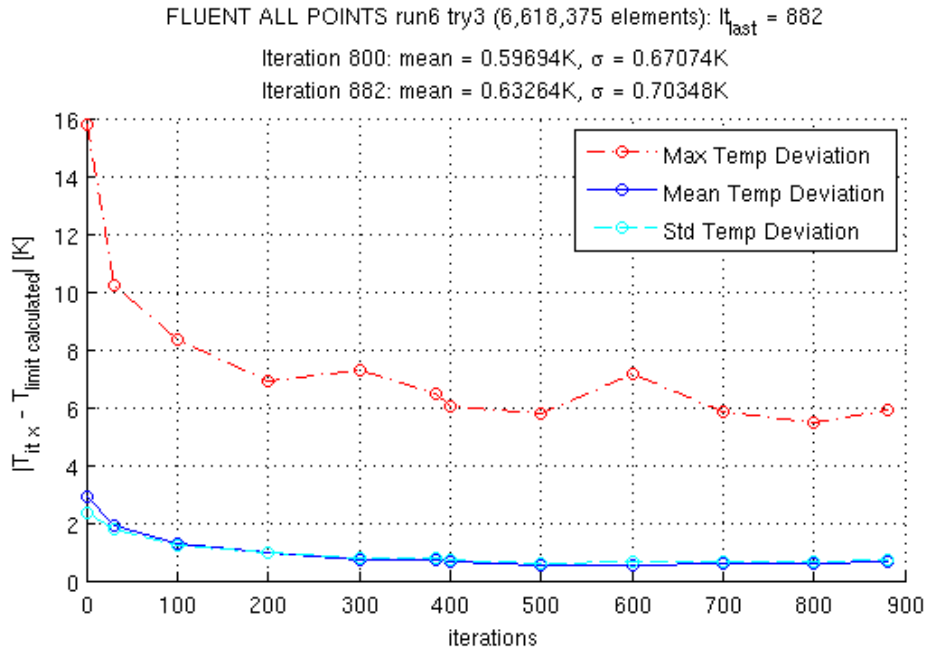
FLUENT ALL POINTS run6 try3 (6,618,375 elements): It$_{last}$ = 882
Iteration 800: mean = 0.59694K, σ = 0.67074K
Iteration 882: mean = 0.63264K, σ = 0.70348K
Max Temp Deviation
Mean Temp Deviation
Std Temp Deviation
|T$_{it\ x}$ - T$_{limit\ calculated}$| [K]
iterations

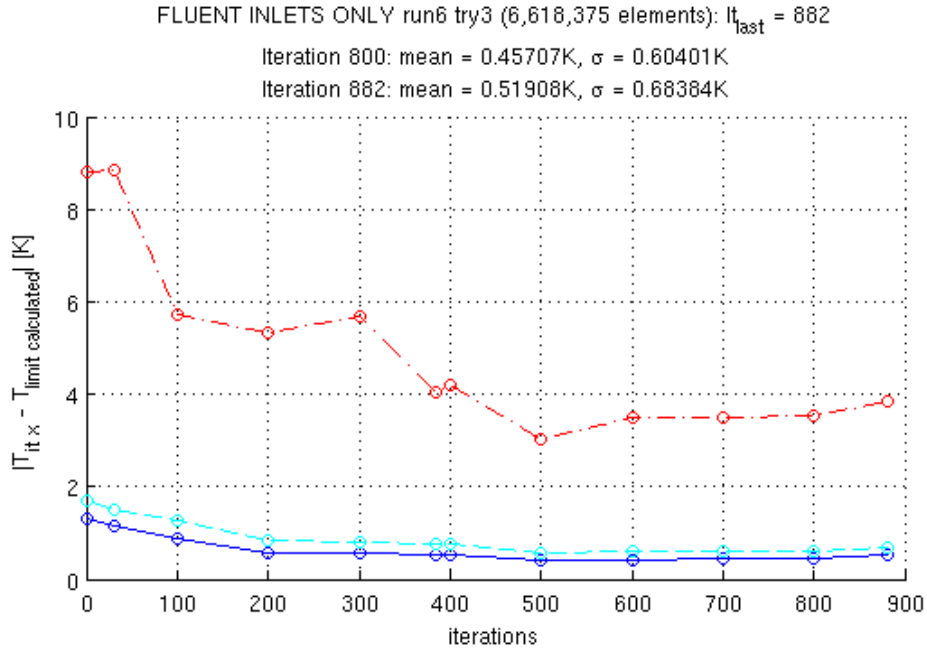
FLUENT INLETS ONLY run6 try3 (6,618,375 elements): It$_{last}$ = 882
Iteration 800: mean = 0.45707K, σ = 0.60401K
Iteration 882: mean = 0.51908K, σ = 0.68384K
|T$_{it\ x}$ - T$_{limit\ calculated}$| [K]
iterations

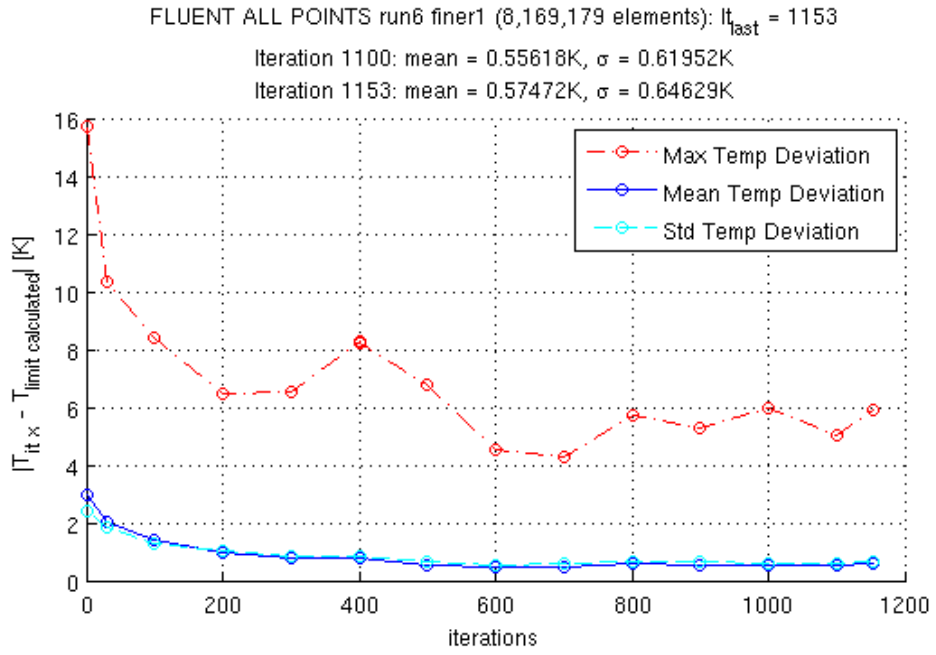
FLUENT ALL POINTS run6 finer1 (8,169,179 elements): It$_{last}$ = 1153
Iteration 1100: mean = 0.55618K, σ = 0.61952K
Iteration 1153: mean = 0.57472K, σ = 0.64629K
Max Temp Deviation
Mean Temp Deviation
Std Temp Deviation
|T$_{it\ x}$ - T$_{limit\ calculated}$| [K]
iterations
0
2
4
6
8
10
12
14
16
0
200
400
600
800
1000
1200

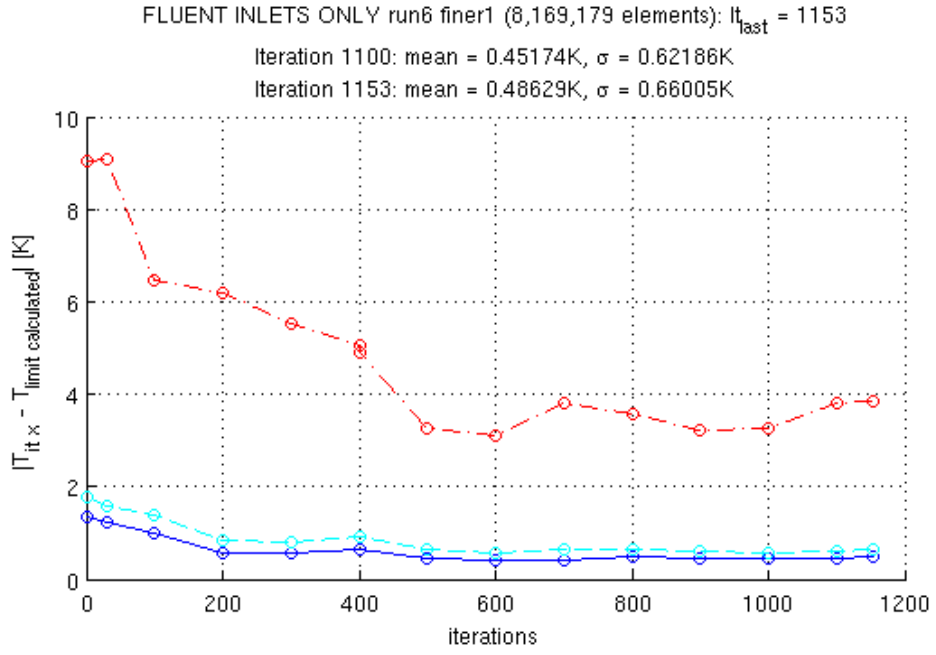
FLUENT INLETS ONLY run6 finer1 (8,169,179 elements): It$_{last}$ = 1153
Iteration 1100: mean = 0.45174K, σ = 0.62186K
Iteration 1153: mean = 0.48629K, σ = 0.66005K
|T$_{it\ x}$ - T$_{limit\ calculated}$| [K]
iterations
0
2
4
6
8
10
0
200
400
600
800
1000
1200

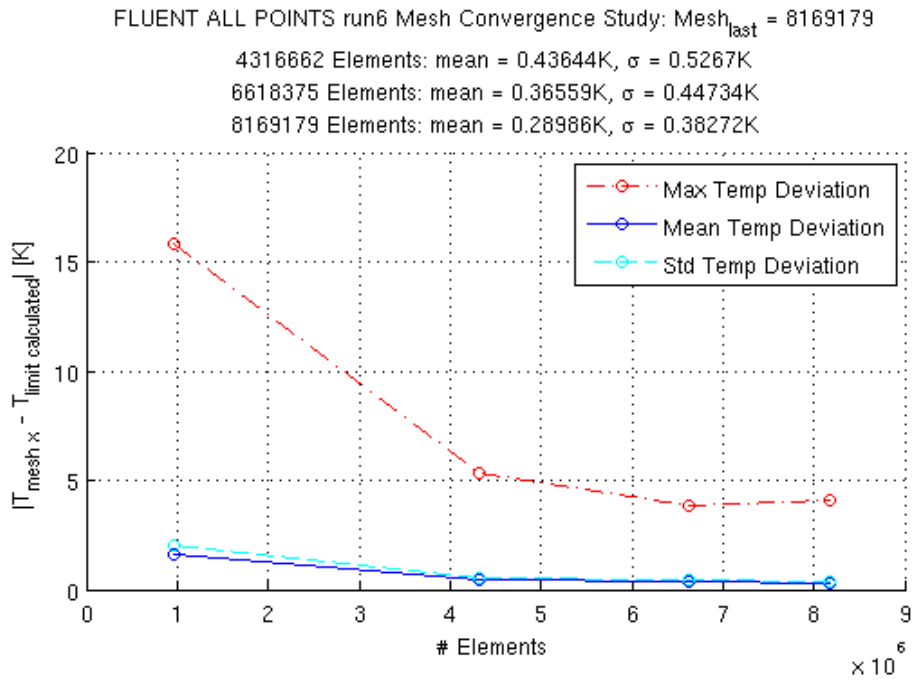
FLUENT ALL POINTS run6 Mesh Convergence Study: Mesh$_{last}$ = 8169179
4316662 Elements: mean = 0.43644K, σ = 0.5267K
6618375 Elements: mean = 0.36559K, σ = 0.44734K
8169179 Elements: mean = 0.28986K, σ = 0.38272K
Max Temp Deviation
Mean Temp Deviation
Std Temp Deviation
|T$_{mesh\ x}$ - T$_{limit\ calculated}$| [K]
Elements
x 10^{6}

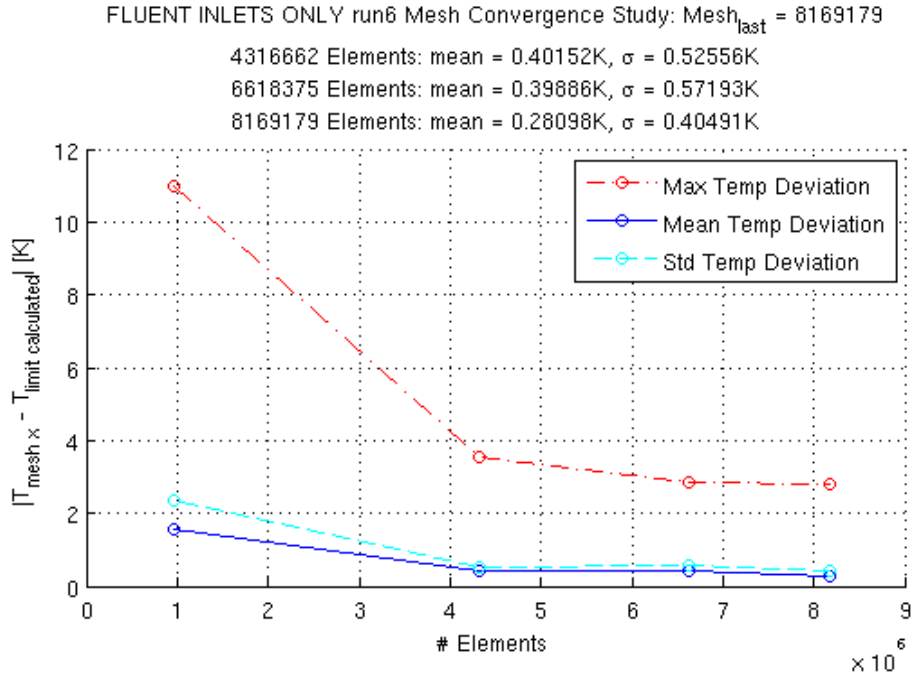
FLUENT INLETS ONLY run6 Mesh Convergence Study: Mesh$_{last}$ = 8169179
4316662 Elements: mean = 0.40152K, σ = 0.52556K
6618375 Elements: mean = 0.39886K, σ = 0.57193K
8169179 Elements: mean = 0.28098K, σ = 0.40491K
Max Temp Deviation
Mean Temp Deviation
Std Temp Deviation
|T$_{mesh\ x}$ - T$_{limit\ calculated}$| [K]
Elements
x 10^{6}

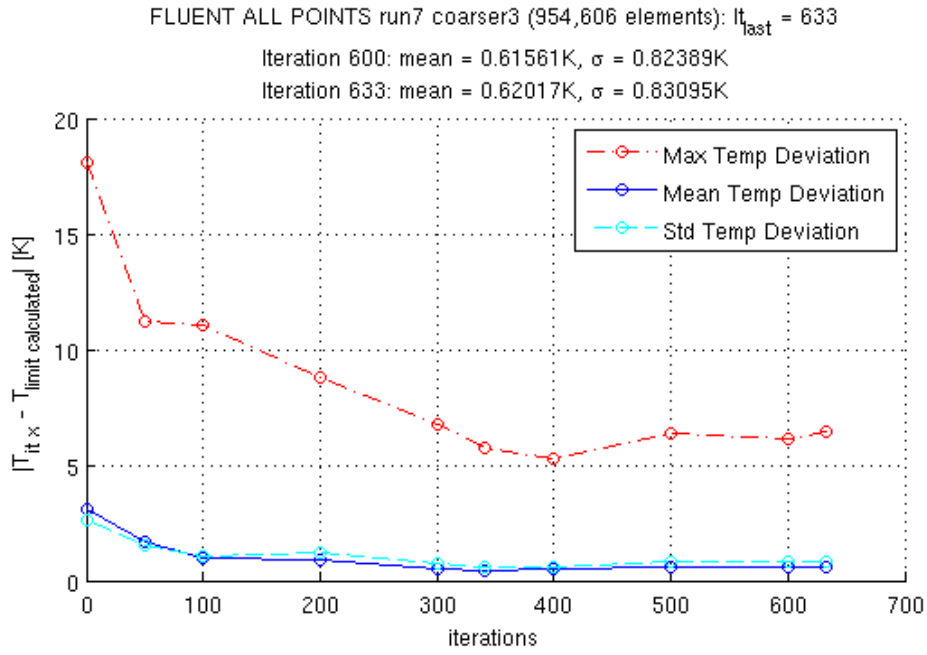
FLUENT ALL POINTS run7 coarser3 (954,606 elements): It$_{last}$ = 633
Iteration 600: mean = 0.61561K, σ = 0.82389K
Iteration 633: mean = 0.62017K, σ = 0.83095K
Max Temp Deviation
Mean Temp Deviation
Std Temp Deviation
|T$_{it\ x}$ - T$_{limit\ calculated}$| [K]
iterations
0
5
10
15
20
0
100
200
300
400
500
600
700

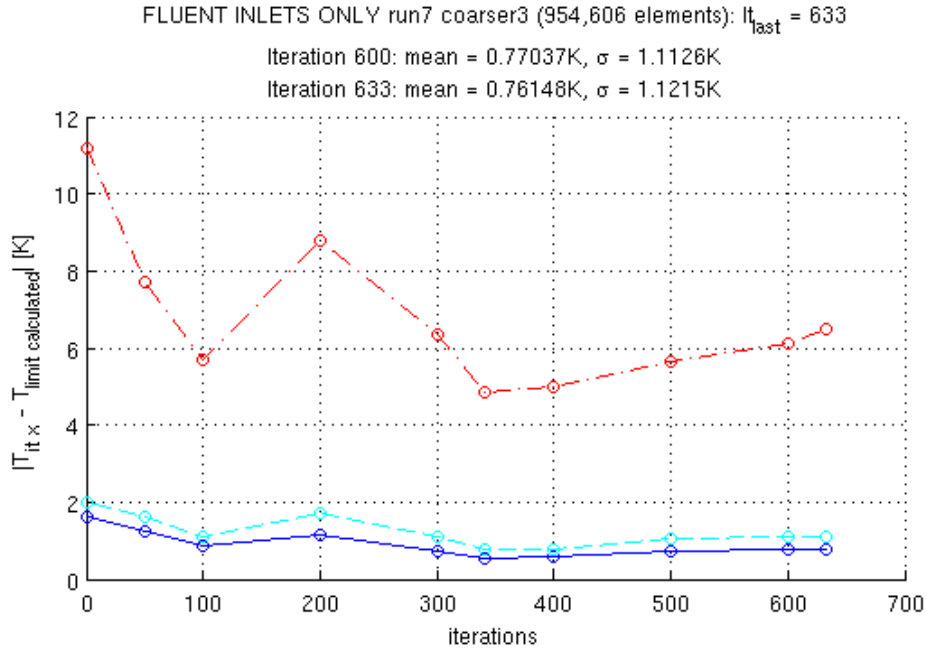
FLUENT INLETS ONLY run7 coarser3 (954,606 elements): It$_{last}$ = 633
Iteration 600: mean = 0.77037K, σ = 1.1126K
Iteration 633: mean = 0.76148K, σ = 1.1215K
|T$_{it\ x}$ - T$_{limit\ calculated}$| [K]
iterations
0
2
4
6
8
10
12
0
100
200
300
400
500
600
700

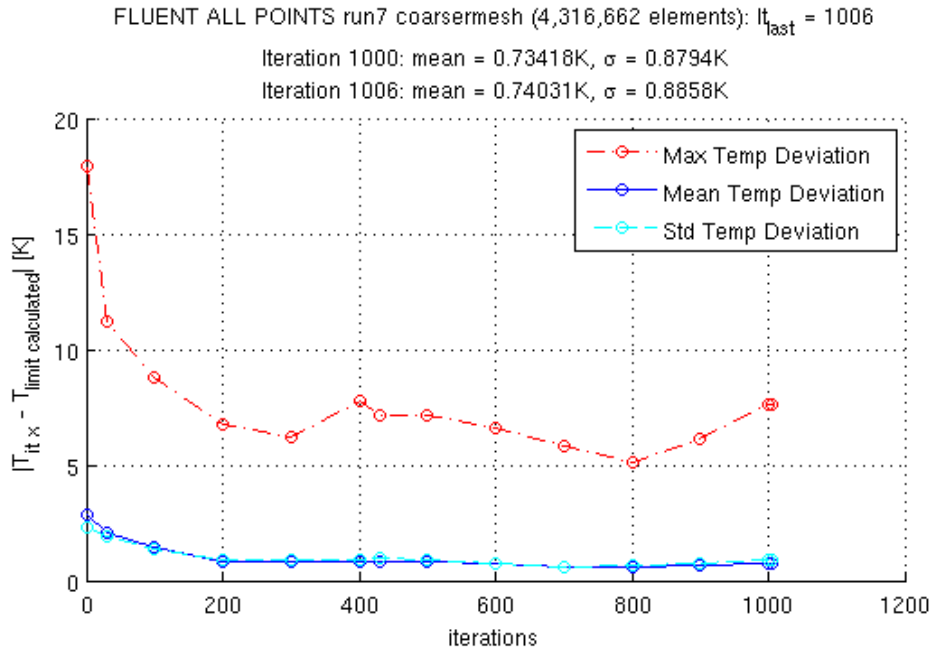
FLUENT ALL POINTS run7 coarsermesh (4,316,662 elements): It_last = 1006
Iteration 1000: mean = 0.73418K, σ = 0.8794K
Iteration 1006: mean = 0.74031K, σ = 0.8858K
Max Temp Deviation
Mean Temp Deviation
Std Temp Deviation
|T_it x - T_limit calculated| [K]
iterations
0
5
10
15
20
0
200
400
600
800
1000
1200

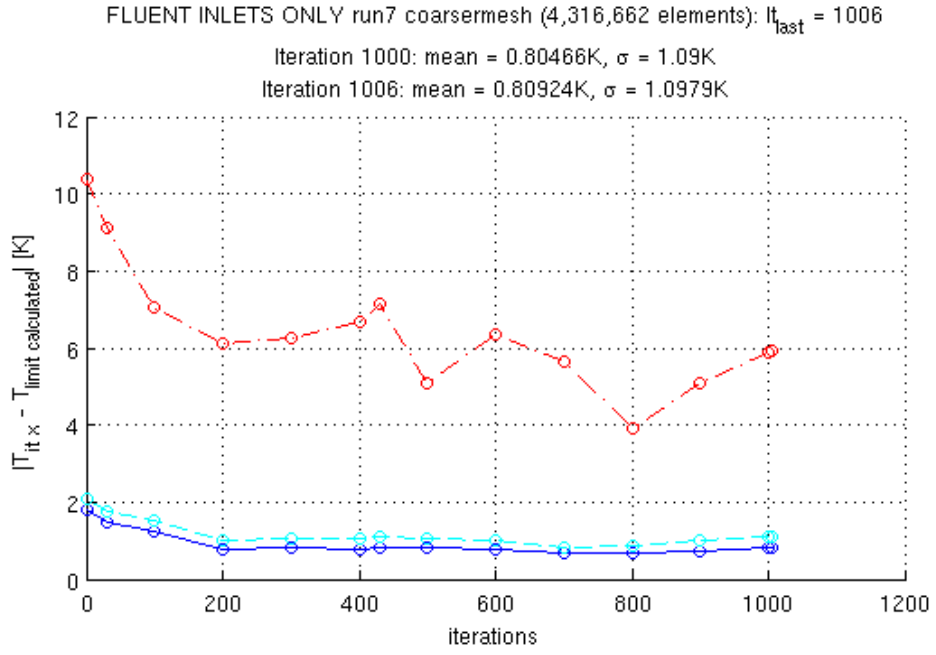
FLUENT INLETS ONLY run7 coarsermesh (4,316,662 elements): It_last = 1006
Iteration 1000: mean = 0.80466K, σ = 1.09K
Iteration 1006: mean = 0.80924K, σ = 1.0979K
|T_it x - T_limit calculated| [K]
iterations
0
2
4
6
8
10
12
0
200
400
600
800
1000
1200

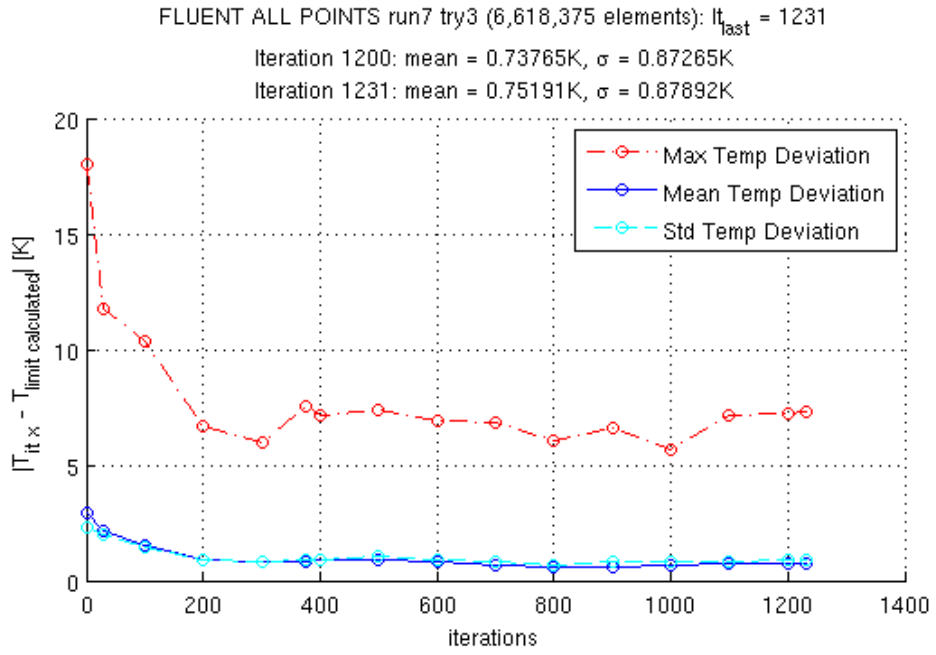
FLUENT ALL POINTS run7 try3 (6,618,375 elements): It$_{last}$ = 1231
Iteration 1200: mean = 0.73765K, σ = 0.87265K
Iteration 1231: mean = 0.75191K, σ = 0.87892K
Max Temp Deviation
Mean Temp Deviation
Std Temp Deviation
|T$_{it\ x}$ - T$_{limit\ calculated}$| [K]
iterations
0
5
10
15
20
0
200
400
600
800
1000
1200
1400

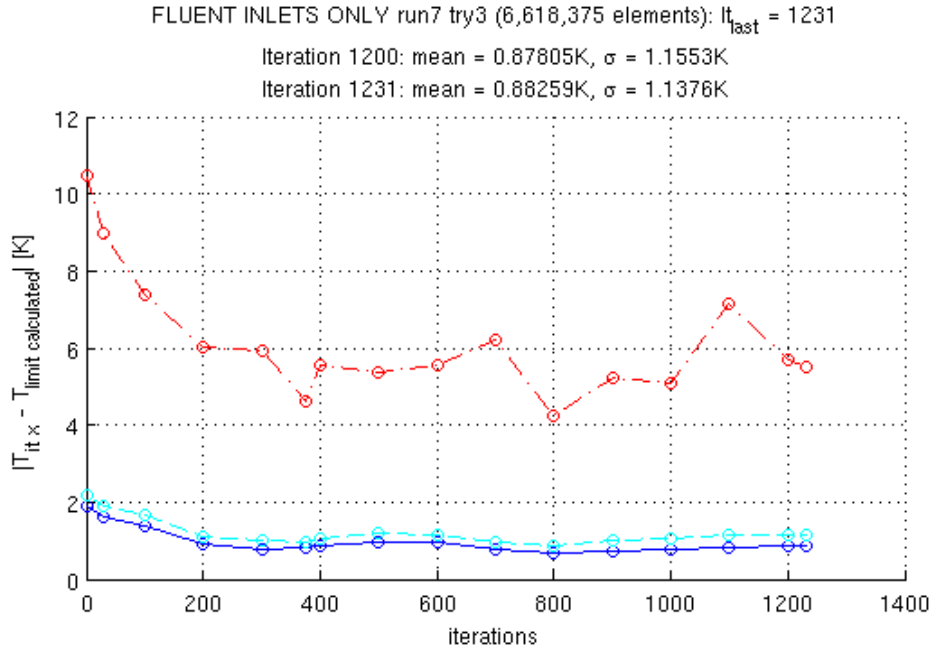
FLUENT INLETS ONLY run7 try3 (6,618,375 elements): It$_{last}$ = 1231
Iteration 1200: mean = 0.87805K, σ = 1.1553K
Iteration 1231: mean = 0.88259K, σ = 1.1376K
|T$_{it\ x}$ - T$_{limit\ calculated}$| [K]
iterations
0
2
4
6
8
10
12
0
200
400
600
800
1000
1200
1400